N83-33322

JPL NO. 9950-847

DRL No. 161
DRD Line Item No. SE-2

DOE/JPL 956061-7
Distribution Category UC-63

FLAT-PLATE SOLAR ARRAY PROJECT

ADVANCED MATERIALS RESEARCH TASK

FINAL REPORT

ON

INVESTIGATION OF THE HYDROCHLORINATION OF $SiCl_4$

(Covering the Period July 9, 1981 to April 8, 1983)

JPL CONTRACT NO. 956061

TO

JET PROPULSION LABORATORY
CALIFORNIA INSTITUTE OF TECHNOLOGY

BY

JEFFREY Y. P. MUI

April 15, 1983.

The JPL Flat-Plate Solar Array Project is sponsored by the U. S. Department of Energy and forms part of the Solar Photovoltaic Conversion Program to initiate a major effort toward the development of low-cost solar arrays. This work was performed for the Jet Propulsion Laboratory, California Institute of Technology by agreement between NASA and DOE.

SOLAREELECTRONICS, INC.

P.O. BOX 141, BELLINGHAM, MASS. 02019

FLAT-PLATE SOLAR ARRAY PROJECT

ADVANCED MATERIALS RESEARCH TASK

JPL Contract No. 956061

"Investigation of the Hydrochlorination of $SiCl_4$"

FINAL REPORT

Period Covered: July 9, 1981 - April 8, 1983

by

Jeffrey Y. P. Mui

SOLARELECTRONICS, INC.
Bellingham, Massachusetts

ABSTRACT

The hydrochlorination of silicon tetrachloride with hydrogen and metallurgical grade (m.g.) silicon metal,

$$3\ SiCl_4 + 2\ H_2 + Si \rightleftharpoons 4\ SiHCl_3$$

has been shown to be an efficient process to produce trichlorosilane. Trichlorosilane is presently the most widely used raw material for the production of high purity, polycrystalline silicon metal used by the electronics industry. It is also the starting material in the Union Carbide, silane-to-silicon process and in the Hemlock Semiconductor dichlorosilane chemical vapor deposition process to produce low-cost silicon metal for high efficiency solar cells.

A research and development program was carried out to study the hydrochlorination reaction over a wide range of reaction conditions. Equilibrium constant and reaction kinetics measurements were made to provide the basis for a theoretical study on the hydrochlorination process. Thermodynamic properties of the hydrochlorination reaction were also measured. The effects of

temperature, pressure and concentration on the equilibrium constant, K_p, were studied. The variation of K_p as a function of temperature provided a measurement on the heat of reaction, ΔH, for the hydrochlorination process. The reaction was found to be slightly endothermic with a value of ΔH equaled to 10.4 Kcal/mole (Si). Reaction kinetics measurements on the hydrochlorination of $SiCl_4$ and m.g. silicon metal were carried out over a wide range of temperature, pressure and concentration. Theoretical treatment of the experimental rate data showed that the hydrochlorination reaction followed a pseudo-first order kinetics. The rate constant, k_1, for the pseudo-first order rate equation was measured over a wide range of reaction conditions. The variation of k_1 as a function of temperature provided a measurement of the activation energy, ΔE, for the hydrochlorination reaction. The value of ΔE was calculated to give 13.2 Kcal/mole from a plot of the Arrhenius equation.

The mechanism of the hydrochlorination reaction was also investigated. A small quartz reactor was constructed to study the deuterium kinetics isotope effects. The reaction rates for the hydrochlorination of $SiCl_4$ and m.g. silicon metal in the presence of hydrogen and deuterium were measured under identical reaction conditions. Results showed that no significant deuterium kinetics effects were observed. This suggested that hydrogen is not directly involved in the rate-determining step. A plausible reaction mechanism for the hydrochlorination reaction is proposed.

A corrosion study was carried out to evaluate various materials of construction for the hydrochlorination reactor at 500°C and 300 psig. Results showed that a silicide protective film was formed on the metal surface. Analyses of the test samples by Scanning Electron Microscopy showed the diffusion of silicon into the base metal. A plausible corrosion mechanism of metals and alloys under the hydrochlorination reaction enviroment is proposed. Results of this study showed that stainless steel, Incoloy 800H and Hastelloy B-2 are suitable material of construction for the hydrochlorination reactor.

4

TABLE OF CONTENTS

7

I. SUMMARY

A basic research and development program was carried out to study the hydrochlorination of silicon tetrachloride with hydrogen and metallurgical grade (m.g.) silicon metal to form trichlorosilane,

$$3\ SiCl_4 + 2\ H_2 + Si \rightleftharpoons 4\ SiHCl_3$$

This reaction was shown to be an efficient process to produce $SiHCl_3$. Trichlorosilane is presently the most widely used raw material for the production of polycrystalline silicon metal used by the electronics industry. It is also the starting material in the Union Carbide, silane-to-silicon process and in the Hemlock Semiconductor dichlorosilane chemical vapor deposition process for the production of low-cost, solar grade silicon metal for high efficiency solar cells. All these silicon processes based on trichlorosilane as starting material also produce $SiCl_4$ as the major by-product. While the hydrochlorination reaction produces trichlorosilane, it also consumes silicon tetrachloride, a by-product generated from these silicon processes. Thus, the hydrochlorination reaction provides a mean to recycle the by-product $SiCl_4$ and it also fits perfectly into a closed-loop process scheme for the production of high purity silicon metal.

A laboratory scale reactor was constructed to collect experimental data on the hydrochlorination reaction over a wide range of reaction conditions. The reaction was studied at temperature range of 350°C to 700°C, pressure range of 0 to 300 psig and concentration range at $H_2/SiCl_4$ feed ratio of 1 to 5. The hydrochlorination of $SiCl_4$ and m.g. silicon metal is a typical equilibrium reaction. The equilibrium constant, K_p, was measured as a function of temperature, pressure and concentration. The effect of temperature on the equilibrium constant was studied over a temperature range of 500°C to 700°C. The equilibrium constant increased with increasing temperature. The heat of reaction, ΔH, was determined by the Second Law Method. The

9

value of ΔH was calculated to give 10.4 Kcal/mole (Si) by plotting the logarithm of K_p versus the inversed temperature, 1/T, in the Van't Hoff equation. Thus, the hydrochlorination is a slightly endothermic process. The equilibrium constant was also measured as a function of concentration over a range of $H_2/SiCl_4$ feed ratio of 1 to 5. In agreement with theory, the equilibrium constant remained constant within experimental error with respect to the varying $H_2/SiCl_4$ feed ratios. On the other hand, the effect of pressure on the equilibrium constant was found to be more complex. The equilibrium constant, K_p, did not remain constant with respect to the varying pressures. A larger K_p value was observed at the higher pressure range of 150 psig to 500 psig.

Reaction kinetics measurements on the hydrochlorination of $SiCl_4$ and m.g. silicon metal were carried out over a wide range of reaction conditions. A kinetic model was developed to fit the experimental rate data. Results of this theoretical study showed that the hydrochlorination reaction followed the pseudo-first order kinetics. A rate equation was developed. The rate constant, k_1, for the pseudo-first order rate equation was measured as a function of temperature, pressure and concentration. The effect of temperature on the rate constant was studied over a temperature range of 450°C to 550°C. The rate constant increased with increasing reaction temperature. This is in agreement with the previous experimental study which showed a faster reaction rate at a higher reaction temperature. The activation energy, ΔE, for the hydrochlorination reaction was determined from the Arrhenius equation to give a value of 13.2 Kcal/mole by plotting the logarithm of k_1 versus the inversed temperature, 1/T. The effect of pressure on the reaction rate was also studied. The rate constant decreased with increasing pressure indicating a slower reaction rate at higher pressures. The effect of $SiCl_4$ and H_2 concentrations on the hydrochlorination reaction was studied over a range of $H_2/SiCl_4$ feed ratios of 1 to 5. Results of the rate constant measurements showed that the reaction rate increased at a higher concentration of hydrogen gas. The effect of pressure

10

and the effect of hydrogen concentration on the rate constant suggested that the hydrochlorination reaction is also a diffusion-controlled process.

The reaction mechanism for the hydrochlorination process was investigated. The kinetics isotope effects of deuterium on the hydrochlorination of $SiCl_4$ and m.g. silicon metal were studied in a small quartz reactor at atmospheric pressure. Reaction kinetics measurements were carried out at 420°C and 450°C, respectively. The relative reaction rates between hydrogen and deuterium were measured under identical reaction conditions. Results of this study showed that there was no significant deuterium kinetics isotope effect observed in the hydrochlorination reaction of $SiCl_4$ and m.g. silicon metal. In this respect, one might rule out hydrogen being directly involved in the rate-determining step. The adsorption of $SiCl_4$ on the silicon metal surface to form an activated species might be the rate-determining step which appeared to fit the results of the reaction kinetics measurements and of the deuterium kinetics isotope effect study. A plausible reaction for the hydrochlorination process is proposed.

A corrosion study was carried out to evaluate a number of materials of construction for the hydrochlorination reactor. This study was originally carried out to support the engineering design work at Union Carbide Corporation (under JPL Contract No. 954334). Samples of conventional metals and alloys were tested and evaluated in a two inch-diameter hydrochlorination reactor at 500°C, 300 psig. Materials included carbon steel, nickel, copper, Alloy 400 (Monel), Type 304 stainless steel, Incoloy 800H and Hastelloy B-2. Results of the corrosion study showed that a silicide protective film was formed on the metal alloy surface. As a result, all the test samples achieved a weight gain. The presence of this silicide protective film protected the metal reactor wall exposed to the hydrochlorination reaction enviroment. Analysis of the test samples by Scanning Electron Microscopy confirmed the diffusion of silicon into

the base metal to form the silicide protective film. The silicon which was deposited onto the metal surface from the reversed hydrochlorination reaction combined with the metallic elements in the alloy to form the various metal-silicon phases. The continuous growth of the silicide film to form a thick scale on the reactor wall over a long period of time constituted a potential corrosion problem. Results of the Scanning Electron Microscopic analysis showed that alloy is more resistent to scale growth than those of the pure metals. Furthermore, alloys containing high melting point elements, such as chromium and molybdenum, are highly resistent to scale growth. Results of the corrosion study showed that stainless steel, Incoloy 800H and Hastelloy B-2 are suitable materials of construction for the hydrochlorination reactor. A corrosion mechanism of metals and alloys in the hydrochlorination reaction enviroment is also proposed.

12

II. INTRODUCTION

The JPL Contract No. 956061 to Solarelectronics, Inc. is part of the Advanced Materials Research Task under the Flat-Plate Solar Array Project managed by the Jet Propulsion Laboratory, California Institute of Technology. The basic research and development contract covered the period from July 9, 1981 to April 8, 1983.

The hydrochlorination of $SiCl_4$ and metallurgical grade (m.g.) silicon metal is the front end step in the Union Carbide silane-to-silicon process[1] developed under the JPL Contract No. 954334. The Union Carbide process may be represented by the following reaction sequences.

$$3\ SiCl_4 + 2\ H_2 + Si\ (m.g.) \rightleftharpoons 4\ SiHCl_3 \qquad (1)$$

$$2\ SiHCl_3 \rightleftharpoons SiCl_4 + SiH_2Cl_2 \qquad (2)$$

$$3\ SiH_2Cl_2 \rightleftharpoons 2\ SiHCl_3 + SiH_4 \qquad (3)$$

$$SiH_4 \xrightarrow{\Delta} 2\ H_2 + Si\ (solar) \qquad (4)$$

The hydrochlorination reaction (Equation 1) completes the closed-loop process scheme by recycling the by-products, $SiCl_4$ and H_2. The overall process merely becomes a purification scheme to convert impure m.g. silicon metal to the high purity, solar grade silicon metal for high efficiency solar cells.

Similarly, the Hemlock Semiconductor dichlorosilane chemical vapor deposition (CVD) process [2] developed under the JPL Contract No. 955533 utilizes the first two steps of the Union Carbide process to produce dichlorosilane. The SiH_2Cl_2 is then decomposed in a Siemens type CVD reactor to produce the high purity, solar grade silicon metal for high efficiency solar cells. Again, the hydrochlorination reaction (Equation 1) completes the closed-loop scheme by recycling the $SiCl_4$ by-product generated in the dichlorosilane synthesis step and in the CVD reactors.

A previous study at the Massachusetts Institute of Technology[3] under the JPL Contract No. 955 382 has shown that the hydrochlorination reaction is an efficient process to make $SiHCl_3$. Trichlorsilane is presently the most widely used raw material for the production of polycrystalline silicon metal by the Siemens type manufacturing process. The Siemens process also produces $SiCl_4$ as a major by-product. While the hydrochlorination reaction produces the needed $SiHCl_3$, it also consumes $SiCl_4$. Thus, the hydrochlorination reaction provides a mean to recycle by-product and to improve the raw material utilization efficiency for the Siemens type process practised by the electronics industry to-day.

The experimental study carried out at Solarelectronics, Inc. on the hydrochlorination of $SiCl_4$ and m.g. silicon was initially designed to supplement the engineering process development activities for the Experimental Process System Development Unit (EPSDU) by Union Carbide. The initial effort included optimization of the reaction conditions and a comprehensive corrosion study to evaluate materialsof construction for the hydrochlorination reactor. As the importance of the hydrochlorination reaction became more evident to other manufacturing processes for low-cost silicon metal, the scope of this research and development effort was expanded to cover a wide range of reaction conditions. The objective is to generate basic reaction kinetic and engineering data so that the potential application of the hydrochlorination process for the production of high purity, solar grade silicon metal can be fully evaluated. This experimental study also produced the needed data for a theoretical study to provide a basic understanding of the hydrochlorination reaction. The theoretical study included the measurement of thermodynamic functions for the hydrochlorination reaction and the development of a rate equation to fit the experimental rate data. Based on the results of these studies, a plausible reaction mechanism for the hydrochlorination process is proposed.

IF

III. DISCUSSIONS

The reaction of $SiCl_4$ and $SiHCl_3$ with hydrogen gas at high temperatures to deposit silicon metal has been extensively studied. It is the basic reaction for the chemical vapor deposition (CVD) of silicon in the Siemens type process for the production of polycrystalline silicon metal. The reaction equilibria in such a silicon-hydrogen-chlorine system are well-established [4,5]. Depending on the reaction conditions, such as temperature and the Cl/H ratio, the reversible reaction can be made to deposit silicon (e.g. the CVD processes) or to consume silicon (e.g. the hydrochlorination reaction). The hydrochlorination of $SiCl_4$ with hydrogen and m.g. silicon metal involves the same elements as the silicon-hydrogen-chlorine system in the Siemens process. However, the reaction temperature of about 500°C for the hydrochlorination reaction is much lower than that of the Siemens CVD process (1,000°C - 1,200°C). The reaction conditions for the hydrochlorination reaction are so chosen as to maximize the formation of $SiHCl_3$. Other than unreacted $SiCl_4$ and hydrogen, $SiHCl_3$ is the only major product present in the reaction mixture. Only a small amount of by-products, SiH_2Cl_2 (0.1 - 0.5%) and HCl (0.1 - 0.3%) are present under normal reaction conditions. Although the reaction mechanism is much more complex, the hydrochlorination of $SiCl_4$ and m.g. silicon metal may be written as,

$$3\ SiCl_4 + 2\ H_2 + Si \rightleftharpoons 4\ SiHCl_3 \qquad (1)$$

to show the stoichiometry of the overall reaction.

Interestingly, this reaction was first observed by O. Ruff and K. Albert [6] in 1905. In their study on the thermo-decomposition of $SiHCl_3$, they reported a reaction identical to the reverse of Equation (1). The hydrochlorination reaction was later studied by Union Carbide in their Tonawanda Laboratory in the late 1940 [1] and it formed the basis of the closed-loop, silane-to-silicon process developed under the JPL Contract No. 954334. This reaction was further studied at the Massachusetts

15

Institute of Technology [3] under the JPL Contract No. 955382.

A. The Hydrochlorination Apparatus

The one inch-diameter stainless steel reactor system constructed at the Massachusetts Institute of Technology under the JPL Contract No. 955382 was transferred to Solarelectronics, Inc. to further the studies on the hydrochlorination reaction. This apparatus was extensively modified to form a two inch-diameter reactor system which is schematically shown in Figure I. A constant flow of hydrogen gas from a standard cylinder is metered through a fine needle valve. The gas flowrate is measured by a mass flowmeter. The hydrogen pressure is controlled by a pressure regulator which is set at about 30 psig above the selected reactor pressure for the hydrochlorination reaction. The ΔP provides the driving force for the gaseous flow through the reactor system. The hydrogen gas is dispersed into a liquid column of $SiCl_4$ contained in a stainless steel cylinder. The $SiCl_4$ liquid is heated by circulating a heat transfer fluid through the heating jacket on the stainless steel cylinder. Since the vapor pressure of $SiCl_4$ is constant at a given temperature, the desired $H_2/SiCl_4$ feed ratio can be conveniently selected by adjusting the $SiCl_4$ liquid temperature and by the applied hydrogen gas pressure. The gaseous $H_2/SiCl_4$ mixture is then fed into the bottom of the two inch-diameter hydrochlorination reactor through heat-traced connecting tubes. The reactor tube is made of Type 304 stainless steel. The reactor is charged 862 g. (718 c.c.) 32 x D (32 mesh to dust) m.g. silicon metal to form a mass bed of about 18 inches high. The reactor tube is heated by four variable sectional heaters which can be individually adjusted so as to give a uniform temperature along the reactor tube. A Nichrome wire electrical heater uniformly wound along the entire reactor tube serves as the control heater to keep reactor at a constant temperature for the hydrochlorination reaction. The arrangement of these heaters is shown in Figure II. The reaction temperature is controlled by a temperature controller with thermocouple located inside the

16

reactor tube at about the mid-point of the silicon mass bed. The two inch-diameter hydrochlorination reactor is a fluidized-bed design with a 5-orifice grid plate located at the bottom of the reactor tube as schematically shown in Figure II. The gaseous $H_2/SiCl_4$ mixture passes through a pre-heater and is dispersed into the silicon mass bed through the grid plate.

The reaction product mixture coming out of the hydrochlorination reactor is analyzed by the in-line gas chromatograph (G.C.). The in-line G.C. is directly connected to the outlet of the reactor tube as shown in Figure I. The in-line arrangement provides instantaneous analysis of the reaction mixture. A gaseous sample from the reactor is drawn into the sample loop through a needle valve and a filter arrangement. All the connecting tubings are heat-traced so that the sample is maintained in a homogeneous vapor state. The sample is then injected into the G.C. column by turning the G.C. sampling valve. The dual G.C. columns are made of 1/8 inch O.D. x 12 feet stainless steel tubing packed with 5% SE-30 silicone gum stationary phase on 150 mesh Chromosorb W. A standard hot wire detector is used for the analysis. The G.C. spectrum is recorded and analyzed by the Hewlett-Packard Model 3380A Recorder/Integrator. The in-line arrangement eliminates the need for external sampling and avoids the contact of the reactive chlorosilane sample with moisture in the atmosphere. The G.C. analysis gives the mole % conversion of $SiHCl_3$ and the unreacted $SiCl_4$. Small amounts of by-product SiH_2Cl_2 (0.1 - 0.5%) is also detected by the G.C. analysis. The hydrogen gas is not analyzed by the gas chromatograph. However, its concentration can be readily calculated. In the reaction kinetic measurements, the $SiHCl_3$ conversion (expressed in mole % based on total chlorosilanes) is measured as a function of residence time. The residence time is varied by changing the $H_2/SiCl_4$ feedrate and the reaction product composition is analyzed by the G.C.

The chlorosilane product mixture coming out of the reactor is condensed by the low temperature condenser. The condenser

is cooled by circulating a coolant from a Dry-Ice bath through the jacket on the condenser. The condenser temperature can be maintained at -65°C. The non-condensable hydrogen gas is passed through a scrubber filled with a solution of sodium hydroxide to remove the trace amount of HCl and residual chlorosilane which may escape the low temperature condenser. The remaining hydrogen gas is safely disposed.

B. Reaction Kinetic Measurements

Previous experimental studies [3] on the hydrochlorination of $SiCl_4$ and m.g. silicon metal were carried out within a rather narrow range of reaction conditions. These earlier experimental works were primarily designed to support the engineering development effort carried out by Union Carbide on the 100 MT/year EPSDU. The operating conditions for the hydrochlorination process were selected by Union Carbide at about 500°C and 500 psig. Previous experimental data on the hydrochlorination reaction were mostly collected at the high pressure range of 300 psig and 500 psig. To expand the study on the effect of pressure, experiments were carried out at the lower pressure range of 25 psig, 100 psig, 150 psig and 200 psig, respectively. The reaction temperature was also expanded to cover a wide range from 350°C to 700°C. The effect of concentration on the hydrochlorination reaction was studied at the expanded range of $H_2/SiCl_4$ feed ratio of 1 to 5. Results of these reaction kinetic measurements are summarized in the following discussions.

(1) Effect of Pressure on the Hydrochlorination Reaction

Since the hydrochlorination of $SiCl_4$ and m.g. silicon metal to form $SiHCl_3$ results in a net volume contraction,

$$3\ SiCl_4 + 2\ H_2 + Si = 4\ SiHCl_3$$

a higher pressure shall produce a higher equilibrium conversion of $SiHCl_3$. Experimental results previously obtained on the hydrochlorination reaction [3] are in agreement with the thermodynamics

prediction. However, thermodynamic properties do not prescribe reaction kinetics. A small pressure effect on the reaction rate, i.e., the rate at which the hydrochlorination reaction reaches its equilibrium $SiHCl_3$ conversion, was noted in the previous experimental studies at 300 psig and at 500 psig. The effect of pressure was systematically studied over a wide range of reaction parameters.

A series of experiments was carried out at 450°C with a $H_2/SiCl_4$ feed ratio of 2.0 and at various pressures of 25 psig, 100 psig, 150 psig and 200 psig, respectively. Results of this series of experiments are summarized in Table I (25 psig), Table II (100 psig), Table III (150 psig) and Table IV (200 psig). Data in these four tables are also presented in Figure III by plotting the % $SiHCl_3$ conversion versus residence time. As predicted by thermodynamics, results in Figure III show that a higher pressure produces a higher conversion of $SiHCl_3$ close to equilibrium at long residence times. On the other hand, the reaction rates are noticable slower at higher pressures. For example at 25 psig, the kinetic curve in Figure III starts leveling off (reaches equilibrium) at about 60 seconds residence time. At pressures over 100 psig, the hydrochlorination reaction is far from equilibrium at 60 seconds residence time as shown in Figure III.

Another series of experiments on the hydrochlorination of $SiCl_4$ and m.g. silicon metal was carried out at a higher temperature of 500°C with the same $H_2/SiCl_4$ feed ratio of 2.0 and at the same pressure range of 25 psig, 100 psig, 150 psig and 200 psig, respectively. Results of the reaction kinetics measurements are summarized in Table V, Table VI, Table VII and Table VIII, respectively for the 25 psig, 100 psig, 150 psig and 200 psig experiments. Data in these four tables are also presented in Figure IV by plotting the % $SiHCl_3$ conversion versus residence time. The profile of the kinetic curves in Figure IV are similar to those in Figure III to show the same effect on the hydrochlorination reaction. The generally higher $SiHCl_3$ conversion at 500°C in Figure IV is the combined results

of the pressure effect and the temperature effect. A higher reaction temperature produces both a faster reaction rate and a higher equilibrium conversion of $SiHCl_3$. For example, the reaction at 25 psig gave an equilibrium conversion of about 18% $SiHCl_3$ at 500°C (Figure IV). At 450°C, the equilibrium conversion of $SiHCl_3$ is only 16% at the same pressure of 25 psig (Figure III). Also, the rate of approaching equilibrium at 500°C is faster than that at 450°C. For example, the reaction takes about 15 seconds residence time to reach 90% of its equilibrium $SiHCl_3$ conversion (0.9 x 18% = 16.2%) at 500°C. At 450°C, the same reaction requires about 26 seconds residence time to reach the same 90% equilibrium $SiHCl_3$ conversion (0.9 x 16% = 14.4%). The effect of temperature on the hydrochlorination reaction is further studied in the following experiments.

(2) Effect of Temperature on the Hydrochlorination Reaction

A series of experiments was carried out to study the effect of temperature on the hydrochlorination reaction at 100 psig with a $H_2/SiCl_4$ feed ratio of 2.0 and at the lower temperature range of 350°C and 400°C to supplement the reaction kinetics data obtained at 450°C and 500°C in Section B (1). Results of these two experiments are summarized in Table IX and Table X for the reaction kinetics data obtained at 350°C and 400°C, respectively. The rate data obtained at these four temperatures are also presented in Figure V by plotting the % $SiHCl_3$ conversion versus residence time. Results in Figure V show the evidence of a large temperature effect on the hydrochlorination reaction. The kinetics curves at 500°C and 450°C level off at the equilibrium conversion of $SiHCl_3$ while the kinetic curves at 400°C and 350°C are far from reaching equilibrium within the residence time scale as shown in Figure V. As previously observed, a higher reaction temperature gives both a faster reaction rate and a higher equilibrium conversion of $SiHCl_3$. For example at 500°C, the hydrochlorination reaction reaches 90% of its equilibrium $SiHCl_3$ conversion in about 35 seconds residence time. At 450°C, about 68 seconds residence time is needed for the hydrochlorination

reaction to achieve the same 90% equilibrium conversion. At 500°C, the equilibrium conversion of $SiHCl_3$ is about 2% to 3% higher than that of the equilibrium $SiHCl_3$ conversion at 450°C.

(3) Effect of Concentration on the Hydrochlorination Reaction

The effect of hydrogen and $SiCl_4$ concentration on the hydrochlorination of $SiCl_4$ and m.g. silicon metal was studied at 100 psig and at 500°C. The reaction temperature and pressure were kept constant while the hydrogen concentration was increased at the $H_2/SiCl_4$ feed ratio of 1.0, 2.0, 2.8, 4.0 and 4.7, respectively. Results of these experiments are summarized in Table XI (1.0), Table VI (2.0), Table XII (2.8), Table XIII (4.0) and Table XIV (4.7). The reaction kinetics data in these Tables are also presented in Figure VI by plotting the % $SiHCl_3$ conversion versus residence time. As results in Figure VI show, a higher $H_2/SiCl_4$ feed ratio produces a higher conversion of $SiHCl_3$ close to equilibrium. This is expected from the equilibrium reaction,

$$3\ SiCl_4 + 2\ H_2 + Si \rightleftharpoons 4\ SiHCl_3$$

An increase of the $H_2/SiCl_4$ feed ratio corresponds to an increase of the hydrogen partial pressure in the hydrochlorination reactor. Since hydrogen is consumed to form $SiHCl_3$, a higher partial pressure of hydrogen gas will drive the equilibrium toward the right hand side of the equation to produce more $SiHCl_3$.

C. Kinetic Modeling of the Hydrochlorination Reaction

The hydrochlorination of $SiCl_4$ with hydrogen and m.g. silicon metal is a typical equilibrium reaction which is illustrated in Figure VII. A mixture of $SiCl_4$ and H_2 is reacted in a mass bed of m.g. silicon metal to form $SiHCl_3$. At time zero, no trichlorosilane is produced. As the residence time increases, the conversion of $SiHCl_3$ also increases at the early stage of the hydrochlorination reaction. As the reaction

approaches equilibrium at long residence times, the $SiHCl_3$ conversion levels off. The kinetic curve for the hydrochlorination reaction in Figure VII may be looked at as two distinct parts. The equilibrium plateau of the kinetic curve may be considered as the thermodynamic properties of the hydrochlorination reaction. The equilibrium compositions are predictable from known thermodynamic parameters. The measurements of the equilibrium constant as a function of temperature provide a mean to determine an important thermodynamic function, ΔH, the heat of reaction for the hydrochlorination process. The curve at the left hand side of the equilibrium plateau is the kinetic curve which is characteristic of the hydrochlorination reaction. The kinetic curve describes the rate of reaction, i.e., the rate at which the hydrochlorination reaction reaches its equilibrium $SiHCl_3$ conversion.

The hydrochlorination of $SiCl_4$ and m.g. silicon metal is strongly affected by the reaction temperature and, to a lesser extend, by the pressure and the concentration parameters. In the following theoretical study, the equilibrium constnat, K_p, is calculated from the equilibrium compositions obtained from the hydrochlorination experiments. The variation of the equilibrium constant as a function of temperature provides a measurement on the heat of reaction, ΔH, for the hydrochlorination process. Equilibrium constant measurements were also carried out as a function of concentration and pressure. Results are discussed in Section C. In the reaction kinetics measurements, the rate of formation of $SiHCl_3$ was measured as a function of residence time. A rate equation was developed to fit the experimental kinetic curve. The rate constant, k_1, for the rate equation was measured as a function of temperature, pressure and concentration. Variation of the rate constant as a function of temperature provides the measurement on the activation energy, ΔE, for the hydrochlorination reaction. Results of these rate constant measurements are discussed in Section D.

D. Equilibrium Constant and Thermodynamic Functions

The equilibrium constant for the hydrochlorination reaction,

$$3\ SiCl_4 + 2\ H_2 + Si \rightleftharpoons 4\ SiHCl_3$$

is calculated in accordance with the stoichiometry of the overall reaction. The equilibrium constant, K, based on the mole fractions of reactants and products is defined as

$$K = \frac{(SiHCl_3)^4}{(SiCl_4)^3(H_2)^2}$$

The activity (concentration) of elemental silicon is taken as unity. The equilibrium constant, K_p, expressed in terms of partial pressure of reactants and products is similarly given by,

$$K_p = \frac{(p_{SiHCl_3})^4}{(p_{SiCl_4})^3(p_{H_2})^2}$$

The partial pressure, p, is obtained by multiplying the mole fraction with the total pressure, P. Thus,

$$K_p = \frac{K}{P}$$

The equilibrium constants were measured as a function of temperature, concentration and pressure. Results are discussed in the following.

(1) Equilibrium Constant as a Function of Temperature

A series of experiments on the hydrochlorination of $SiCl_4$ and m.g. silicon metal was carried out in the two inch-diameter pressure reactor at 100 psig with a $H_2/SiCl_4$ feed ratio of 2.0 and at various reaction temperatures. Sufficiently long residence times were allowed for the reaction so that the hydrochlorination reaction was well within equilibrium. The reaction product composition was then measured by the in-line

G.C. at the reaction temperature of 500°C, 525°C, 550°C and 575°C, respectively. Results of the G.C. measurements are summarized in Table XV. Data in Table XV showed that the equilibrium conversion of $SiHCl_3$ increased with increasing temperature. The mole% of $SiHCl_3$ and $SiCl_4$ in Table XV were converted to mole fractions. The concentration of hydrogen in the reaction product mixture was not determined by the G.C. analysis. However, it can be readily calculated. Since one mole of hydrogen is consumed for every two moles of $SiHCl_3$ produced and since one mole of hydrogen is consumed for every mole of SiH_2Cl_2 produced, the concentration of hydrogen at equilibrium is given by,

$$C_{H_2} = a_{H_2} - \tfrac{1}{2} C_{SiHCl_3} - C_{SiH_2Cl_2}$$

where a_{H_2} is the initial hydrogen concentration in the feed. The values of the equilibrium constants, K and K_p, were calculated from the mole fraction data and from the partial pressure data. Results are summarized in Table XVI. As the results in Table XVI show, the equilibrium constants for the hydrochlorination reaction increase as a function of increasing reaction temperature.

Another series of experiments was carried out to measure the equilibrium constant for the hydrochlorination reaction at a still higher temperature range of 500°C to 700°C. The experiments were carried out in a small quartz reactor at atmospheric pressure with a $H_2/SiCl_4$ feed ratio of 2.0 (H/Cl = 1.0). The quartz reactor was originally designed for the deuterium kinetic isotope effect study. The function of this quartz reactor is described in Section F (A). Results of the equilibrium composition measurements are summarized in Table XVII. The equilibrium data in Table XVII were converted to mole fractions. The equilibrium constant K for the hydrochlorination reaction was calculated from the equilibrium mole fractions of H_2, $SiHCl_3$ and $SiCl_4$ at the temperature range of 500°C, 550°C, 600°C, 650°C and 700°C, respectively. Results are summarized in Table XVIII.

2f

Here K is the same as K_p since the hydrochlorination reaction was carried out at one atmosphere. Again, the data in Table XVIII show that the equilibrium constant increases with an increasing reaction temperature.

The equilibrium compositions for the hydrogen, $SiHCl_3$, $SiCl_4$ and the small amount of SiH_2Cl_2 by-product obtained from the hydrochlorination reaction are in good agreement with the calculated values reported by E. Sirtle,L. P. Hunt and D. H. Sawyer[5]. In Figure Ic of their publication, "High Temperature Reaction in the Silicon-Hydrogen-Chlorine System", the equilibrium gas phase composition at 1 atmosphere total pressure and Cl/H = 1.0 is plotted against various temperature. At 773°K (500°C), the calculated partial pressure (in atmosphere) are approximately 0.002 for SiH_2Cl_2, 0.08 for $SiHCl_3$, 0.28 for $SiCl_4$ and 0.64 for H_2. These calculated equilibrium compositions by E. Sirtle, et. al. are in good agreement with the experimental results given in Table XVI and Table XVIII. The calculated concentration of SiH_2Cl_2 is about 1/30 to 1/40 of the $SiHCl_3$ concentration. This is also in good agreement with the small amount of SiH_2Cl_2 by-product observed in the hydrochlorination of $SiCl_4$ and m.g. silicon metal.

(2) The Heat of Reaction, ΔH

The heat of reaction, ΔH, for the hydrochlorination reaction is calculated by the Second Law Method. Starting from the equation,

$$\Delta F = - RT \ln K$$

by differentiation with respect to T,

$$\frac{d\Delta F}{dT} = - S$$

one obtains the well-known Van't Hoff equation,

$$\Delta H = RT^2 \frac{d \ln K}{d T}$$

where, ΔF is the Free Energy, R is the ideal gas constant, T is the temperature and S is the Entropy. By substituting $dT = - T^2 d(1/T)$, one obtains,

$$\Delta H = - R \frac{d(\ln K)}{d(\frac{1}{T})}$$

Thus, the slope of a ln K versus 1/T plot is $-\Delta H/R$. The logarithm of the equilibrium constant K in Table XVI is then plotted against the inversed temperature, 1/T. Results are given in Figure VIII. The plot in Figure VIII gives a straight line. The heat of reaction, ΔH, is then determined from the slope of the straight line to give a value of 10.6 Kcal/mole for the hydrochlorination reaction. Thus, the hydrochlorination of $SiCl_4$ and m.g. silicon metal to $SiHCl_3$ is a slightly endothermic reaction.

Similarly, the logarithm of the equilibrium constant K obtained at atmospheric pressure and at the temperature range of 500°C - 700°C in Table XVIII is plotted against the inversed temperature, 1/T. Results are summarized in Figure IX. Interestingly, the graph in Figure IX shows a linear plot at the lower temperature range of 500°C - 550°C. At the higher temperature range of 600°C - 700°C, the graph curves and appears to level off at temperature above 700°C. The slope of the linear portion of the graph at the lower temperature range was measured. The heat of reaction, ΔH, was then calculated from the slope which equals to $-\Delta H/R$. Results of the calculation gave a value of 10.1 Kcal/mole for the heat of reaction. This result is in good agreement with the value of ΔH obtained from the same equilibrium constant measurement at 100 psig and at the temperature range of 500°C to 575°C in Figure VIII. The average of the two ΔH values give 10.4 Kcal/mole for the heat of reaction for the hydrochlorination reaction.

The deviation of the graph in Figure IX from linearity may be explained by the fact that, at higher temperatures, other important products are produced from this reaction system containing silicon, hydrogen and chlorine. For example, the

calculated equilibrium composition as reported by Sirtl, Hunt and Sawyer [5] shows that an approximately equal molar amounts of $SiHCl_3$ and HCl are formed at 1,000°C, atmospheric pressure and Cl/H ratio of 1.0 (same as $H_2/SiCl_4$ = 2.0). Evidently, at temperature below 550°C, the hydrochlorination reaction predominates in the silicon-hydrogen-chlorine system. At this temperature, $SiHCl_3$ is the only major product with only small amounts of by-products, SiH_2Cl_2 (0.1 - 0.5%) and HCl (0.1 - 0.3%). At temperature of 600°C and above, the formation of HCl becomes increasingly more important. The above equilibrium constant measurements based on $SiHCl_3$ alone as the only reaction product becomes inadequate at the higher temperature range. The deviation of the graph in Figure IX from linearity merely means that the hydrochlorination reaction becomes less dominant at temperature above 600°C as other parallel reactions come into being.

(3) Equilibrium Constant as a Function of Concentration

One set of experimental data obtained from the hydrochlorination of $SiCl_4$ and m.g. silicon metal at 100 psig, 500°C and at various $H_2/SiCl_4$ feed ratio of 1.0, 2.0, 2.8, 4.0 and 4.7 was analyzed. These experimental data were obtained from the reaction kinetics curves in Figure VI. The equilibrium $SiHCl_3$ conversion at various $H_2/SiCl_4$ feed ratios were directly measured from Figure VI at the point where the kinetic curves leveled off. The equilibrium compositions of $SiHCl_3$ and $SiCl_4$ were converted to mole fractions and partial pressures as shown in Table XIX. The equilibrium constants, K and K_p, were calculated. Results are summarized in the last two columns in Table XIX. The equilibrium constant remains essentially constant within experimental error at the various $H_2/SiCl_4$ feed ratios ranging from 1.0 to 4.7. The standard deviation from this set of equilibrium constant values are well within ± 10%. Thus, the equilibrium constant for the hydrochlorination reaction is constant with respect to H_2 and $SiCl_4$ concentrations. This

observation is in agreement with the theoretical consideration.

(4) Equilibrium Constant as a Function of Pressure

The equilibrium constant, K_p, for the hydrochlorination reaction should also be a constant value with respect to pressure. A collection of equilibrium data previously obtained from the hydrochlorination of $SiCl_4$ and m. g. silicon metal at 500°C and at various pressures (from 0 psig to 500 psig) and $H_2/SiCl_4$ feed ratios (from 1.0 to 4.7) is summarized in Table XX. The equilibrium mole % of $SiHCl_3$ was obtained from the various kinetic curves at the point where the % $SiHCl_3$ conversion has leveled off at long residence times. The 300 psig and the 500 psig equilibrium data in Table XX were obtained from the previous hydrochlorination study carried out at the Massachusetts Institute of Technology [3] with the one inch-diameter reactor system. The 25 psig to 200 psig equilibrium data were collected from the two inch-diameter stainless steel reactor while the atmospheric (0 psig) equilibrium data were obtained from the small quartz reactor system. These equilibrium data were converted to mole fractions. The equilibrium constants, K and K_p, were then calculated and listed in the last two columns in Table XX. The equilibrium constant measurements in Table XX show complex results. The equilibrium constant K_p does not remain constant over the pressure range of 0 psig to 500 psig. The value of K_p appears to increase at the higher pressure range of 150 psig to 500 psig. The reason for the increase of the value of K_p at the higher pressure range is not fully understood at the present time. On the other hand, one might expect a fairly large deviation of experimental error in this collection of equilibrium data, since these results were collected over a period of about three years from three different hydrochlorination reactors. Nevertheless, the effect of pressure on the equilibrium constant K_p appears to show reproducible results. Table XXI summarizes another collection of experimental equilibrium data for the hydrochlorination reaction at a lower temperature of 450°C. The equilibrium constant was calculated from the $SiHCl_3$

and $SiCl_4$ equilibrium compositions over the pressure range of 25 psig to 500 psig. Results are summarized in the last column in Table XXI. Again, a higher value of K_p is observed at the higher pressure range of 150 psig to 500 psig.

E. The Rate Equation, the Rate Constant and the Activation Energy

(1) Development of a Rate Equation

A theoretical treatment of experimental reaction kinetics data is to express the reaction rate in terms of an equation which relates the rate to the concentations of reactants, and sometimes of products or other substance present (e.g. of catalyst). If the reaction has a simple order, one must determine what the order is, and also the rate constant. The hydrochlorination of $SiCl_4$ and m.g. silicon metal frequently expressed as,

$$3\ SiCl_4 + 2\ H_2 + Si \rightleftharpoons 4\ SiHCl_3 \qquad (1)$$

is a balanced equation to show the stoichiometry of the overall equilibrium reaction. The equilibrium constant measurements in Section D above on the hydrochlorination reaction (Equation 1) are in agreement with the stoichiometry as it is written. A number of models for the treatment of experimental rate data was tested with different rate expressions. Results showed that the reaction kinetics on the rate of formation of $SiHCl_3$ fitted well in the pseudo-first order rate equation. The theoretical treatment of experimental rate data is presented in the following discussions.

To start with the simplest situation in which both the forward and reverse reactions are of first order,

$$A \underset{k_{-1}}{\overset{k_1}{\rightleftharpoons}} B$$

If the reaction is started using pure A, of concentration a,

and if after time t the concentration of B is x, that of A is a - x, the rate from left to right is then $k_1(a - x)$, and that from right to left is $k_{-1}x$; the net rate of production of B is thus

$$\frac{dx}{dt} = k_1(a - x) - k_{-1}x$$

At equilibrium, the net rate of production of B is zero, and if the concentration of x is then x_e,

$$k_1(a - x_e) = k_{-1}x_e$$

Elimination of k_{-1} between these two equations gives rise to

$$\frac{dx}{dt} = \frac{k_1 a}{x_e}(x_e - x)$$

The solution to this differential rate equation is

$$\ln \frac{x_e}{x_e - x} = \frac{k_1 a}{x_e} t$$

This simple rate equation can sometimes be applied to a more complex reaction involving more than one reactant and more than one product. It is then called pseudo-first order kinetics. For the rate of conversion of $SiCl_4$ to $SiHCl_3$ in the hydrochlorination reaction, x is the concentration of $SiHCl_3$ at time t, x_e is the equilibrium concentration of $SiHCl_3$ and a is the initial concentration of $SiCl_4$. To test the validity of the pseudo-first order rate equation for the experimental kinetics data, a plot of the logarithm of $x_e/x_e - x$ versus residence time t shall give a straight line. The forward rate constant, k_1, is then obtained from the slope of the straight line, which equals to $k_1 a/x_e$.

(2) Rate Constant as a Function of Temperature

Reaction kinetics measurements on the hydrochlorination of $SiCl_4$ and m.g. silicon metal were carried out at 100 psig with

a $H_2/SiCl_4$ feed ratio of 2.0. Results of the kinetic measurements at 450°C and 500°C have already been summarized in Table II and Table VI, respectively. Another series of kinetic measurements on the hydrochlorination reaction was carried out at a still higher reaction temperature, 550°C. Results of this experiment are summarized in Table XXII. The reaction kinetics measurements at 450°C, 500°C and 550°C were presented in Figure X by plotting the % $SiHCl_3$ conversion versus residence time. The resulting kinetic curves in Figure X were analyzed by fitting the experimental rate data in the pseudo-first order rate equation. As an illustration, the analysis for the 500°C reaction kinetic curve in Figure X is summarized in Table XXIII. The % $SiHCl_3$ conversion at 10, 20, 30, 40 and 60 seconds residence times were taken from the smooth kinetic curve in Figure X. The mole % of $SiHCl_3$ and $SiCl_4$ were converted to mole fractions and partial pressures (psia) and recorded in column 3 of Table XXIII. The hydrogen concentration was not measured. However, it can be calculated in the same manner as shwon in Section C(1). The initial partial pressure of $SiCl_4$, a, was calculated from the $H_2/SiCl_4$ feed ratio and from the total pressure (i.e. 1/3 of 114.7 psia). The equilibrium partial pressure of $SiHCl_3$, x_e, was measured at the point where the kinetic curve leveled off at long residence times. The logarithm of $x_e/x_e - x$ at each of the selected residence time was computed. These kinetic data were then applied to the pseudo-first order rate equation by plotting ln x_e/x_e-x versus the residence time t. Results are summarized in Figure XI. The plot in Figure XI gives a straight line to show a good fit between the experimental rate data and the rate equation.

Similarly, the experimental kinetics data obtained at 450°C and at 500°C were treated by the same theoretical consideration. The plot of the pseudo-first order rate equation at these two temperatures are also presented in Figure XI. Again, a straight line is obtained from the plots at 450°C and 500°C. The rate constants, k_1, at 550°C, 500°C and 450°C were determined from the slopes of the straight lines, which equal to k_1a/x_e. By

substituting the known values of a and x_e, the rate constant k_1 was calculated to give 19.2 x 10^{-3} $sec.^{-1}$, 12.7 x 10^{-3} $sec.^{-1}$ and 6.5 x 10^{-3} $sec.^{-1}$ at the three reaction temperatures of 550°C, 500°C and 450°C, respectively. In agreement with previous observations , the rate constant increases with temperature indicating a faster reaction rate at higher reaction temperatures.

(3) Activation Energy, ΔE

The activation energy, ΔE, for a chemical reaction is given by the Arrhenius equation.

$$k_1 = C\, e^{-\Delta E/RT} \qquad \text{or,} \qquad \ln k_1 = \ln C - \frac{\Delta E}{R}\left(\frac{1}{T}\right)$$

where R is the ideal gas constant (1.987 cal/mole/ K) and C is a constant. Thus, a plot of the logarithm of the rate constant k_1 versus the inversed temperature, 1/T, produces a straight line with a slope equals to $-\Delta E/R$. The rate constants obtained at 550°C, 500°C and 450°C in Section E(2) above were then plotted against 1/T as shown in Figure XII. A straight line was drawn. The activation energy, ΔE, was then calculated from the slope of the straight line to give a value of 13.2 Kcal/mole for the hydrochlorination reaction.

(4) Rate Constant as a Function of Concentration

A set of reaction kinetics data obtained from the hydrochlorination of $SiCl_4$ and m.g. silicon metal at 100 psig, 500°C and at various $H_2/SiCl_4$ feed raios of 1.0, 2.0, 2.8, 4.0 and 4.7 was analyzed by the same theoretical treatment with the pseudo-first order rate equation. These experimental rate data were shown by the kinetic curves in Figure VI. The % $SiHCl_3$ conversions at various residence times of 10, 20, 30, 40 and 60 seconds were directly measured from the smooth kinetic curves and summarized in Table XXIV. The equilibrium composition of $SiHCl_3$, x_e, was taken at the point where the kinetic curve leveled off. The initial partial pressure of $SiCl_4$, a, was calculated from the composition of $H_2/SiCl_4$ feed and the total

pressure. These experimental rate data were applied to the pseudo-first order rate equation by plotting the logarithm of x_e/x_e-x versus the residence time t. The rate constant k_1 was calculated from the slopes of the resulting set of straight lines. Results are summarized in Table XXIV. Data in Table XXIV show that the rate constant slightly increases at a higher $H_2/SiCl_4$ feed ratio. These results suggest that the hydrochlorination of $SiCl_4$ and m.g. silicon metal proceeds at a slightly faster rate at a higher concentration of hydrogen gas.

(5) Rate Constant as a Function of Pressure

A similar theoretical treatment of the reaction kinetic data obtained from the hydrochlorination of $SiCl_4$ and m.g. silicon metal at various pressures was performed. A set of kinetic curves obtained at 500°C with a $H_2/SiCl_4$ feed ratio of 2.0 and at various pressures of 25 psig, 100 psig and 200 psig was reproduced in Figure XIII. The % $SiHCl_3$ conversions were read from the smooth kinetic curves at 10, 20, 30, 40 and 60 seconds residence time. The mole % data were converted to partial pressures for H_2, $SiHCl_3$ and $SiCl_4$. The equilibrium conversion of $SiHCl_3$ was measured at the point where the kinetic curves leveled off. The logarithm of x_e/x_e-x was calculated and plotted against the residence time t. The rate constants were calculated from the slopes of the resulting straight lines. Results are summarized in Table XXV. Two more data points on the rate constant measurements at 73 psig and at 500 psig were obtained by the same theoretical treatment. These two data points were obtained from the same hydrochlorination reaction at a slightly higher $H_2/SiCl_4$ feed ratio of 2.8 (instead of 2.0). Results in Table XXV show that the rate constant gradually decreases as a function of increasing pressure. In other words, the hydrochlorination reaction rate decreases at a higher pressure. Thus, to a certain extend, the hydrochlorination of $SiCl_4$ with hydrogen in a mass bed of m.g. silicon metal is also a diffusion-controlled process. The diffusion of reactants and products to and from the solid surfaces may also be rate-limiting.

A plausible reaction mechanism for the hydrochlorination of $SiCl_4$ and m.g. silicon metal is proposed in Section F in the following.

F. Reaction Mechanism Study

Previous experimental studies [1,3] on the hydrochlorination of $SiCl_4$ and m.g. silicon metal showed that a plausible reaction mechanism may involve two stepwise reactions,

$$SiCl_4 + H_2 \xrightleftharpoons{\text{slow}} SiHCl_3 + HCl$$

$$3\,HCl + Si \xrightleftharpoons{\text{fast}} SiHCl_3 + H_2$$

The hydrogenation of a Si-Cl bond by hydrogen to form $SiHCl_3$ and HCl was postulated as the slow, rate-determining step. The reaction of HCl with silicon is a well-known reaction which occurs rapidly at about 350°C. At the hydrochlorination reaction temperature of 500°C, the HCl + Si reaction is expected to go very fast. Based on this postulated mechanism, one may propose an activation process involving hydrogen and $SiCl_4$ to form an activated complex species which, through one or more reaction pathways, produces the product $SiHCl_3$. A experimental study was thus proposed to replace hydrogen with deuterium isotope in the hydrochlorination reaction. A positive kinetic isotope effect will not only produce the needed experimental evidence to prove the mechanism, but also, it provides informations on the nature of the activated complex. Kinetic isotope effect is a powerful tool to study reaction mechanism. It provides useful infromations on the activation process and on the nature of the activated complex at the molecular level.

(1) The Quartz Hydrochlorination Reactor

The two inch-diameter stainless steel reactor is primarily designed to study the hydrochlorination reaction under pressure. With a large internal volume and large size storage tanks, this apparatus is not suitable for the planned experiments to study the deuterium kinetic isotope effects. A small, 0.75 inch-diameter

quartz reactor system was designed with a mininum volume of dead space inside the apparatus in order to conserve the relatively expensive deuterium isotope. This quartz reactor system is schematically shown in Figure XIV. The $H_2/SiCl_4$ and the $D_2/SiCl_4$ feed system is designed in such a way that either hydrogen gas or deuterium gas can be fed into the hydrochlorination reactor at any time during an experiment. This is accomplished by a 3-way ball valve arrangement as shown in Figure XIV. The cylinder pressure is reduced by a regulator to a few psig above atmospheric pressure to provide the driving force for the gaseous flow through the reactor system. The flowrate of H_2 or D_2 is controlled by a fine metering valve and measured by a calibrated flowmeter. The gas is bubbled into a liquid column of $SiCl_4$ maintained at a constant temperature. The $H_2/SiCl_4$ or $D_2/SiCl_4$ feed ratio can be readily adjusted by the $SiCl_4$ liquid temperature. The gaseous mixture is then fed into the bottom of the quartz hydrochlorination reactor. The reaction product mixture coming out of the reactor is analyzed by the in-line gas chromatograph. The small amounts of chlorosilane and hydrogen (or deuterium) gas are disposed off by venting into a scrubber. The reactor system at the right hand side of the flowmeter as shown in Figure XIV is made of Pyrex glass with the exception of the reactor tube and the heating jackets, which are made of quartz (Vycor). The H_2- $D_2/SiCl_4$ feed system and the reactor assembly are formed into a single piece of glassware by standard glass blowing technique. By keeping the dead space inside the apparatus small, the residual gas inside the reactor can be readily flushed out with a mininum amount of deuterium gas. With this design feature, one can switch deuterium from hydrogen and vice versa for every data point in the reaction kinetic measurements. Past experience has shown that one can get a better reproducible data point measured within the span of a single experiment than that obtained in two separated experiments carried out under "identical" reaction conditions. In this way, one can accurately measure the relative reaction rates between hydrogen and

deuterium in the hydrochlorination reaction. The in-line gas chromatograph is calibrated for the analysis of the deuterated product, $SiDCl_3$. The sensitivity factor (or response factor) for the G.C. analysis was determined with a pure sample of $SiDCl_3$. Results of the G.C. calibration showed that the sensitivity factor for $SiDCl_3$ is essentially the same as that of $SiHCl_3$ within experimental error. This is not unexpected in view of the very close physical properties between $SiHCl_3$ and $SiDCl_3$.

(2) Deuterium Kinetic Isotope Effects

A series of experiments was carried out at 450°C and at atmospheric pressure (15 psia) with a $H_2/SiCl_4$ or $D_2/SiCl_4$ feed ratio of 2.0. The $SiCl_4$ liquid temperature in the feed assembly (see Figure XIV) was kept at 27°C. The vapor pressure of $SiCl_4$ at this temperature is 253 mmHg (1/3 of an atmosphere). At one atmosphere (760 mmHg), the feed ratio of $H_2/SiCl_4$ and $D_2/SiCl_4$ became 2.0. Hydrogen gas was first fed into the quartz reactor; starting with a slower feedrate and then gradually increased to a higher feedrate. At each hydrogen gas feedrate, several analyses for the reaction product composition were made by the in-line gas chromatograph until two or more consecutive analyses agreed within ± 2%. The hydrogen gas was then switched to deuterium gas. The feedrate of D_2 was adjust to give the same feedrate as the last hydrogen experiment. After the system had stabilized and after the hydrogen gas was completely displaced by the deuterium gas, several G.C. analyses were made on the reaction product mixture until two or more consecutive analyses agreed within ± 2%. Afterwards, the deuterium gas was switched back to hydrogen. A new,higher feedrate of hydrogen was selected for another data point in the reaction kinetic measurements. After the hydrogen experiment was completed, the same measurement was repeated with deuterium. Results of these reaction kinetic measurements with hydrogen and deuterium in the hydrochlorination reaction are summarized in Table XXVI. Data in Table XXVI show

that the % conversion of $SiHCl_3$ and $SiDCl_3$ at various residence times are essentially the same within experimental error. The reaction kinetic data in Table XXVI are also presented in Figure XV by plotting the % $SiHCl_3$ conversion and the % $SiDCl_3$ conversion versus residence time. The resulting kinetic curve in Figure XV shows that there is no significant difference in the hydrochlorination reaction rate between hydrogen and deuterium.

Another series of the same experiment on the deuterium kinetic isotope effects was carried out at a lower temperature of 420°C. Results of this series of experiments are summarized in Table XXVII. As in the 450°C experiment above, data in Table XXVII show that the % $SiHCl_3$ conversion and the % $SiDCl_3$ conversion at various residence times are essentially the same within experimental error. The reaction kinetic data in Table XXVII are also plotted in Figure XV. The resulting kinetic curve in Figure XV at 420°C shows that there is no significant difference in the hydrochlorination reaction rates between hydrogen and deuterium.

(3) A Plausible Reaction Mechanism for the Hydrochlorination of $SiCl_4$ and M.G. Silicon Metal

The new experimental results on the deuterium kinetic isotope effects suggest that hydrogen is not directly involved in the rate-determining step for the hydrochlorination of $SiCl_4$ and m.g. silicon metal. This may imply that the slow, rate-limiting activation process must involve $SiCl_4$. The new experimental evidence does not necessarily invalid the previously postulated stepwise reactions [1,3] for the hydrochlorination of $SiCl_4$ and m.g. silicon metal.

$$SiCl_4 + H_2 \rightleftharpoons SiHCl_3 + HCl \qquad (5)$$

$$3\,HCl + Si \rightleftharpoons SiHCl_3 + H_2 \qquad (6)$$

The deuterium kinetic isotope effects study suggests that the hydrogenation of a Si-Cl bond by hydrogen in the above stepwise reaction is not the rate-determining step.

The reaction mechansim for the chemical vapor deposition (CVD) of silicon has been extensively studied. In the case of epitaxy from $SiCl_4$, a set of chemical reactions is proposed by Nishizawa and Nihira[8].

$$SiCl_4 + H_2 \rightleftharpoons SiHCl_3 + HCl \quad (7)$$

$$SiHCl_3 \rightleftharpoons SiCl_2 + HCl \quad (8)$$

$$SiHCl_3 + H_2 \rightleftharpoons SiH_2Cl_2 + HCl \quad (9)$$

$$SiH_2Cl_2 \rightleftharpoons SiCl_2 + H_2 \quad (10)$$

$$SiCl_4 + H_2 \rightleftharpoons SiCl_2 + 2\,HCl \quad (11)$$

$$SiCl_2 + H_2 \rightleftharpoons Si + 2\,HCl \quad (12)$$

Thermodynamic data for these homogeneous gas phass reactions (equation 7 - 12) are published by the work of Hunt and Sirtl[5]. The despostion of silicon (equation 12) is described as the reduction of $SiCl_2$ by hydrogen on the silicon surface [8]. A model based on these chemical reactions for the epitaxial growth of silicon from SiH_2Cl_2, $SiHCl_3$ and $SiCl_4$ is recently reported by J. Korec [9]. The mechanism for the deposition of silicon (Equation 12) is postulated as an initial adsorption of $SiCl_2$ at a surface vacancy followed by the surface migration of the adsrobed $SiCl_2$ to form an activated complex, $SiCl_2$-H_2*. The rate-determining step is assumed to be the chemical reaction between adsorbed $SiCl_2$ and gaseous H_2[9].

The hydrochlorination of $SiCl_4$ with hydrogen and m.g. silicon metal is basically the reverse of the chemical vapor deposition of silicon, since both systems contain the same number of elements, silicon-hydrogen-chlorine. It is conceivable that the same intermediate species, $SiCl_2$, is involved in the hydrochlorination reaction. However, a very important difference between these two processes is the reaction temperature. The hydrochlorination reaction is normally carried out at about 500°C in comparison with 1000°C - 1200°C for the CVD silicon

process. Another important factor is that the hydrochlorination of $SiCl_4$ and m.g. silicon metal is also a catalytic process. Copper has been shown to be an effective catalyst [3] for the hydrochlorination reaction. Even the metallic impurities in the m.g. silicon metal have a strong catalytic effect on the reaction. On the other hand, the much higher temperature CVD silicon process involves mostly homogeneous vapor phase reactions and non-catalyzed surface reactions. At the much lower reaction temperature of 500°C, one may expect the equilibria for the homogeneous gas phase reactions (Equation 7-11) in the CVD silicon process to lie far to the left hand side of the equation. For example, the calculations based on reported thermodynamic data by Sirtl, Hunt and Sawyer [5] show that the vapor pressure of $SiCl_2$ is less than 10^{-5} atmosphere at temperature below 600°C with a total pressure of one atmosphere and a Cl/H ratio of 1.0. In contrast, the concentration of $SiCl_2$ approaches that of $SiHCl_3$ in the same reaction system at 1100°C. Thus, it is very unlikely that the homogeneous gas phase reaction of $SiCl_4$ and H_2 is the source of $SiCl_2$ for the hydrochlorination reaction at 500°C. Another plausible reaction pathway to $SiCl_2$ at lower temperatures is the reaction of $SiCl_4$ with Si on the silicon metal surface.

$$SiCl_4 + Si \rightleftharpoons 2\ SiCl_2 \qquad (13)$$

This reaction is proposed by Bloem, Claassen and Valkenbury[10] to supplement the formation of $SiCl_2$ on the silicon surface in the epitaxy from $SiCl_4$ at 900°C, since the homogeneous vapor phase formation of $SiCl_2$ falls off rapidly below 1000°C. The reaction of $SiCl_4$ and Si (Equation 13) is also the basic reaction for the etching effect produced by $SiCl_4$ on a silicon surface in an inert ambient (e.g. helium to replace hydrogen). $SiCl_4$ attacks silicon, giving volatile $SiCl_2$. This etching effect is exactly the opposite to the CVD silicon process, whereby silicon is consumed.

One may propose a similar reaction mechanism for the hydrochlorination reaction in which the reactive intermediate $SiCl_2$

is formed by the adsorption of $SiCl_4$ at the catalytic sites on the silicon metal surface. The activation of $SiCl_4$ at the catalytic site to form $SiCl_2$ may be postulated as the slow, rate-determining step. This catalytic reaction may account for the much lower reaction temperature (500°C) needed for the hydrochlorination of $SiCl_4$ and m.g. silicon metal. The subsequent reaction of $SiCl_2$ with HCl and H_2 produces the observed reaction products, $SiHCl_3$ and SiH_2Cl_2. A plausible reaction mechanism is summarized in the following.

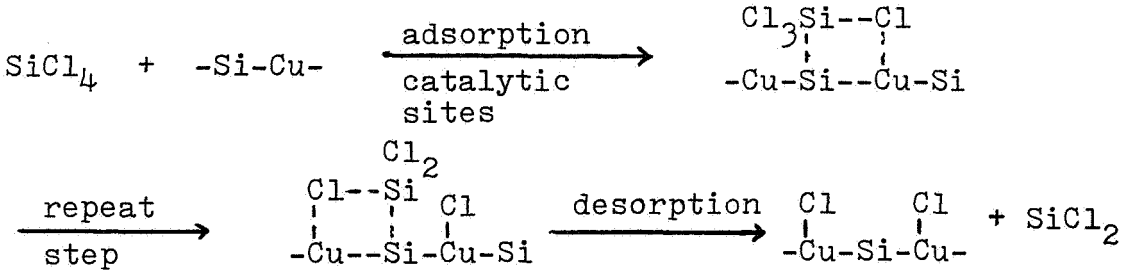

followed by,

$$2\ \text{-Si-Cu-Cl} + H_2 \rightleftharpoons 2\ \text{-Si-Cu} + 2\ HCl$$

$$3\ HCl + Si \longrightarrow SiHCl_3 + H_2$$

$$SiCl_2 + HCl \longrightarrow SiHCl_3$$

$$SiCl_2 + H_2 \longrightarrow SiH_2Cl_2$$

$$SiH_2Cl_2 + HCl \rightleftharpoons SiHCl_3 + H_2$$

At 500°C, the reaction of $SiCl_2$ with HCl and H_2 to form $SiHCl_3$ and SiH_2Cl_2 is very favorable.

The above reaction mechanism can conceivably explain the experimental results observed on the hydrochlorination of $SiCl_4$ and m.g. silicon metal to form $SiHCl_3$. The pseudo-first order kinetics is postulated by a slow, rate-determining adsorption of $SiCl_4$ at a catalytic site on the silicon metal surface. The activation process produces the reactive intermediate $SiCl_2$ which subsequently reacts with H_2 and HCl to form $SiHCl_3$.

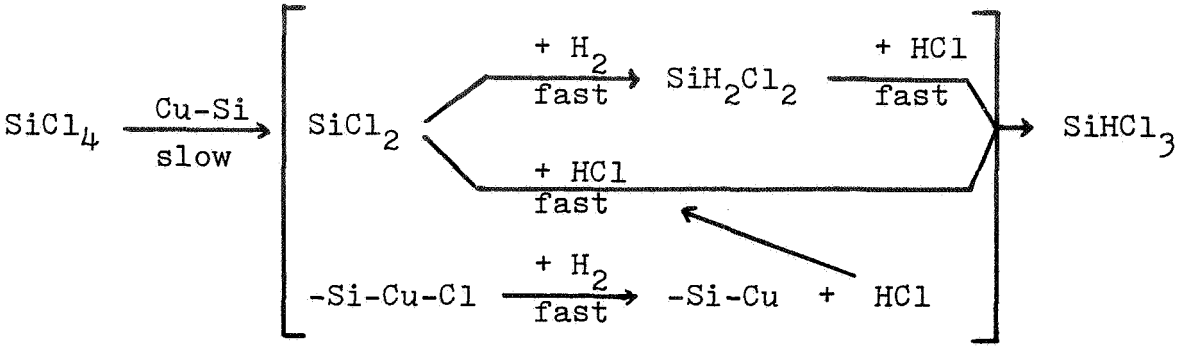

The overall reaction,

$$SiCl_4 \underset{k_{-1}}{\overset{k_1}{\rightleftharpoons}} SiHCl_3$$

accounts for the observed pseudo-first order kinetics. Also, the rate-determining step involves $SiCl_4$ and silicon but not hydrogen. This reaction mechanism can account for the experimentally observed negative deuterium kinetic isotope effects. The moderate pressure effect on the reaction rate also suggested that the hydrochlorination of $SiCl_4$ in a mass bed of m.g. silicon metal is diffusion-controlled to a certain extent. For example, the pseudo-first order rate constant k_1 is reduced by a factor of about two (see last column of Table XXV) with an increase of pressure from 25 psig to 500 psig. A diffusion-controlled kinetics is operative when the rate-determining reaction step occurs faster than the rate of diffusion of the reactants and/or products to and from the solid surfaces. In view of the relatively small change in the reaction rate over such a wide pressure range, the hydrochlorination of $SiCl_4$ in a mass bed of m.g. silicon metal is not very strongly influenced by these diffusion and mass transfer parameters.

G. Corrosion Study

At elevated temperatures, HCl is producted in variable amounts in the silicon-hydrogen-chlorine system. A small amount of HCl was detected and measured in the reaction mixture obtained from the hydrochlorination of $SiCl_4$ and m.g. silicon metal at 500°C, 300 psig with a $H_2/SiCl_4$ feed ratio of 2.0. Results of these HCl analyses are summarized in

Table XXVIII. The small amounts of HCl (0.1 - 0.5%) are in fairly good agreement with the calculated equilibrium concentration of HCl for the silicon-hydrogen-chlorine system in the publication by Sirtl, Hunt and Sawyer[5]. The operating temperature of 500°C and above for the hydrochlorination reaction is a concern for the reactor constructed with conventional metal alloys. Metals and alloys offer little or no resistance to high concentrations of HCl gas at temperature above 450°C [11]. Under these conditions, the usual oxide protective film on the metal surface is replaced by a metal chloride film. The covalent nature of the metal chlorides exhibits a much higher vapor pressure than those of their oxide counterparts. At elevated temperatures, the metal chloride film begins to evaporate off. Corrosion becomes a serious problem as the material of construction of the reactor is constantly removed from the reactor wall as metal chlorides.

Contradiction to this corrosion mechanism was noted in a previous corrosion study [3]. The corrosion study on Incoloy 800H showed that a silicide protective film was formed on the metal surface. A metal chloride film did not appear to involve under the hydrochlorination reaction enviroment. The corrosion study is further expanded to include a variety of metals and alloys. The objective of the present experimental work is to provide a basic understanding on the mechanism of corrosion inside the hydrochlorination reactor and to evaluate a variety of metal alloys as the material of construction for the hydrochlorination reactor.

(1) Corrosion Test Results

Samples of material of construction for the hydrochlorination reactor were prepared for the corrosion test. Materials include nickel, copper, Alloy 400 (Monel), carbon steel, Type 304 stainless steel, Incoloy 800H and Hastelloy B-2. The approximate compositions of these alloys are given in Table XXIX. The test samples were weighed and their total surface area measured. They were mounted on a stainless steel rack which was

fitted inside the two inch-diameter hydrochlorination reactor tube. In this manner, all the test samples would be exposed to the same reaction enviroment throughout the corrosion test. The reactor was charged 862 grams of m.g. silicon metal (32 mesh x dust) to form a mass bed of about 18 inches high. All the test samples were buried in the silicon metal during the entire corrosion test experiment.

The corrosion test was carried out at a reactor pressure of 300 psig, temperature of 500°C and a $H_2/SiCl_4$ feed ratio of 2.0 for a total of 87 hours. After 87 hours of the hydrochlorination reaction, the test samples were removed from the reactor. Each of the test samples was cleaned and re-weighed with an analytical balance. Results of these weigh data are summarized in Table XXX. As the results in Table XXX show, all the corrosion test samples achieve a gain in weigh. The weigh gain is due to the chemical vapor deposition of silicon from the reverse hydrochlorination reaction. Interestingly, the weigh gain per unit surface area (last column in Table XXX) varies greatly between different metals and alloys. The deposited silicon penetrates the alloy body to form a silicide film. The weigh gain per unit surface area data also qualitatively show how much and how far the deposited silicon penetrates the alloy body.

The thickness of the silicide protective film formed under the hydrochlorination reaction enviroment after 87 hours was measured for each of the test samples. The corrosion test samples were embedded in a mold of epoxy resin. A cross section of the samples was prepared. The thickness of the silicide deposits on the metal alloy surface was measured under a microscope. Several measurements were made on the cross section of the silicide deposits to give an average value. Results are summarized in Table XXXI. The growth rates of the silicide film based on the 87 hour test were calculated and listed in the last column in Table XXXI. The growth rate in mils/year was calculated to give a convenient, practical

number to show approximately the extend of silicon penetration into the alloy body. This calculation does not imply a linear (or a non-linear) growth rate of the silicide film. The important result obtained from the corrosion test is that alloys such as stainless steel, Incoloy 800H and Hastelloy B-2 show a very slow growth of the silicide film at a projected rate of about 30 to 50 mils/year. Eventhough these projected growth rates are not very accurate, the rather slow rate of silicon penetration into the alloy body suggests that these alloys are reasonable choice as the material of construction for the hydrochlorination reactor.

(2) Scanning Electron Microscopy

The silicide protective film on nickel, Alloy 400 and Incoloy 800H test sample was analyzed by a Scanning Electron Microscope (SEM). Carbon was used to coat the sample surface in the standard sample preparation for the SEM analysis. In Figure XVI, the SEM photographs show the surface morphology of the silicide film on the pure nickel sample at 500, 1900 and 5000 magnifications. These photographs show particles of the order of 3 to 10 microns on the surface of the silicide deposits. There appears to be two types of particles, one type has a rather smooth surface and the other type has a laminated structure. Spot analysis by the x-ray microprobe and EDAX of the smooth particles showed an atomic composition of 47.5% Si and 52.5% Ni. This composition corresponds approximately to a nickel-silicon phase NiSi. Aanlysis of the other type of particles having a laminated structure showed an atomic composition of 96.2% Si and 3.8% Ni. Thus, these particles appear to be pure silicon deposited from the reverse hydrochlorination reaction, since the known metallic impurities, such as iron and aluminum, in the m.g. silicon metal are absent from the SEM analysis. Furthermore, the m.g. silicon metal particles from the mass bed are too large to account for the 3 to 10 micron size particles on the silicide film surface. The surface morphology of the silicide film appears to indicate that an initial chemical vapor

deposition of silicon from the reverse hydrochlorination reaction is followed by the combination of the deposited silicon with the base metal to form nickel-silicon phases, NiSi.

A cross section of the test sample was cut and polished for the SEM analysis. Figure XVII shows the SEM photographs of a cross sectional area of the nickel test sample. A well-defined layer of the silicide deposit is seen on both sides of the nickel base metal. At a higher magnification (500 X), the silicide film shows a rather porous structure with many void spaces . This porous structure is charateristic of a silicon deposit obtained from a CVD process carried out at high deposition rates. The composition of the silicide film was analyzed by the X-ray microprobe and the EDAX analyzer. Figure XVIII shows that X-ray distribution maps of silicon and nickel as well as the EDAX analysis on four different areas of a cross sectional area of the nickel test sample. The X-ray map of silicon shows a rather uniform distribution of Si throughout the cross section of the silicide film. Similarly, the nickel X-ray distribution shows a rather uniform distribution of Ni throughout the silicide film. There does not appear to be a gradual decrease in the silicon concentration across the silicide film-nickel base metal boundary. The silicide film on the nickel test sample is well-defined. The X-ray microprobe and EDAX analyses at the four different areas of the cross section of the test sample are also summarized in Figure XVIII. Results show that the bulk of the silicide film has the atomic composition of 40% to 50% Si with the balance being Ni. This composition corresponds to the nickel-silicon phases, Ni_3Si_2 (m.p. 964°C) and NiSi (m.p. 992°C), which are the most stable nickel-silicon phases having the lowest melting points.

Another analysis on the Alloy 400 test sample was made by the Scanning Electron Microscope. Figure XIX shows the SEM photographs of the surface of the silicide protective film on Alloy 400 at various magnifications. The surface morphology also has a rather porous structure. However, the appearance of

of the silicide film surface is quite different from that of the nickel test sample (Figure XVI).This porous structute is also seen in the SEM photograph of a cross sectional area of the silicide film in Figure XX. The X-ray distribution maps of nickel, copper and silicon in Figure XX show some interesting results. The copper X-ray distribution map shows a copper-rich zone at the surface of the silicide film and at the surface of the base alloy. On the other hand, the nickel X-ray distribution map shows that nickel is depleted at the surface of the base alloy where the copper concentration is enriched. The segregation of copper and nickel in the silicide film is in contrast to the rather uniformally distributed nickel and copper concentrations in the alloy body. The X-ray microprobe and the EDAX analysis on the four different areas at the cross section of the silicide film also confirms the segregation of copper and nickel in the silicide film. Results are summarized in Figure XXI. The atomic composition of Area #1 near the surface of the silicide film shows a high concentration of copper (52.22%). The nickel concentration in Area #1 (11.22%) is low in comparison with those in Area #2 (48.42%) and in Area # 3 (55.31%) at the middle section of the silicide film. In the middle section, the copper concentrations are low (Area #2, 9.24% and Area #3, 3.99%) in comparison with that of Area #1 (52.22%). On the other hand, the silicon concentrations are relatively uniform in these three areas: Area #1, 36.55%; Area #2, 40.88% and Area #3,38.77%. The base alloy (Area #4) has the atomic composition of about 61% nickel and 35% copper in good agreement with the specific composition of Alloy 400.

The Scanning Electron Microscopic analysis on the Incoloy 800H test sample shows a complex silicide protective film. The Incoloy 800H test sample was obtained from a previous corrosion study carried out at the Massachusetts Institute of Technology[3]. The corrosion test on this sample was carried out under similar reaction conditions at 500°C, 300 psig and $H_2/SiCl_4$ ratio of 2.0 but for a longer duration of 238 hours. The SEM photograph of a cross sectional area of the Incoloy 800H sample is shown

in Figure XXII. The SEM photograph shows a well-defined silicide deposit which is slightly broken off from the base alloy. The test sample has been briefly exposed to the atmosphere. The action of moisture on the reactive silicide film may cause the breakage. Analysis by the X-ray microprobe and EDAX was carried out at four different areas of the cross section of the Incoloy 800H test sample. The atomic compositions of silicon, iron, nickel and chromium at these four different areas are summarized in Figure XXII. Results show a high degree of segregation of these elements at different locations of the silicide film. This is also seen in the X-ray distribution maps of Si, Fe, Ni and Cr of the same cross sectional area as the SEM photograph in Figure XXII. These X-ray distribution maps are presented in Figure XXIII. It is interesting to note that the the X-ray distribution maps of iron, nickel and chromium show a rather uniform distribution of the elements in the Incoloy 800H alloy body. However, these elements are highly segregated and concentrated at different areas of the silicide film. In contrast to the Alloy 400 test sample, the silicon is also highly segregated in different area of the silicide film on the Incoloy 800H sample. Results of the SEM analysis appear to indicate that the rather uniformally distributed iron, nickel and chromium in the alloy body are broken up and segregated in their combination with the deposited silicon to form various metal-silicon phases. The mechanism on the formation of the silicide protective film is discussed in Section G(3) in the following.

(3) Corrosion Mechanism Inside The Hydrochlorination Reactor

a. Chemical Process

The deposition of silicon on the metal alloy surface may be postulated as the result of a chemical vapor deposition process from the reverse hydrochlorination reaction.

$$4\ SiHCl_3 \rightleftharpoons 3\ SiCl_4 + 2\ H_2 + Si$$

At the start of the hydrochlorination reaction, the activity (concentration) of silicon on the metal surface is zero. As the reaction proceeds, silicon is deposited until the activity of Si on the metal surface reaches at steady state concentration. A dynamic equilibrium exists between the silicon on the metal surface and the reaction mixture in the gas phase. The forward hydrochlorination reaction can consume the deposited silicon on the metal surface. However, as silicon is consumed, the reduced activity of silicon causes the hydrochlorination reaction to re-deposit silicon on the metal surface until an equilibrium concentration is again reached. Although HCl is known to be highly corrosive to metals and alloys at temperature above 450°C, the concentration of HCl in the hydrochlorination reactor is very small. The gas phase contains approximately 0.03 - 0.1 % HCl under normal operating conditions. At 500°C, HCl can certainly attack the silicide protective film. However, the reaction will be slow because of its low concentrations. Furthermore, HCl is more reactive toward Si than the metals, Fe, Ni and Cr. HCl is most likely consumed to form $SiHCl_3$ and $SiCl_4$ which are far more volatile than those of $FeCl_2$, $NiCl_2$ and $CrCl_3$. As Si is reacted away by HCl, the reverse hydrochlorination reaction re-deposits silicon to restore its equilibrium concentration on the silicide film surface. Results of the corrosion test show no loss of materials from the samples. Therefore, one may conclude that there is no significant corrosion of metals and alloys inside the hydrochlorination reactor due to chemical reactions.

(b) Physical Process

If the silicide protective film is produced by the chemical process alone, one would expect only a very thin deposit on the metal surface, since a chemical reaction on a solid surface does not normally involve surface atoms more than 10 to 20 atomic layers deep. Once a steady state equilibrium is reached, the silicide film shall stop growing. Results of the corrosion tests show that this is certainly not the case. Therefore, other physical process must be operative in order to account for the

continuous growth of the silicide film on the metal alloy surface. At the rather high reaction temperature of 500°C, a thermal diffusion process of silicon to form metal-silicon phases may be postulated. In the case of nickel and copper, some metal-silicon phases are formed at relatively low temperatures, e.g., Cu_3Si (558°C, 802°C), Ni_3Si_2 (845°C, 964°C) and NiSi (992°C). Thus, the continuous diffusion of silicon into the metal alloy body to from the various metal-silicon phases may be postulated as the mechanism for the continuous growth of the silicide film in the hydrochlorination reaction enviroment. The continuous growth of the silicide film to a thick scale after long periods of operation of the hydrochlorination reactor constitutes a potential corrosion of the reactor wall. A thick scale can weaken the reactor wall. Fortunately, some alloys are highly resistant to scale growth.

The corrosion test results in Table XXXI show very high growth rate of the silicide film on pure metals, nickel and copper. Carbon steel which is basically iron also has a high growth rate. Interestingly, the growth rate of an alloy of nickel and copper, Alloy 400 (2/3 Ni and 1/3 Cu at 90 mils/year), is much slower than those of the pure metals, nickel (435 mils/year) and copper (451 mils/year). A plausible explanation is that there are metal-metal phases in an alloy. As silicon is deposited onto the metal surface, the metal combines with silicon to form metal-silicon phases. In the case of nickel and copper, the corrosion test results appear to indicate that the most stable form of nickel-silicon and copper-silicon phases are produced in the course of the thermal diffusion process. In the case of Alloy 400, the nickel-copper phases in the alloy must be broken up in order to form the nickel-silicon and the copper-silicon phases. Thus, the extra energy required may explain the slower growth rate of the silicide film on Alloy 400 in comparison with those of pure nickel and copper.

One may apply the same argument for the multi-component alloy system, such as, stainless steel, Incoloy 800H and

Hastelloy B-2 to account for the still slower growth of the silicide film on these alloys. However, there is another factor involved in the thermal diffusion process. Stainless steel, Incoloy 800H and Hastelloy B-2 contain a third metallic element, chromium (m.p. 1890°C) and molybdenum (m.p. 2620°C), which has a melting temperature much higher than those of silicon (m.p. 1420°C), nickel (m.p. 1455°C), copper (m.p. 1083°C) and iron (m.p. 1535°C). The corresponding chromium-silicon and molybdenum-silicon phases are also form at a much higher temperature than those of nickel and copper, viz., $CrSi_2$ (1550°C), CrSi (1600°C), $MoSi_2$ (1870°C) and Mo_3Si (2190°C). The silicide films on stainless steel, Incoloy 800H and Hastelloy B-2 do not necessarily contain these discrete Cr-Si and Mo-Si phases. The generalization is that a higher temperature is needed to alloy silicon with Cr and Mo than those of nickel and copper. Consequently, stainless steel, Incoloy 800H and Hastelloy B-2 are the most resistant to scale growth.

(4) Optimum Material of Construction for the Hydrochlorination Reactor

The present experimental study on the subject of corrosion is primarily concerned with what happens to the metal reactor in the hydrochlorination reaction enviroment. There are other forms of corrosion which must be taken into account in selecting the proper material of construction for the hydrochlorination reactor. In fact, potential problems should be traced all the way back to the manufacturing process of the alloy which must meet the desired metallurgical specifications. The mechanical and thermal process (forming, welding, etc.) which fabricates the alloy to form the piece of equipment can alter the property of the alloy. A classical example of the potential corrosion problem is the "sensitization" of austenitic stainless steel. The sensitization may be resulted from an uncontrolled thermal cycle, such as, in a welding process. Precipitation of chromium carbide ($Cr_{23}C_6$) can deplete the chromium at the grain boundary. The net result is a sharp reduction in the alloy's resistance to chemical attack.

Contamination of foreign material in the testing procedure, storage and transportation of the equipment could be another potnetial problem area. The atmospheric enviroment in which the reactor is installed is an important factor in selecting the proper material of construction. The atmospheric enviroment inside a chlorosilane processing plant may be considered as corrosive. The presence of acid chlorides, HCl and chlorosilane vapor contribute to the corrosive nature of the enviroment. Interaction of these acidic chlorides with moisture in the atmosphere produces a strong acid. "Chloride Stress Corrosion Crack" is a serious corrosion problem in the presence of a high level of chloride in the enviroment. Austenitic stainless steels are particularly sensitive to this type of structural failure which is generally believed to be the result of a transgranular attack by chloride accelerated by internal stress. The operating temperature of 500°C and above will also subject the outside wall of the hydrochlorination reactor to a high temperature enviroment. Oxidation and the presence of potentially corrosive contaminant (chloride, etc.) at these high temperatures represent still another potential corrosion of the hydrochlorination reactor. After the reactor has been in operation, there will be periods of shutdown for service and repair. Exposure of the inside wall of the reactor to air and moisture can readily destroy the silicide protective film. Hydrolysis of residual metal chlorides and chlorosilanes produces a strong acid which can further corrode the exposed metal alloy.

Pure nickel and copper used in the corrosion study are primarily for theoretical interest. Pure metals are generally not very good material of construction, which is characterized by poor mechanical strength. In the case of carbon steel, the prospect of forming a thick silicide scale is a potentially serious corrosion problem. Furthermore, in the presence of hydrogen gas at high temperature and pressure, hydrogen embrittlement is potentially another serious corrosion problem for carbon steel. Although carbon steel is a low-cost material

of construction, it does not appear to be a suitable material of construction for the hydrochlorination reactor. Stainless steel, Incoloy 800H and Hastelloy B-2 produce a stable silicide protective film on the metal surface. The silicide film does not penetrate deeply into the base metal at a rapid rate to form a thick scale. These alloys also show good resistence to the other forms of corrosion such as those in a high chloride level and high temperature oxidative enviroments. Although at a lower cost, stainless steel is somewhat less satisfactory as the material of construction for the hydrochlorination reactor, since it is more susceptable to chloride strss corrosion crack. In general, the type of alloys with high Ni, Cr and Mo contents similar to those of stainless steel, Incoloy 800H and Hastelloy B-2 are suitable material of construction for the hydrochlorination reactor.

Finally, there is the important element of cost. The cost of the base metal alloy, the cost of fabrication and the cost of repair are important factors in selecting the optimum material of construction for the hydrochlorination reactor. In general, the higher the nickel, chromium and molybdenum contents in a given alloy, the better is its corrosion resistance properties but also at a higher price. Therefore, the optimum material of construction for the hydrochlorination reactor is the choice of a good compromise between the performance of the piece of equipment and the cost of building it.

IV. CONCLUSIONS

The research and development work carried out under the JPL Contract No. 956061 at Solarelectronics, Inc. has fulfilled all the program objectives. The expanded study on the hydrochlorination of $SiCl_4$ and m.g. silicon metal carried out over a wide range of temperature, pressure and concentration has provided the basic reaction kinetic data for the hydrochlorination process. The hydrochlorination reaction has been shown

to be an efficient process for the production of $SiHCl_3$. The process can be operated under a wide range of practical reaction conditions. The corrosion study has shown that conventional alloys, such as stainless steel, Incoloy 800H and Hastelloy B-2, are suitable material of construction for the hydrochlorination reactor.

A theoretical study on the hydrochlorination of $SiCl_4$ and m.g. silicon metal to $SiHCl_3$ has been completed. A rate equation has been developed to describe the experimental kinetic data for the hydrochlorination reaction. The equilibrium constant and the rate constant are measured as a function of temperature, pressure and concentration. Thermodynamic functions for the hydrochlorination reaction are measured. A plausible reaction mechanism has been postulated and proposed. The experimental study has provided a basic understanding on the hydrochlorination reaction. The corrosion study has also provided a basic understanding on the mechanism of corrosion of metals and alloys in the hydrochlorination reaction enviroment.

V. RECOMMENDATIONS

The reaction kinetic measurements on the hydrochlorination of $SiCl_4$ and m.g. silicon metal have shown that the highest practical reaction temperature and pressure are desirable to maxinum conversion to $SiHCl_3$. Additional corrosion data on metals and alloys under the hydrochlorination reaction enviroment at temperature above 500°C are very useful informations for the reactor design. Recommendations for further experimental study on the subject of corrosion may include,

- Time dependency on the growth rate of the silicide protective film as a function of time,
- Growth rate of the silicide film as a function of temperature,

- Corrosion measurements at temperature above 500°C,
- Upper temperature limit on selected alloys at which corrosion becomes excessive.

VI. REFERENCES

(1) Final Report, JPL Contract No. 954334, "Feasibility of the Silane Process for Producing Semiconductor-Grade Silicon", Union Carbide Corporation, June 1979.

(2) Quarterly Reports, JPL Contract No. 955533, "Development of a Polysilicon Process Based on Chemical Vapor Deposition", Hemlock Semiconductor Corporation, 1979 - 1982.

(3) Final Report, JPL Contract No. 955382, "The Hydrogenation of $SiCl_4$" by Jeffrey Y. P. Mui and Dietmar Seyferth, Massachusetts Institute of Technology, April 15, 1981.

(4) R. F. Lever, "The Equilibrium Behavior of the Silicon-Hydrogen-Chlorine System", IBM Journal, p. 460, September, 1964.

(5) L. P. Hunt and E. Sirtl, J. Electrochem., p. 1741, Vol. 119 1972.

E. Sirtl, L. P. Hunt and D. H. Sawyer, J. Electrochem., p. 919, Vol. 121, 1974.

(6) O. Ruff and K. Albert, "Unber das Silicium Chloroform", Chem. Ber., p. 2222, Vol. 38, 1905.

(7) R. J. H. Voorhoeve and J. C. Vlngter, J. Catalysis, p. 123, Vol. 4, 1965.

(8) J. Nishizawa and H. Nihira, J. Crystal Growth, p. 82-89, Vol. 45, 1978.

(9) J. Korec, J. Crystal Growth, p. 32-44, Vol. 61, 1983.

(10) J. Bloem, W. A. P. Claassen and W. G. J. N. Valkenburg, J. Crystal growth, p. 177-184, Vol. 57, 1982.

VII. APPENDICES

Table I through Table XXXI, Figure I through XXIII.

5f

TABLE I

THE HYDROCHLORINATION OF $SiCl_4$ AND M.G. SILICON METAL AT 25 PSIG, 450°C AND $H_2/SiCl_4$ FEED RATIO OF 2.0

Sample No.	Hydrogen Feedrate SLM (1)	Residence Time Second	Product Composition, Mole % SiH_2Cl_2	$SiHCl_3$	$SiCl_4$
1	0.37	81.9	0.09927	15.98	83.92
2	0.37	81.9	0.08745	16.13	83.78
3	0.55	55.1	0.1071	15.37	84.52
4	0.55	55.1	0.1458	15.52	84.33
5	0.88	34.4	0.09545	14.72	85.18
6	0.88	34.4	0.1098	14.96	84.93
7	1.17	25.9	0.07396	14.32	85.61
8	1.17	25.9	0.08641	14.31	85.60
9	1.48	20.5	<0.05	13.70	86.30
10	1.48	20.5	<0.05	13.77	86.23
11	1.89	16.0	<0.05	12.98	87.02
12	1.89	16.0	<0.05	13.11	86.89

(1) SLM, Standard Liter per Minute

TABLE II

THE HYDROCHLORINATION OF $SiCl_3$ AND M.G. SILICON METAL AT 100 PSIG, 450° C AND $H_2/SiCl_4$ FEED RATIO OF 2.0

Sample No.	Hydrogen Feedrate SLM	Residence Time Second	Product Composition, Mole % SiH_2Cl_2	$SiHCl_3$	$SiCl_4$
1	0.5	179	0.3040	19.74	79.95
2	0.5	179	0.3119	20.13	79.56
3	1.1	81.4	0.2515	18.24	81.51
4	1.1	81.4	0.2525	18.60	81.15
5	2.1	42.6	0.1764	15.47	84.35
6	2.1	42.6	0.2408	15.42	84.33
7	4.2	21.3	< 0.05	12.47	87.52
8	4.2	21.3	< 0.05	11.72	88.28

TABLE III

THE HYDROCHLORINATION OF $SiCl_4$ AND M.G. SILICON METAL AT 150 PSIG, 450°C AND $H_2/SiCl_4$ FEED RATIO OF 2.0

Sample No.	Hydrogen Feedrate SLM	Residence Time Second	Product Composition, Mole % SiH_2Cl_2	$SiHCl_3$	$SiCl_4$
1	0.67	183	0.6027	23.64	75.73
2	0.67	183	0.5873	23.90	75.51
3	1.02	120	0.4889	22.04	77.47
4	1.02	120	0.4401	22.09	77.47
5	1.57	78.1	0.3653	19.45	80.15
6	1.57	78.1	0.2910	18.94	80.77
7	2.35	52.2	0.2729	16.91	82.81
8	2.35	52.2	0.1756	17.17	82.66
9	3.8	32.3	0.1191	13.47	86.41
10	3.8	32.3	0.09731	13.21	86.69

TABLE IV

THE HYDROCHLORINATION OF $SiCl_4$ AND M.G. SILICON METAL AT 200 PSIG, 450° C AND $H_2/SiCl_4$ FEED RATIO OF 2.0

Sample No.	Hydrogen Feedrate SLM	Residence Time Second	Product Composition, Mole % SiH_2Cl_2	$SiHCl_3$	$SiCl_4$
1	0.86	198	0.6480	25.94	73.41
2	0.86	198	0.7101	26.05	73.24
3	1.25	136	0.4718	24.61	74.92
4	1.25	136	0.4971	24.16	75.34
5	1.96	86.9	0.3052	20.03	79.66
6	1.96	86.9	0.2842	20.29	79.43
7	2.65	64.3	0.2192	17.98	81.80
8	2.65	64.3	0.2380	17.61	82.16
9	4.05	42.0	0.1724	14.82	85.01
10	4.05	42.0	0.08395	15.07	84.85

TABLE V

THE HYDROCHLORINATION OF $SiCl_4$ AND M.G. SILICON METAL AT 25 PSIG, 500° C AND $H_2/SiCl_4$ FEED RATIO OF 2.0

Sample No.	Hydrogen Feedrate SLM (1)	Residence Time Second	Product Composition, Mole % SiH_2Cl_2	$SiHCl_3$	$SiCl_4$
1	0.38	73.8	0.1684	18.16	81.67
2	0.38	73.8	0.1483	18.13	81.73
3	0.55	51.0	0.1354	17.89	81.97
4	0.55	51.0	0.1373	17.88	81.98
5	0.82	34.2	0.1841	17.43	82.39
6	0.82	34.2	0.1389	17.63	82.23
7	1.48	18.9	0.1639	16.96	82.87
8	1.48	18.9	0.1312	17.05	82.82
9	2.10	13.4	0.1022	16.41	83.49
10	2.10	13.4	0.1091	16.40	83.49

(1) SLM, Standard Liter per Minute

TABLE VI

THE HYDROCHLORINATION OF $SiCl_4$ AND M.G. SILICON METAL AT 100 PSIG, 500° C AND $H_2/SiCl_4$ FEED RATIO OF 2.0

Sample No.	Hydrogen Feedrate SLM	Residence Time Second	Product Composition, Mole % SiH_2Cl_2	$SiHCl_3$	$SiCl_4$
1	0.6	137	0.4614	22.90	76.64
2	0.6	137	0.4954	22.77	76.74
3	1.2	68.5	0.4091	21.97	77.62
4	1.2	68.5	0.3854	22.08	77.54
5	2.4	34.3	0.3316	20.53	79.13
6	2.4	34.3	0.3203	20.46	79.22
7	4.8	17.1	0.2423	18.20	81.56
8	4.8	17.1	0.2068	17.62	82.17

TABLE VII

THE HYDROCHLORINATION OF $SiCl_4$ AND M.G. SILICON METAL AT 150 PSIG, 500°C AND $H_2/SiCl_4$ FEED RATIO OF 2.0

Sample No.	Hydrogen Feedrate SLM	Residence Time Second	Product Composition, Mole % SiH_2Cl_2	$SiHCl_3$	$SiCl_4$
1	0.65	173	0.7586	27.47	71.77
2	0.65	173	0.7333	27.65	71.62
3	0.98	115	0.7298	26.85	72.42
4	0.98	115	0.7043	26.39	72.90
5	1.43	78.6	0.5694	24.37	75.06
6	1.43	78.6	0.4978	24.39	75.11
7	2.1	53.5	0.3594	22.48	77.16
8	2.1	53.5	0.4680	22.72	76.81
9	3.3	34.1	0.3718	19.14	80.49
10	3.3	34.1	0.3366	19.02	80.64

TABLE VIII

THE HYDROCHLORINATION OF $SiCl_4$ AND M.G. SILICON METAL AT 200 PSIG, 500° C AND $H_2/SiCl_4$ FEED RATIO OF 2.0

Sample No.	Hydrogen Feedrate SLM	Residence Time Second	Product Composition, Mole % SiH_2Cl_2	$SiHCl_3$	$SiCl_4$
1	0.82	190	0.7714	30.77	68.46
2	0.82	190	0.8315	30.67	68.50
3	1.24	126	0.8581	29.85	69.30
4	1.24	126	0.8830	30.05	69.06
5	1.82	85.6	0.6148	26.99	72.39
6	1.82	85.6	0.5398	27.35	72.11
7	2.50	62.3	0.4637	23.99	75.54
8	2.50	62.3	0.4790	24.18	75.34
9	3.75	41.5	0.3171	21.66	78.03
10	3.75	41.5	0.4346	21.56	78.00

TABLE IX

THE HYDROCHLORINATION OF $SiCl_4$ AND M.G. SILICON METAL AT 100 PSIG, 350° C AND $H_2/SiCl_4$ FEED RATIO OF 2.0

Sample No.	Hydrogen Feedrate SLM (1)	Residence Time Second	Product Composition, Mole % SiH_2Cl_2	$SiHCl_3$	$SiCl_4$
1	0.6	167	< 0.05	6.038	93.96
2	0.6	167	< 0.05	6.232	93.77
3	1.5	66.8	< 0.05	2.723	97.28
4	1.5	66.8	< 0.05	2.876	97.12
5	2.8	35.8	< 0.05	1.836	98.16
6	2.8	35.8	< 0.05	1.964	98.04
7	4.0	25.1	< 0.05	1.254	98.75
8	4.0	25.1	< 0.05	1.411	98.59

(1) SLM, Standard Liter per Minute

TABLE X

THE HYDROCHLORINATION OF $SiCl_4$ AND M.G. SILICON METAL AT 100 PSIG, 400°C AND $H_2/SiCl_4$ FEED RATIO OF 2.0

Sample No.	Hydrogen Feedrate SLM	Residence Time Second	Product Composition, Mole % SiH_2Cl_2	$SiHCl_3$	$SiCl_4$
1	0.6	161	0.07554	13.18	86.74
2	0.6	161	0.08251	13.55	86.36
3	1.2	80.5	< 0.05	8.986	91.01
4	1.2	80.5	< 0.05	9.183	90.82
5	1.9	50.8	< 0.05	7.494	92.51
6	1.9	50.8	< 0.05	7.646	92.35
7	3.3	29.2	< 0.05	5.608	94.39
8	3.3	29.2	< 0.05	5.656	94.34

TABLE XI

THE HYDROCHLORINATION OF $SiCl_4$ AND M.G. SILICON METAL AT 100 PSIG, 500°C AND $H_2/SiCl_4$ FEED RATIO OF 1.0

Sample No.	Hydrogen Feedrate SLM (1)	Residence Time Second	Product Composition, Mole % SiH_2Cl_2	$SiHCl_3$	$SiCl_4$
1	0.4	154	0.3730	18.98	80.65
2	0.4	154	0.3464	18.71	80.94
3	0.7	88.0	0.2847	18.34	81.38
4	0.7	88.0	0.3317	18.29	81.38
5	1.1	56.0	0.2877	17.77	81.95
6	1.1	56.0	0.2420	17.62	82.14
7	2.0	30.8	0.2161	16.44	83.34
8	2.0	30.8	0.2103	16.25	83.54
9	3.5	17.6	0.1775	15.07	84.75
10	3.5	17.6	0.1729	14.33	85.50

(1) SLM, Standard Liter per Minute

TABLE XII

THE HYDROCHLORINATION OF $SiCl_4$ AND M.G. SILICON METAL AT 100 PSIG, 500°C AND $H_2/SiCl_4$ FEED RATIO OF 2.8

Sample No.	Hydrogen Feedrate SLM	Residence Time Second	Product Composition, Mole % SiH_2Cl_2	$SiHCl_3$	$SiCl_4$
1	0.6	154	0.5759	24.49	74.94
2	0.6	154	0.5298	24.46	75.01
3	1.2	77.0	0.4124	23.64	75.95
4	1.2	77.0	0.5521	23.84	75.61
5	2.1	44.0	0.3953	23.09	76.51
6	2.1	44.0	0.5299	22.73	76.74
7	4.15	22.3	0.4223	21.29	78.29
8	4.15	22.3	0.4329	20.69	78.88

TABLE XIII

THE HYDROCHLORINATION OF $SiCl_4$ AND M.G. SILICON METAL AT 100 PSIG, 500° C AND $H_2/SiCl_4$ FEED RATIO OF 4.0

Sample No.	Hydrogen Feedrate SLM	Residence Time Second	Product Composition, Mole % SiH_2Cl_2	$SiHCl_3$	$SiCl_4$
1	0.7	145	0.6050	26.54	72.86
2	0.7	145	0.5453	26.85	72.61
3	1.2	84.6	0.5820	26.50	72.92
4	1.2	84.6	0.5479	26.72	72.73
5	2.1	48.3	0.4983	25.66	73.84
6	2.1	48.3	0.4669	25.23	74.30
7	4.2	24.2	0.4479	22.11	77.44
8	4.2	24.2	0.4267	21.81	77.76

TABLE XIV

THE HYDROCHLORINATION OF $SiCl_4$ AND M.G. SILICON METAL AT 100 PSIG, 500°C AND $H_2/SiCl_4$ FEED RATIO OF 4.7

Sample No.	Hydrogen Feedrate SLM	Residence Time Second	Product Composition, Mole % SiH_2Cl_2	$SiHCl_3$	$SiCl_4$
1	0.65	163	0.6244	28.12	71.26
2	0.65	163	0.7960	27.85	71.35
3	0.9	118	0.6961	27.47	71.83
4	0.9	118	0.6743	27.70	71.62
5	1.2	88.3	0.6617	26.61	72.73
6	1.2	88.3	0.6504	27.18	72.17
7	2.4	44.1	0.6020	25.84	73.56
8	2.4	44.1	0.5812	26.06	73.36
9	4.1	25.8	0.2576	24.64	75.10
10	4.1	25.8	0.2655	24.51	75.23

TABLE XV

EQUILIBRIUM COMPOSITIONS OF CHLOROSILANE PRODUCTS FOR THE HYDROCHLORINATION OF $SiCl_4$ AND M.G. SILICON METAL AT 100 PSIG, $H_2/SiCl_4$ = 2.0 AND AT VARIOUS TEMPERATURES

Sample No.	Reaction Temperature °C	Residence Time Second	Product Composition, Mole % SiH_2Cl_2	$SiHCl_3$	$SiCl_4$
I	500	148	0.3726	22.29	77.33
I	500	148	0.3596	21.98	77.66
I	500	148	0.3779	22.15	77.47
I	500	148	0.3600	22.11	77.53
		Average =	0.3675	22.13	77.50
II	525	138	0.4781	23.25	76.27
II	525	138	0.3651	22.98	76.66
II	525	138	0.4141	22.92	76.66
II	525	138	0.4359	22.93	76.64
		Average =	0.4233	23.02	76.56
III	550	101	0.5750	24.05	75.38
III	550	101	0.5125	23.98	75.51
III	550	101	0.5099	24.21	75.28
III	550	101	0.5650	23.98	75.45
		Average =	0.5406	24.06	75.40
IV	575	98	0.5857	24.89	74.53
IV	575	98	0.5294	24.84	74.63
IV	575	98	0.5070	24.85	74.64
IV	575	98	0.4828	24.92	74.60
		Average =	0.5262	24.88	74.60

TABLE XVI EQUILIBRIUM CONSTANTS FOR THE HYDROCHLORINATION OF $SiCl_4$ AND M.G. SILICON AT 100 PSIG, $H_2/SiCl_4$ = 2.0 AND AT VARIOUS TEMPERATURES

Expt'l No.	Reaction Temp. °C	Mole Fractions at Equilibrium				Equilibrium Constant	
		SiH_2Cl_2	$SiHCl_3$	$SiCl_4$	H_2	K x 10^{-3}	K_p x 10^{-4} Atm.$^{-1}$
I	500	0.001326	0.079855	0.27965	0.63916	4.55	5.83
II	525	0.001533	0.083363	0.27725	0.63786	5.57	7.14
III	550	0.001967	0.087535	0.27432	0.63618	7.03	9.01
IV	575	0.001920	0.090774	0.27218	0.63513	8.35	10.7

TABLE XVII

EQUILIBRIUM COMPOSITION OF THE HYDROCHLORINATION REACTION MIXTURE AT ATMOSPHERIC PRESSURE WITH A $H_2/SiCl_4$ RATIO OF 2.0 AT VARIOUS TEMPERATURES

Run No.	Temperature °C	Residence Time Second	Product Composition,* Mole % $SiHCl_3$	$SiCl_4$
1	500	81.9	16.82	83.18
2	550	51.3	18.12	81.88
3	600	48.3	19.24	80.76
4	650	45.7	19.69	80.31
5	700	43.3	19.93	80.07

* Average of four to six analyses

TABLE XVIII EQUILIBRIUM CONSTANTS FOR THE HYDROCHLORINATION OF $SiCl_4$ AND M.G. SILICON AT VARIOUS TEMPERATURES

Temperature	Equilibrium Composition Mole Fractions			Equilibrium Constant
°C	$SiHCl_3$	$SiCl_4$	H_2	K x 10^{-3}
500	0.05940	0.2937	0.6469	1.17
550	0.06428	0.2905	0.6452	1.67
600	0.06853	0.2876	0.6438	2.24
650	0.07024	0.2865	0.6433	2.50
700	0.07116	0.2859	0.6429	2.65

TABLE XIX EQUILIBRIUM CONSTANTS FOR THE HYDROCHLORINATION OF $SiCl_4$ AND M.G. SILICON AT 500°C, 100 PSIG AND AT VARIOUS $H_2/SiCl_4$ FEED RATIOS

$\frac{H_2}{SiCl_4}$ Ratio	Equilibrium (1) Composition Mole % $SiHCl_3$	Mole % $SiCl_4$	Mole Fractions at Equilibrium $SiHCl_3$	$SiCl_4$	H_2	Equilibrium Constant K x 10^{-3}	K_p x 10^{-3} $Atm.^{-1}$
4.7	28.0	72.0	0.05353	0.1376	0.8088	4.81	0.617
4.0	26.7	73.3	0.05806	0.1594	0.7825	4.58	0.587
2.8	24.5	75.5	0.06988	0.2153	0.7148	4.67	0.599
2.0	22.8	77.2	0.08225	0.2785	0.6392	5.19	0.665
1.0	18.5	81.5	0.09939	0.4379	0.4627	5.43	0.696

(1) Data from Figure VI.

TABLE XX EQUILIBRIUM CONSTANTS FOR THE HYDROCHLORINATION OF $SiCl_4$ AND M.G. SILICON AT 500°C AND AT VARIOUS PRESSURES AND $H_2/SiCl_4$ FEED RATIOS

Reactor Pressure		$\frac{H_2}{SiCl_4}$	Equilibrium Composition Mole %		Mole Fraction at Equilibrium			Equilibrium Constant K	Equilibrium Constant K_p
psig	Atm.	Ratio	$SiHCl_3$	$SiCl_4$	$SiHCl_3$	$SiCl_4$	H_2	$\times 10^{-3}$	$\times 10^{-3} Atm.^{-1}$
0	1.0	2.0	16.82	83.18	0.05940	0.2937	0.6469	1.17	1.17
25	2.70	2.0	18.5	81.5	0.06572	0.2895	0.6448	1.85	0.685
73	5.97	2.8	23.7	76.3	0.06741	0.2170	0.7155	3.95	0.661
100	7.80	1.0	18.5	81.5	0.09939	0.4379	0.4627	5.43	0.696
100	7.80	2.0	22.8	77.2	0.08225	0.2785	0.6392	5.19	0.665
100	7.80	2.8	24.5	75.5	0.06988	0.2153	0.7148	4.67	0.599
100	7.80	4.0	26.7	73.3	0.05806	0.1594	0.7825	4.58	0.587
100	7.80	4.7	28.0	72.0	0.05353	0.1376	0.8088	4.81	0.617
150	11.2	2.0	27.9	72.1	0.1025	0.2650	0.6325	14.9	1.33
200	14.6	2.0	30.5	69.5	0.1132	0.2579	0.6289	24.2	1.65
300	21.4	2.8	35.0	65.0	0.1035	0.1923	0.7041	32.6	1.52
500	35.0	2.8	37.0	63.0	0.1102	0.1877	0.7020	45.3	1.29

TABLE XXI EQUILIBRIUM CONSTANTS FOR THE HYDROCHLORINATION OF $SiCl_4$ AND M.G. SILICON AT 450°C AND AT VARIOUS PRESSURES AND $H_2/SiCl_4$ FEED RATIOS

Reactor Pressure		$\frac{H_2}{SiCl_4}$	Equilibrium Composition Mole %		Mole Fraction at Equilibrium			Equilibrium Constant	
								K	K_p
psig	Atm.	Ratio	$SiHCl_3$	$SiCl_4$	$SiHCl_3$	$SiCl_4$	H_2	$\times 10^{-3}$	$\times 10^{-3}$ Atm.$^{-1}$
25	2.70	2.0	16.2	83.8	0.05708	0.2953	0.6476	0.983	0.364
73	5.96	2.8	20.8	79.2	0.05858	0.2231	0.7183	2.06	0.345
100	7.80	2.0	20.4	79.6	0.07296	0.2847	0.6424	2.98	0.382
150	11.2	2.0	24.0	76.0	0.08696	0.2754	0.6377	6.73	0.601
150	11.2	2.8	26.5	73.5	0.07611	0.2111	0.7128	7.02	0.627
200	14.6	2.0	27.0	73.0	0.09890	0.2674	0.6337	12.5	0.854
300	21.4	2.8	31.0	69.0	0.09043	0.2013	0.7083	16.3	0.764
300	21.4	1.0	25.0	75.0	0.1379	0.4138	0.4483	25.4	1.19
500	35.0	2.8	33.0	67.0	0.09695	0.1968	0.7062	23.2	0.664

TABLE XXII

THE HYDROCHLORINATION OF $SiCl_4$ AND M.G. SILICON METAL AT 550°C, 100 PSIG AND $H_2/SiCl_4$ FEED RATIO OF 2.0

Sample No.	Hydrogen Feedrate SLM	Residence Time Second	Product Composition, Mole % SiH_2Cl_2	$SiHCl_3$	$SiCl_4$
1	0.65	109	0.6471	24.72	74.64
2	0.65	109	0.6821	24.46	74.86
3	1.00	70.9	0.6317	24.36	75.00
4	1.00	70.9	0.6733	24.25	75.08
5	1.60	44.3	0.6532	23.61	75.74
6	1.60	44.3	0.5337	24.31	75.15
7	2.40	29.5	0.5069	23.29	76.21
8	2.40	29.5	0.5456	23.34	76.11
9	3.40	20.8	0.4188	22.08	77.50
10	3.40	20.8	0.4848	21.83	77.68
11	5.10	13.9	0.3894	20.16	79.45
12	5.10	13.9	0.4431	20.57	78.99

TABLE XXIII THE HYDROCHLORINATION OF $SiCl_4$ AND M.G. SILICON METAL TO $SiHCl_3$

Pressure 114.7 psia, Temperature 500 °C, $H_2/SiCl_4$ Feed Ratio 2.0 .

Time t sec.	Composition Mole % $SiHCl_3$	Composition Mole % $SiCl_4$	Composition at Time t (psia)/Mole Fraction H_2	Composition at Time t (psia)/Mole Fraction $SiHCl_3$	Composition at Time t (psia)/Mole Fraction $SiCl_4$	Initial Partial Press. $SiCl_4$ a	Equil. Partial Press. $SiHCl_3$ x_e	$\ln \frac{x_e}{x_e - x}$	Rate Constant k_1 x 10^{-3} $sec.^{-1}$
10	12.2	87.8	(74.85) 0.6525	(4.862) 0.04239	(34.99) 0.3051	38.23	-	0.7193	
20	18.1	81.9	(74.01) 0.6453	(7.365) 0.06421	(33.32) 0.2905	38.23	-	1.500	
30	19.9	80.1	(73.75) 0.6430	(8.149) 0.07105	(32.80) 0.2860	38.23	-	1.964	
40	20.9	79.1	(73.60) 0.6417	(8.589) 0.07488	(32.51) 0.2834	38.23	-	2.366	
60	22.0	78.0	(73.44) 0.6403	(9.077) 0.07914	(31.18) 0.2806	38.23	-	3.160	
Eq.	22.9	77.1	(73.31) 0.6391	(9.479) 0.08264	(31.91) 0.2782	38.23	9.479	-	12.2

Reference To: Figure III, fourth Quarterly Report, April 9 - July 8, 1982.

TABLE XXIV RATE CONSTANTS FOR THE HYDROCHLORINATION OF $SiCl_4$ AT 100 PSIG, 500°C AS A FUNCTION OF $H_2/SiCl_4$ FEED RATIO

$H_2/SiCl_4$ Feed Ratio	Equilibrium Composition Mole %		Rate Constant k_1 x 10^{-3} $Sec.^{-1}$
	$SiHCl_3$	$SiCl_4$	
4.7	28.0	72.0	12.7
4.0	26.8	73.2	12.2
2.8	24.5	75.5	11.4
2.0	22.8	77.2	10.9
1.0	18.8	81.2	9.30

TABLE XXV SUMMARY OF RATE CONSTANTS FOR THE HYDROCHLORINATION OF $SiCl_4$ AT 500°C AS A FUNCTION OF REACTOR PRESSURE

Reactor Pressure psig.	Atm.	$H_2/SiCl_4$ Ratio	Equilibrium Mole % $SiHCl_3$	Equilibrium Mole % $SiCl_4$	Rate Constant k_1 x 10^{-3} $sec.^{-1}$
25	2.70	2.0	18.4	81.6	14.5
73	5.97	2.8	23.4	76.6	13.0
100	7.80	2.0	22.9	77.1	12.2
200	14.6	2.0	31.0	69.0	8.33
500	35.0	2.8	37.5	62.5	7.06

TABLE XXVI RELATIVE REACTION RATES BETWEEN HYDROGEN AND DEUTERIUM IN THE HYDROCHLORINATION OF $SiCl_4$ AND M.G. SILICON AT 450°C, 15 PSIA AND $H_2/SiCl_4$ AND $D_2/SiCl_4$ RATIO OF 2.0

Run No.	Residence Time Second	Reaction Products Composition, Mole %					
		SiH_2Cl_2	$SiHCl_3$	$SiCl_4$	SiD_2Cl_2	$SiDCl_3$	$SiCl_4$
1	142	0.3756	16.15	83.48			
1	142	0.3971	16.38	83.22			
1	142	0.2545	15.66	84.08			
1	142	0.1648	15.84	84.00			
	Ave.	0.2980	16.01	83.70			
2	142				0.2534	16.06	83.68
2	142				0.2704	16.23	83.50
2	142				0.2711	16.46	83.27
2	142				0.2838	16.44	83.28
				Ave.	0.2697	16.30	83.43
3	60.2	0.1675	15.71	84.12			
3	60.2	0.1816	15.98	83.84			
3	60.2	0.1933	15.82	83.99			
	Ave.	0.1808	15.84	83.98			
4	60.2				0.1768	15.48	84.34
4	60.2				0.2010	15.85	83.95
4	60.2				0.1876	15.69	84.12
				Ave.	0.1885	15.67	84.14
5	30.2	0.1467	14.51	85.34			
5	30.2	0.1612	14.73	85.11			
5	30.2	0.1387	14.29	85.57			
	Ave.	0.1487	14.51	85.34			
6	30.2				0.1318	14.92	84.95
6	30.2				0.1701	14.80	85.03
6	30.2				0.1485	14.46	85.39
				Ave.	0.1501	14.73	85.12

TABLE XXVII RELATIVE REACTION RATES BETWEEN HYDROGEN AND DEUTERIUM IN THE HYDROCHLORINATION OF $SiCl_4$ AND M.G. SILICON AT 420°C, 15 PSIA AND $H_2/SiCl_4$ AND $D_2/SiCl_4$ RATIO OF 2.0

Run No.	Residence Time Second	Reaction Product Composition in Mole % *			
		$SiHCl_3$	$SiCl_4$	$SiDCl_3$	$SiCl_4$
1	196	14.93	85.07		
1	196	14.88	85.12		
	Ave.	14.91	85.09		
2	196			14.83	85.17
2	196			15.00	85.00
				Ave. 14.92	85.08
3	76.7	14.71	85.29		
3	76.7	14.72	85.28		
3	76.7	14.55	85.45		
3	76.7	14.40	85.60		
	Ave.	14.60	85.40		
4	76.7			14.28	85.72
4	76.7			14.47	85.53
4	76.7			14.34	85.66
4	76.7			14.50	85.50
				Ave. 14.40	85.60
5	43.0	12.52	87.48		
5	43.0	12.87	87.13		
5	43.0	12,54	87.46		
5	43.0	12.86	87.14		
	Ave.	12.70	87.30		
6	43.0			12.87	87.13
6	43.0			13.52	86.48
6	43.0			12.97	87.03
6	43.0			12.44	87.56
				Ave. 12.95	87.05
7	24.8	10.84	89.16		
7	24.8	11.09	89.91		
7	24.8	10.99	89.01		
	Ave.	10.97	89.36		
8	24.8			11.29	88.71
8	24.8			11.11	88.89
8	24.8			10.99	89.01
				Ave. 11.13	88.87

* The amount of SiH_2Cl_2 and SiD_2Cl_2 is too small to be determined accurately.

TABLE XXVIII HCl ANALYSIS ON THE HYDROCHLORINATION OF $SiCl_4$ AT 500° C, 300 PSIG AND $H_2/SiCl_4$ RATIO OF 2.0

Sample No.	Residence Time Second	Reaction Product Composition, Area % HCl	SiH_2Cl_2	$SiHCl_3$	$SiCl_4$
4*	209	0.5970	0.7512	32.66	64.04
5*	209	0.5875	0.7611	31.64	66.66
1	96	0.1235	0.4878	26.69	71.98
2	96	0.1388	0.5163	26.75	71.92
3	138	0.3326	0.7961	31.75	66.57
4	138	0.4343	0.3325	31.84	66.80
5	209	0.5962	0.7303	31.95	65.82
6	209	0.5735	0.8337	31.93	66.05

* from a separated analysis

TABLE XXIX APPROXIMATE COMPOSITION OF THE METAL ALLOYS FOR CORROSION TEST

Metals, Alloys	Approximate Compositions
Carbon Steel	Basically Iron, + 95% Fe
Nickel	Pure
Copper	Pure
Stainless Steel (Type 304)	68% Fe, 19% Cr, 10% Ni, 2% Mn, 1% Si
Alloy 400 (Monel)	2/3 Ni, 1/3 Cu
Incoloy 800 H	45% Fe, 30% Ni, 23% Cr, 1% Mn, 0.6% Si
Hastelloy B-2	68% Ni, 28% Mo, 2% Fe, 1% Cr, 1% Mn

TABLE XXX CORROSION TESTS FOR METALS AND ALLOYS AT 500°C, 300 PSIG AND $H_2/SiCl_4$ RATIO OF 2.0 FOR 87 HOURS

Sample Metal Alloy	Total Surface Area sq. cm.	Weigh before Reaction g.	Weigh after Reaction g.	Weigh Gain m.g.	Weigh Gain per Unit Area m.g./sq. cm.
Nickel	20.8	4.9808	5.3098	329.0	15.8
Nickel	20.3	4.8638	5.2190	355.2	17.5
Copper	24.3	8.7066	8.9283	221.7	9.13
Copper	23.1	8.2623	8.5986	336.3	14.6
Alloy 400	31.2	21.3429	21.4448	101.9	3.27
Alloy 400	27.8	19.0018	19.1307	128.9	4.64
Carbon Steel	15.6	3.6100	3.7435	133.5	8.56
Carbon Steel	16.8	3.8900	4.0259	135.9	8.90
Stainless Steel	19.5	11.9436	11.9923	48.7	2.50
Stainless Steel	20.0	12.2397	12.2972	57.5	2.88
Incoloy 800H	28.7	13.4049	13.4561	51.2	1.78
Incoloy 800H	30.3	14.1411	14.1935	52.4	1.73
Hastelloy B-2	32.2	23.1987	23.2417	43.0	1.34
Hastelloy B-2	30.3	21.8447	21.9001	55.4	1.83

TABLE XXXI CORROSION TEST AT 500 C, 300 PSIG, $H_2/SiCl_4$ RATIO OF 2.0 FOR 87 HOURS

Test Sample	Total Surface Area cm^2	Weigh Gain g.	Weith Gain per Unit Area $g/cm^2 \times 10^3$	Silicide Film Thickness cm x 10^4	Silicide Film Growth Rate cm/hr x 10^4	mils/year
Nickel	20.3	0.3552	17.5	110	1.26	435
Copper	24.3	0.2217	9.1	114	1.31	451
Alloy 400	31.2	0.1019	3.3	23	0.26	90
Carbon Steel	16.8	0.1359	8.9	56	0.64	221
Stainless Steel	19.5	0.0487	2.5	12	0.14	48
Incoloy 800H	30.3	0.0524	1.7	8	0.09	31
Hastelloy B-2	32.2	0.0430	1.3	7	0.08	28

FIGURE I APPARATUS FOR THE HYDROCHLORINATION OF $SiCl_4$ AND M.G. SILICON METAL TO $SiHCl_3$

(DRAWING NOT TO SCALE)

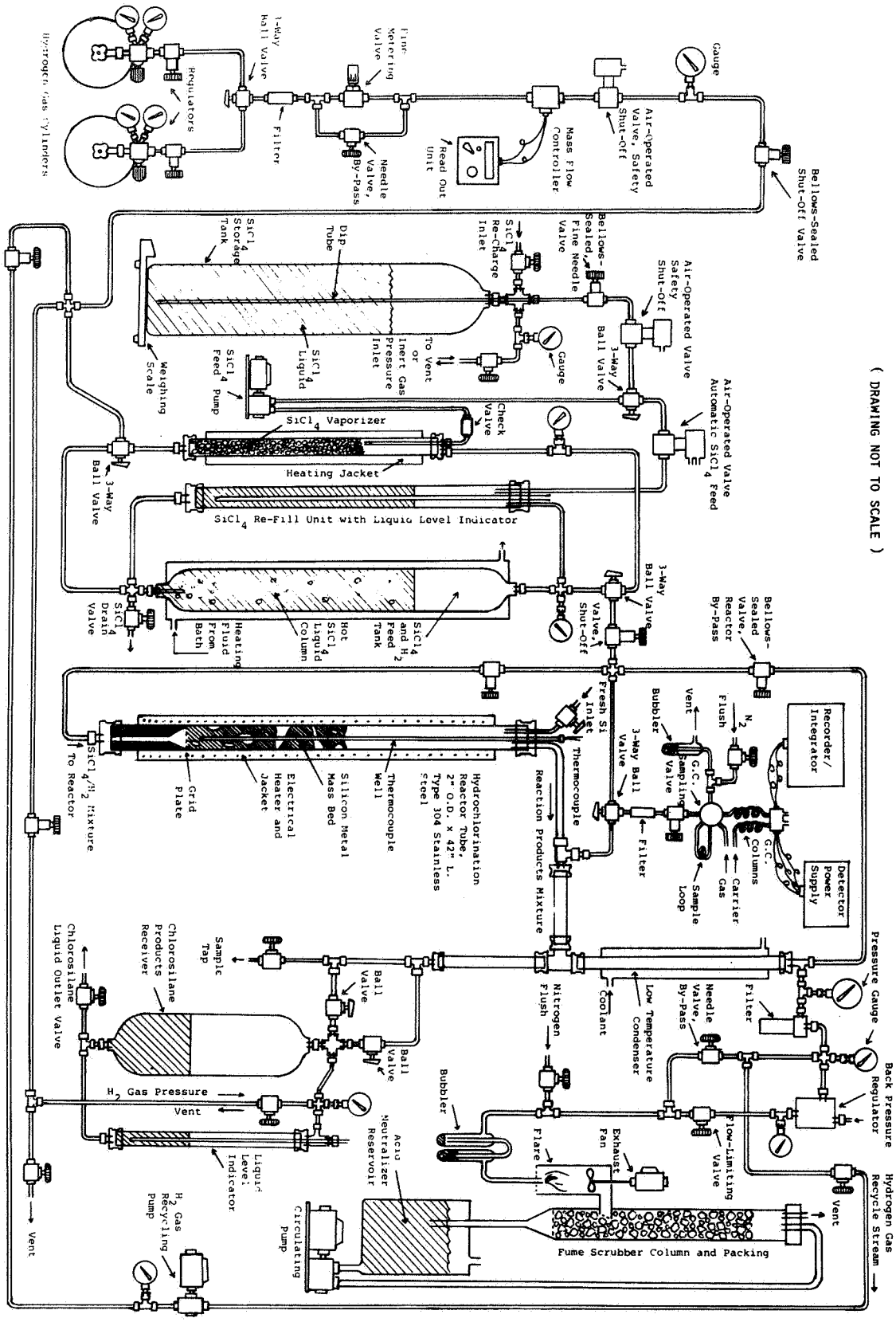

FIGURE II THE FLUIDIZED-BED REACTOR AND GRID DESIGN

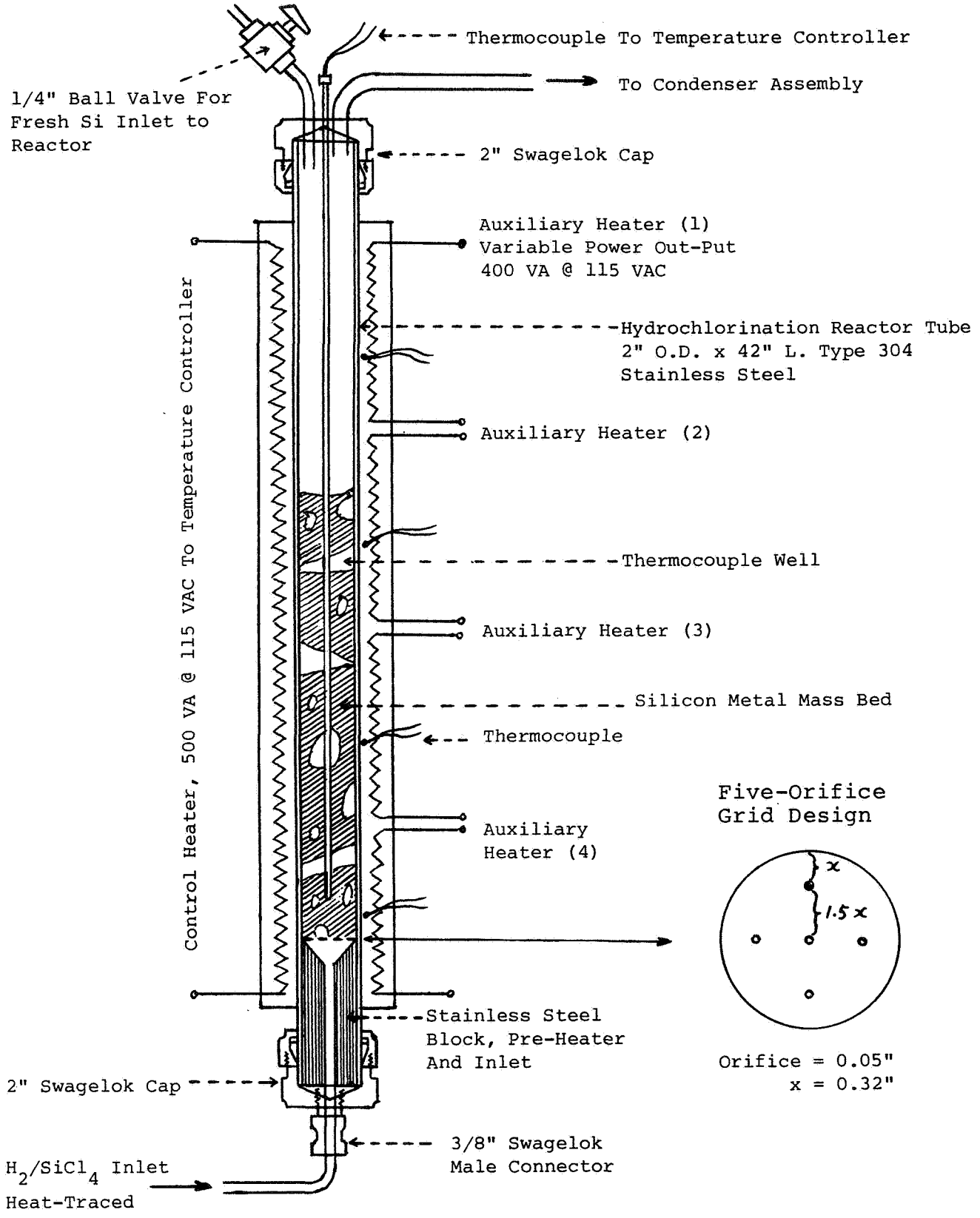

9950-847

FIGURE III HYDROCHLORINATION OF $SiCl_4$ AND M.G. SILICON AT 450°C, $H_2/SiCl_4$ RATIO OF 2.0 AND AT VARIOUS PRESSURES

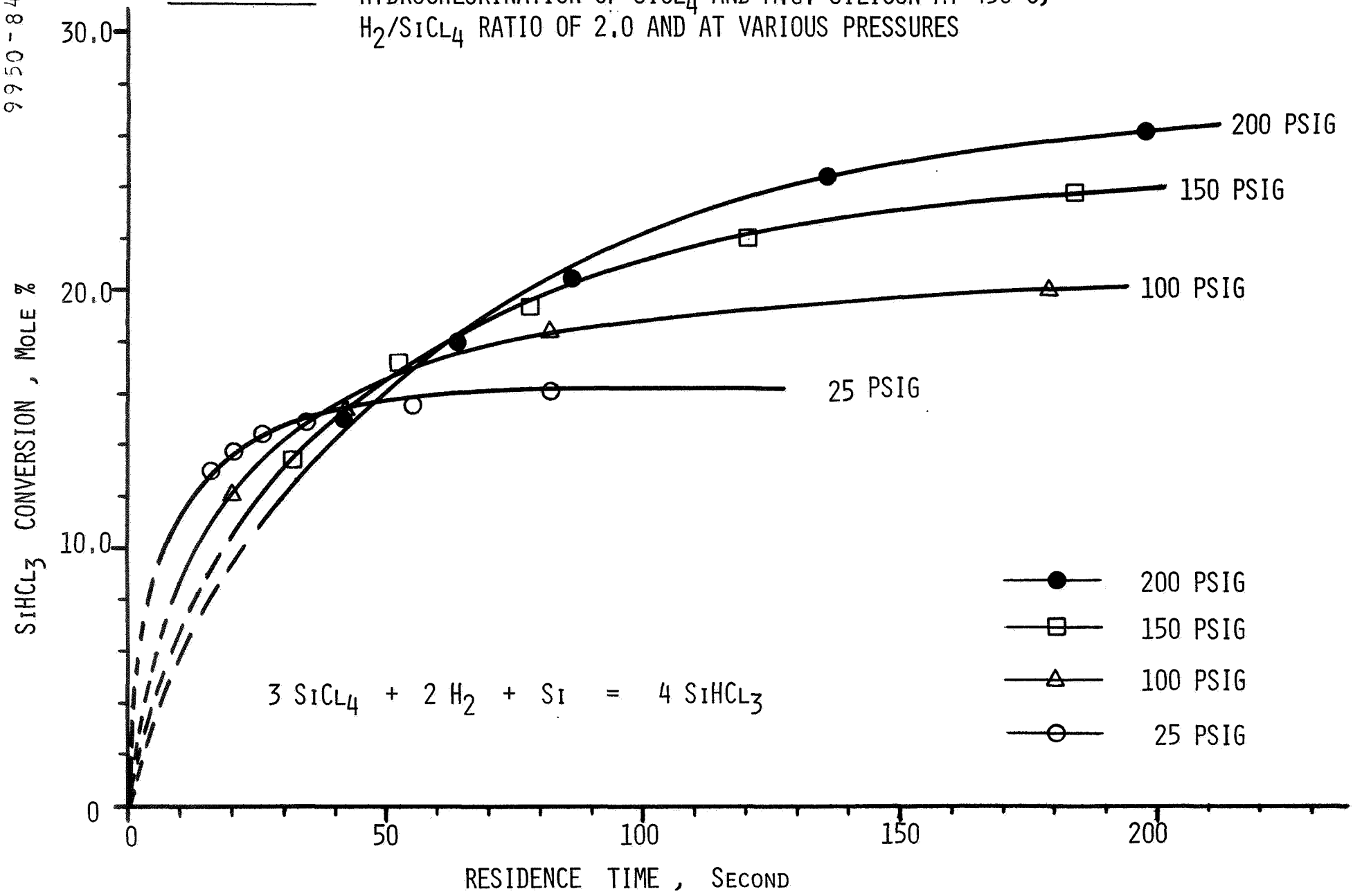

FIGURE IV HYDROCHLORINATION OF $SiCl_4$ AND M.G. SILICON AT 500°C, $H_2/SiCl_4$ RATIO OF 2.0 AND AT VARIOUS PRESSURES

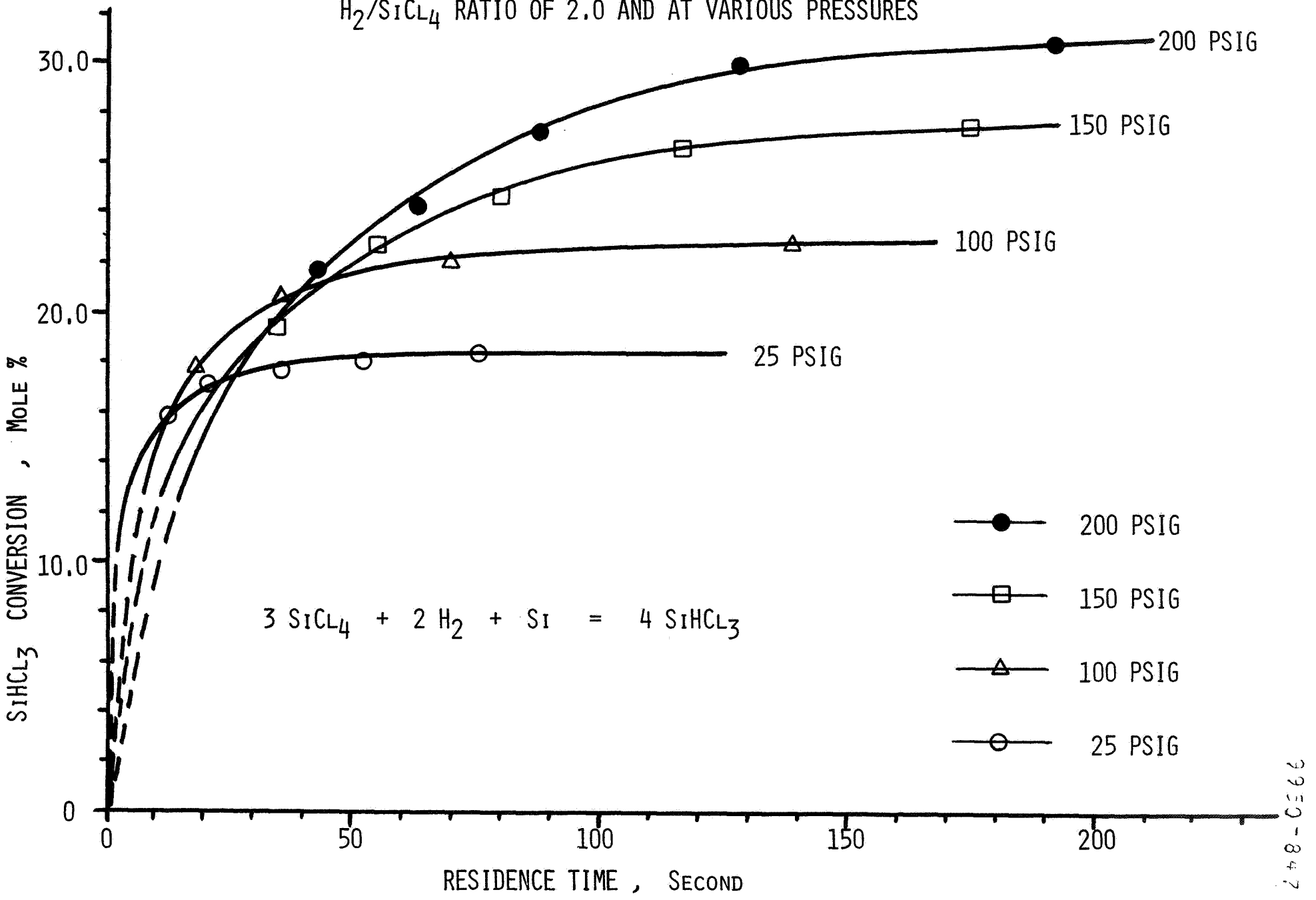

FIGURE V THE EFFECT OF TEMPERATURE ON THE HYDROCHLORINATION OF $SiCl_4$ AND M.G. SILICON AT 100 PSIG AND $H_2/SiCl_4$ MOLAR RATIO OF 2.0

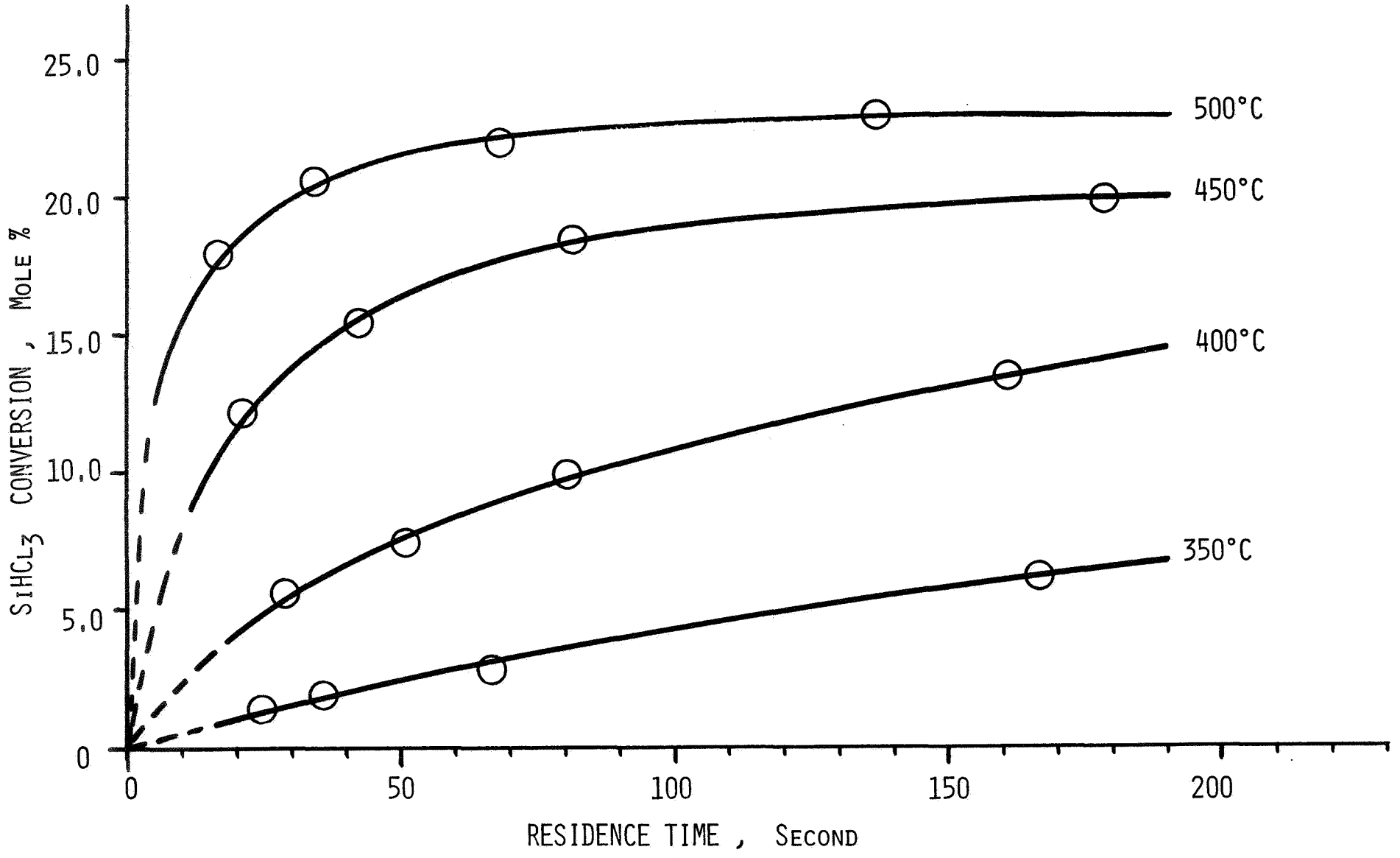

FIGURE VI HYDROCHLORINATION OF $SiCl_4$ AT 100 PSIG, 500°C AND AT VARIOUS MOLAR RATIOS OF H_2 : $SiCl_4$

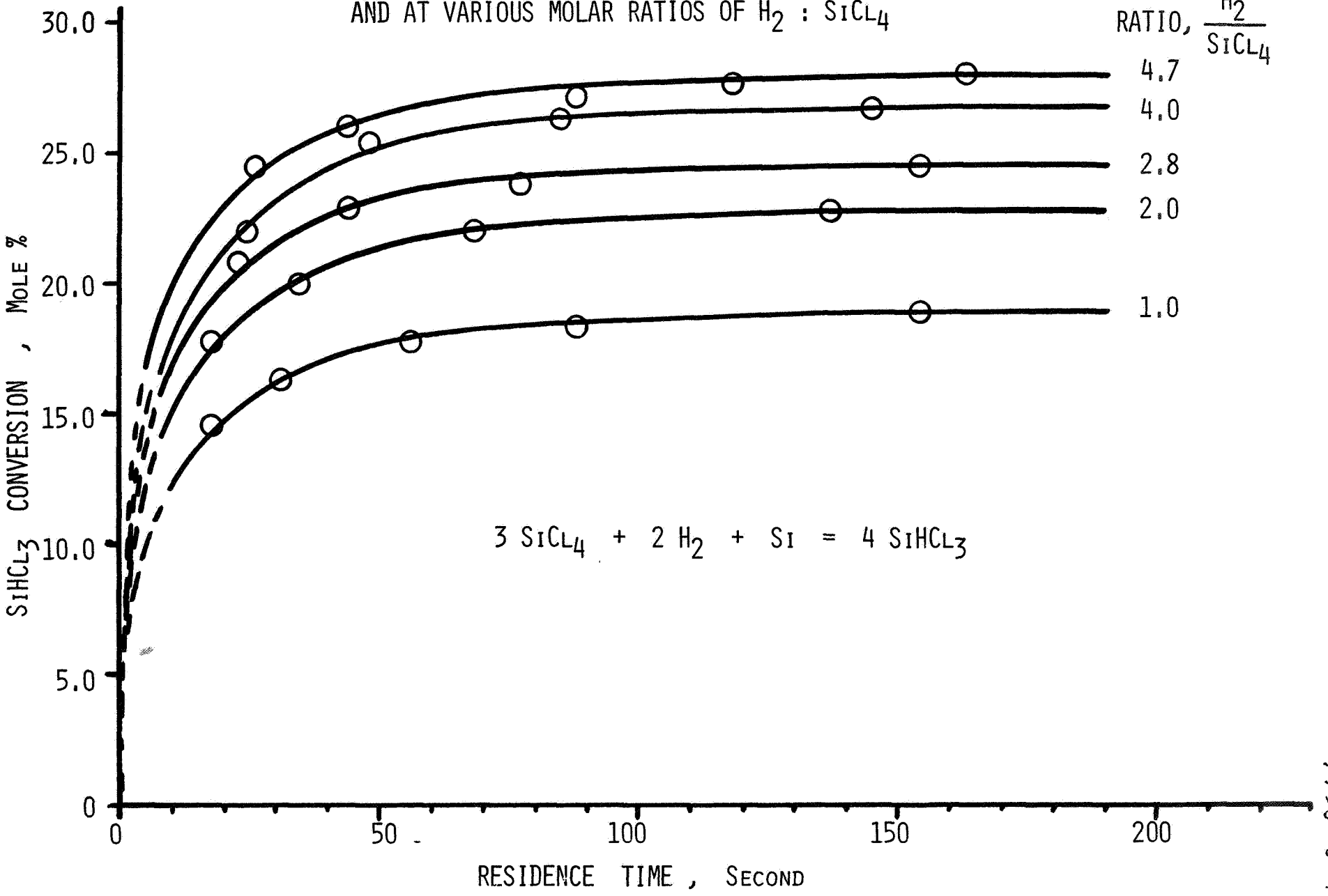

7933-847

9950-847

FIGURE VII KINETIC MODELING OF A TYPICAL EQUILIBRIUM REACTION

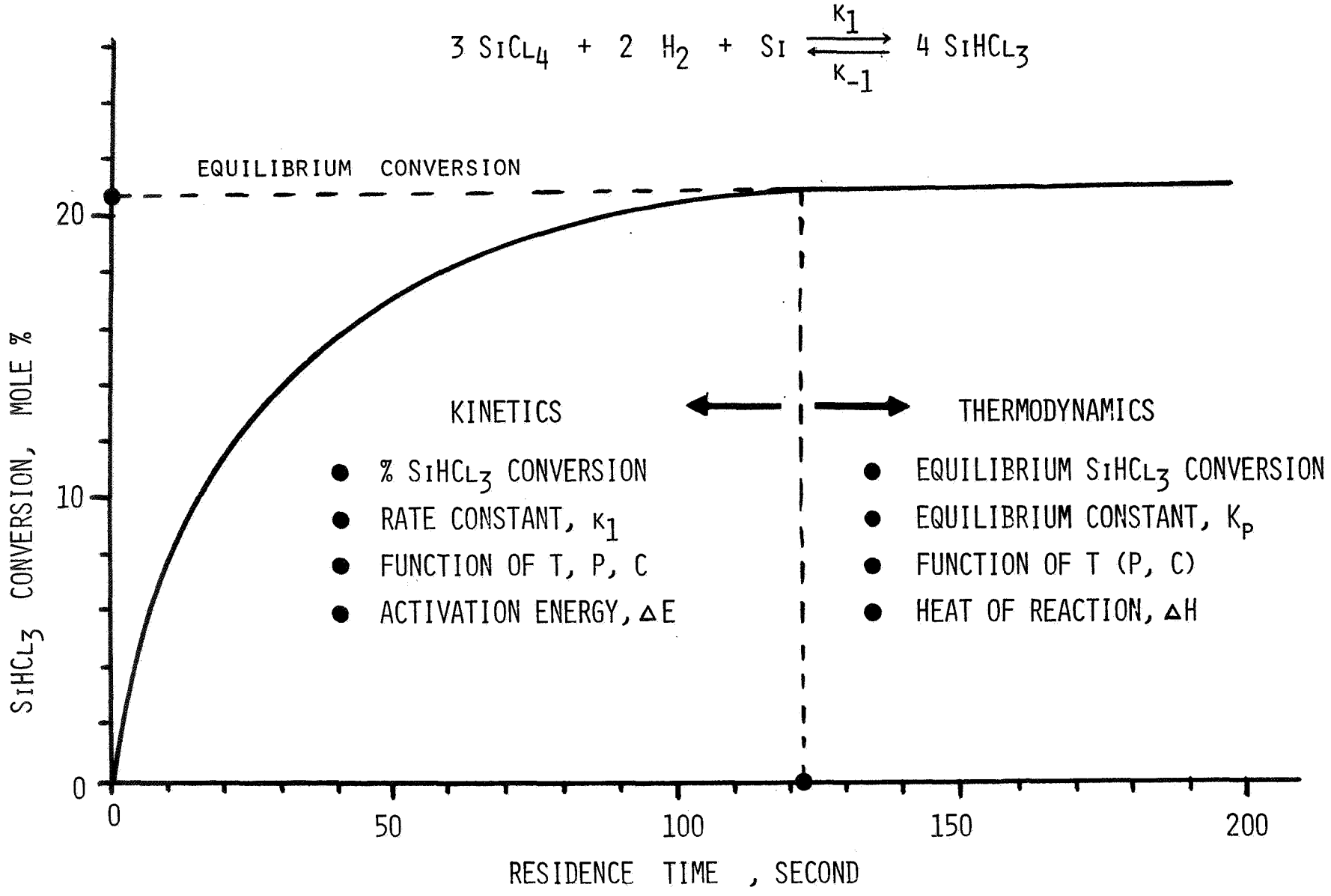

FIGURE VIII PLOT OF THE VAN'T HOFF EQUATION
LN K VERSUS INVERSED TEMPERATURE, 1/T

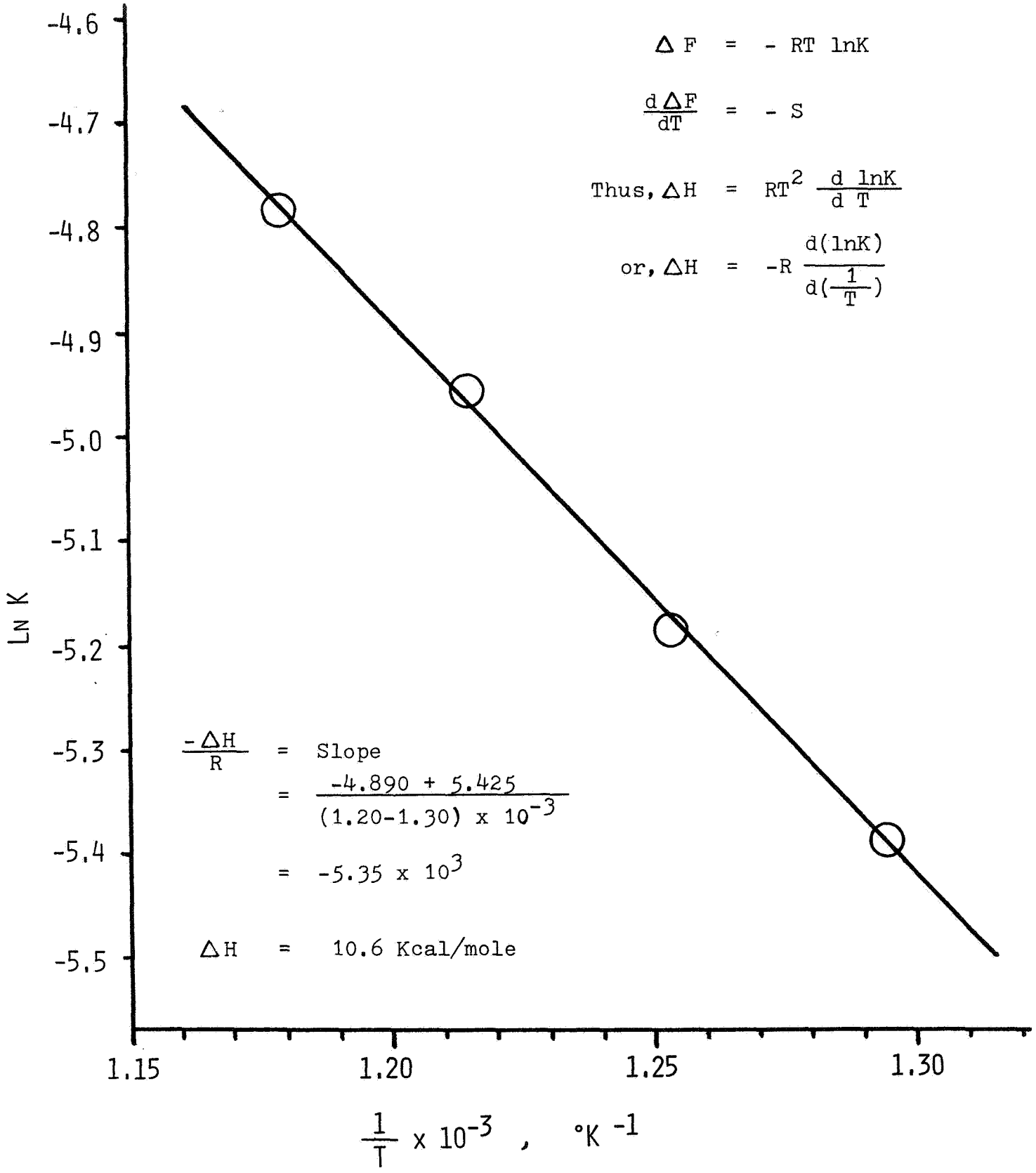

$$\Delta F = - RT \ln K$$

$$\frac{d\Delta F}{dT} = - S$$

$$\text{Thus, } \Delta H = RT^2 \frac{d \ln K}{d T}$$

$$\text{or, } \Delta H = -R \frac{d(\ln K)}{d(\frac{1}{T})}$$

$$\frac{-\Delta H}{R} = \text{Slope} = \frac{-4.890 + 5.425}{(1.20-1.30) \times 10^{-3}} = -5.35 \times 10^3$$

$$\Delta H = 10.6 \text{ Kcal/mole}$$

FIGURE IX PLOT OF THE EQUILIBRIUM CONSTANT, LN K VERSUS THE INVERSED TEMPERATURE, 1/T

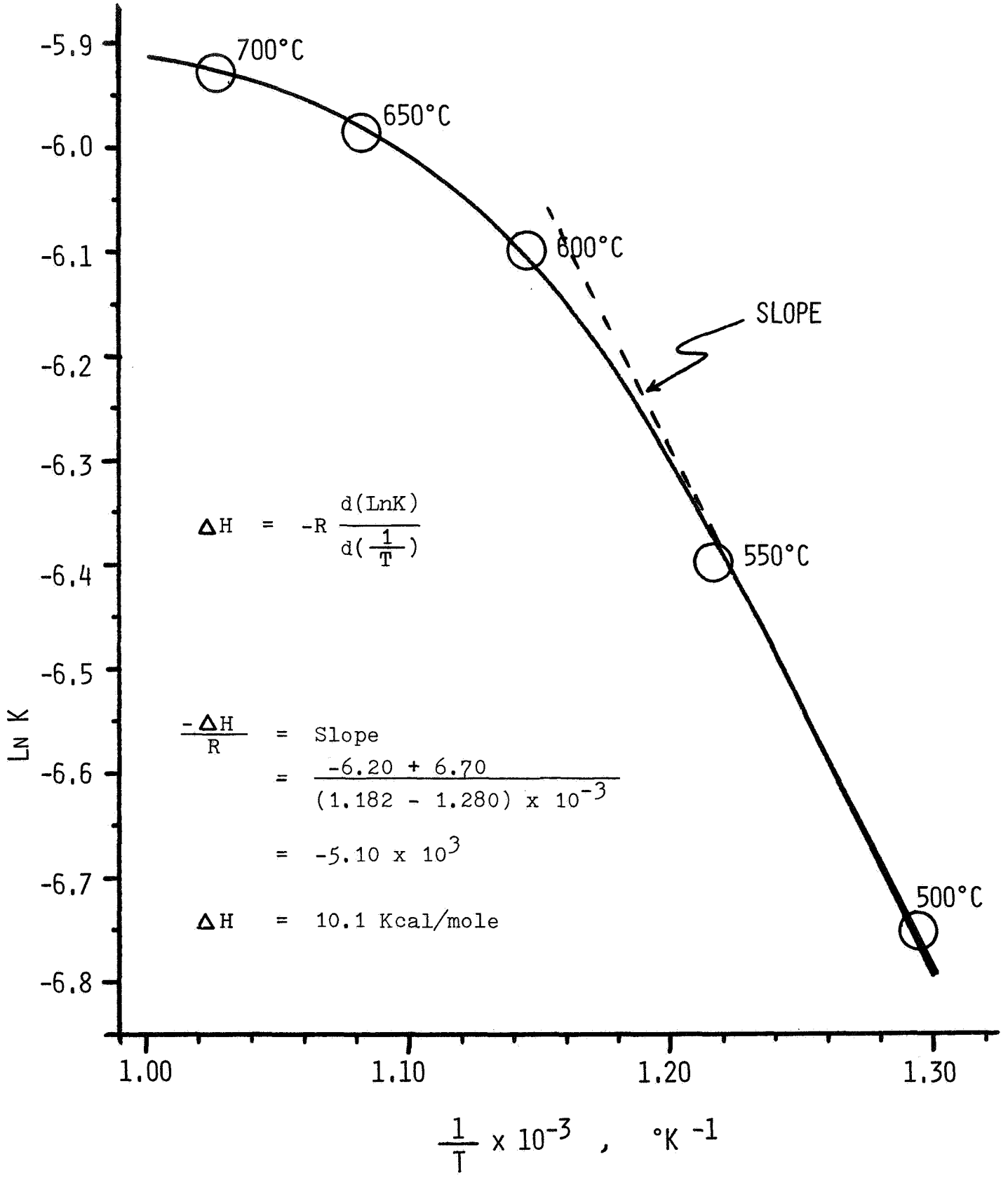

FIGURE X HYDROCHLORINATION OF $SiCl_4$ AT 100 PSIG AND $H_2/SiCl_4$ RATIO OF 2.0

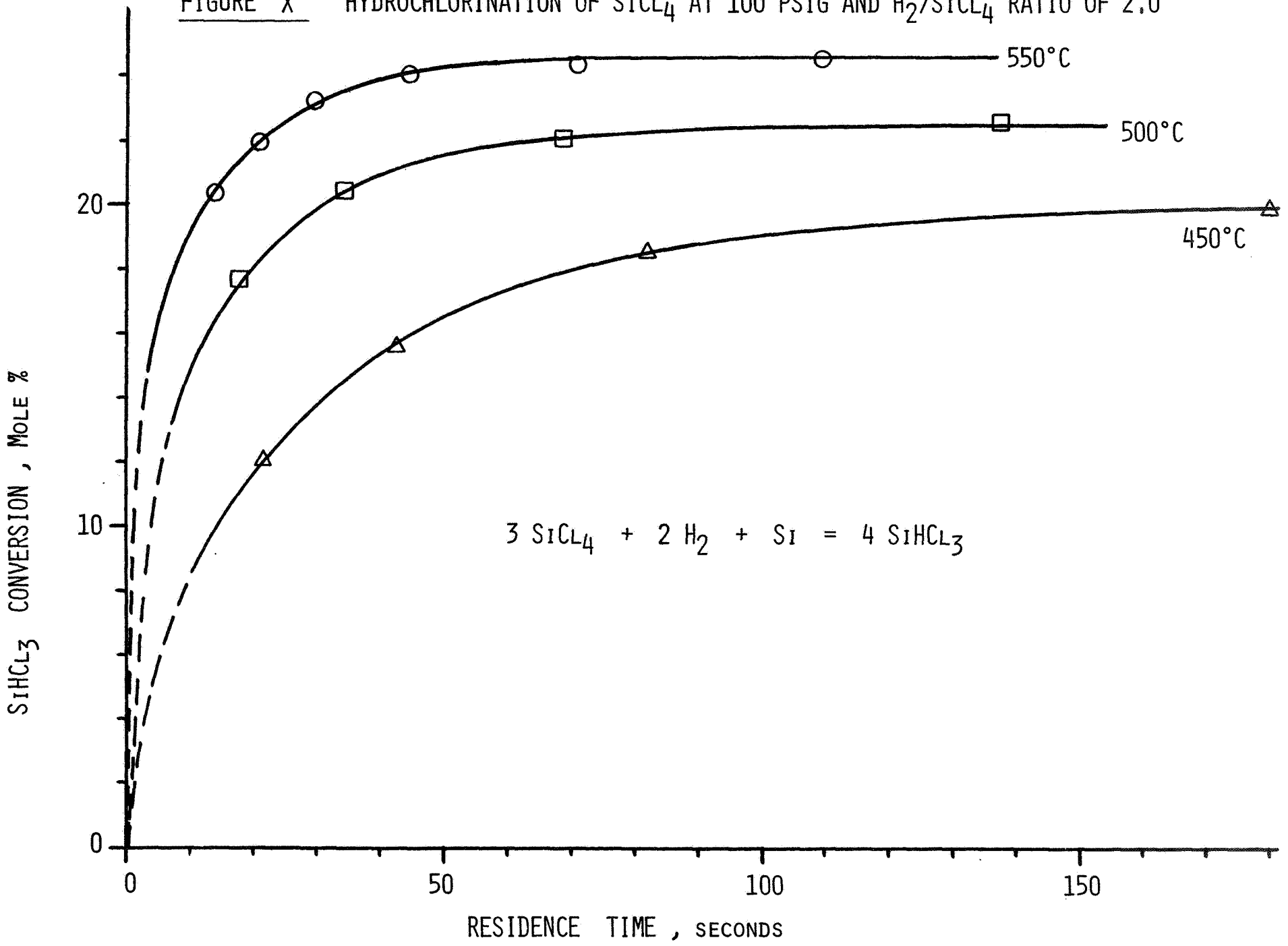

FIGURE XI PLOT OF PSUEDO-FIRST ORDER RATE EQUATION

$$A \underset{k_{-1}}{\overset{k_1}{\rightleftharpoons}} B \qquad \ln \frac{x_e}{x_e - x} = \frac{k_1 a}{x_e} t$$

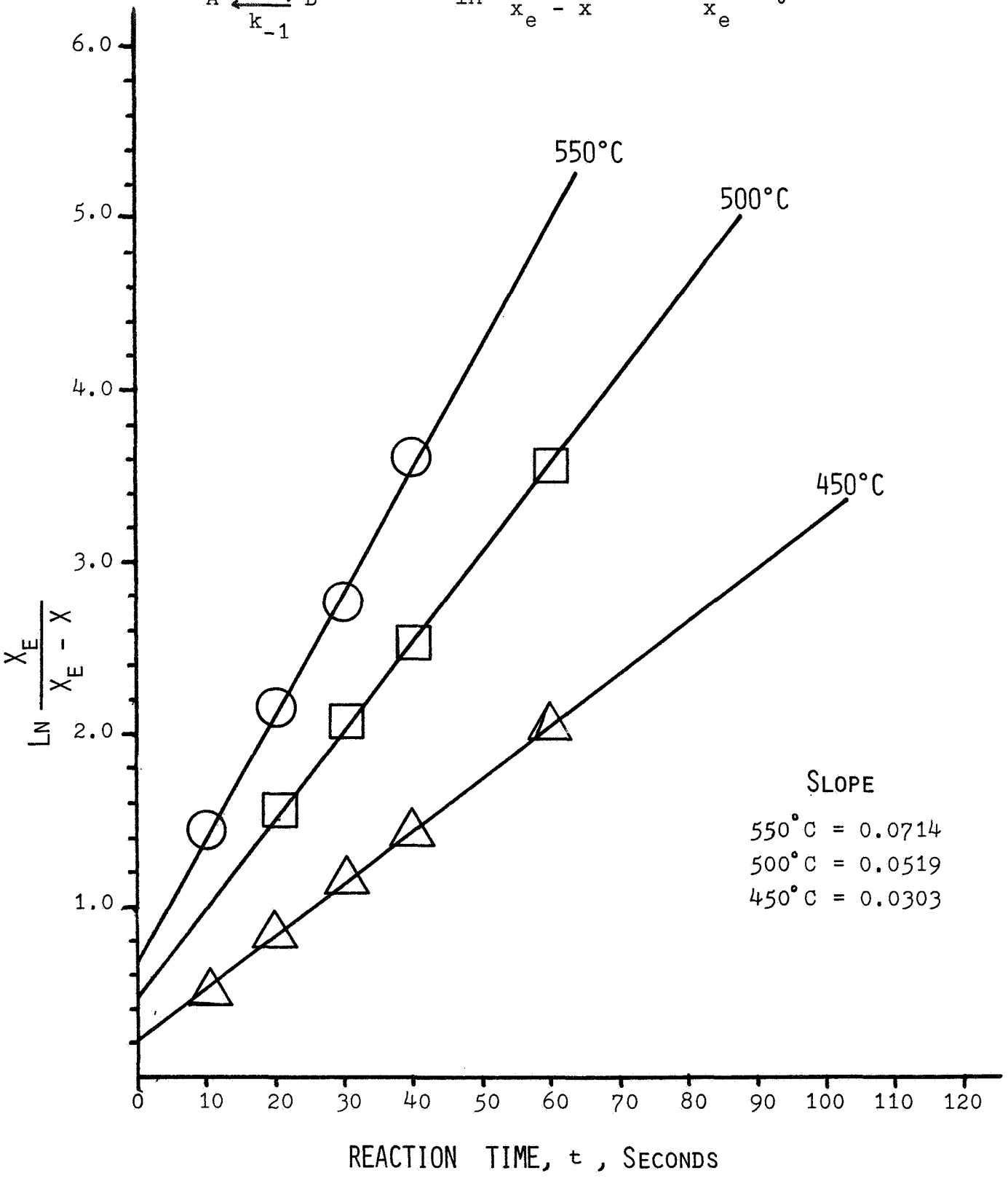

FIGURE XII PLOT OF THE ARRHENIUS EQUATION

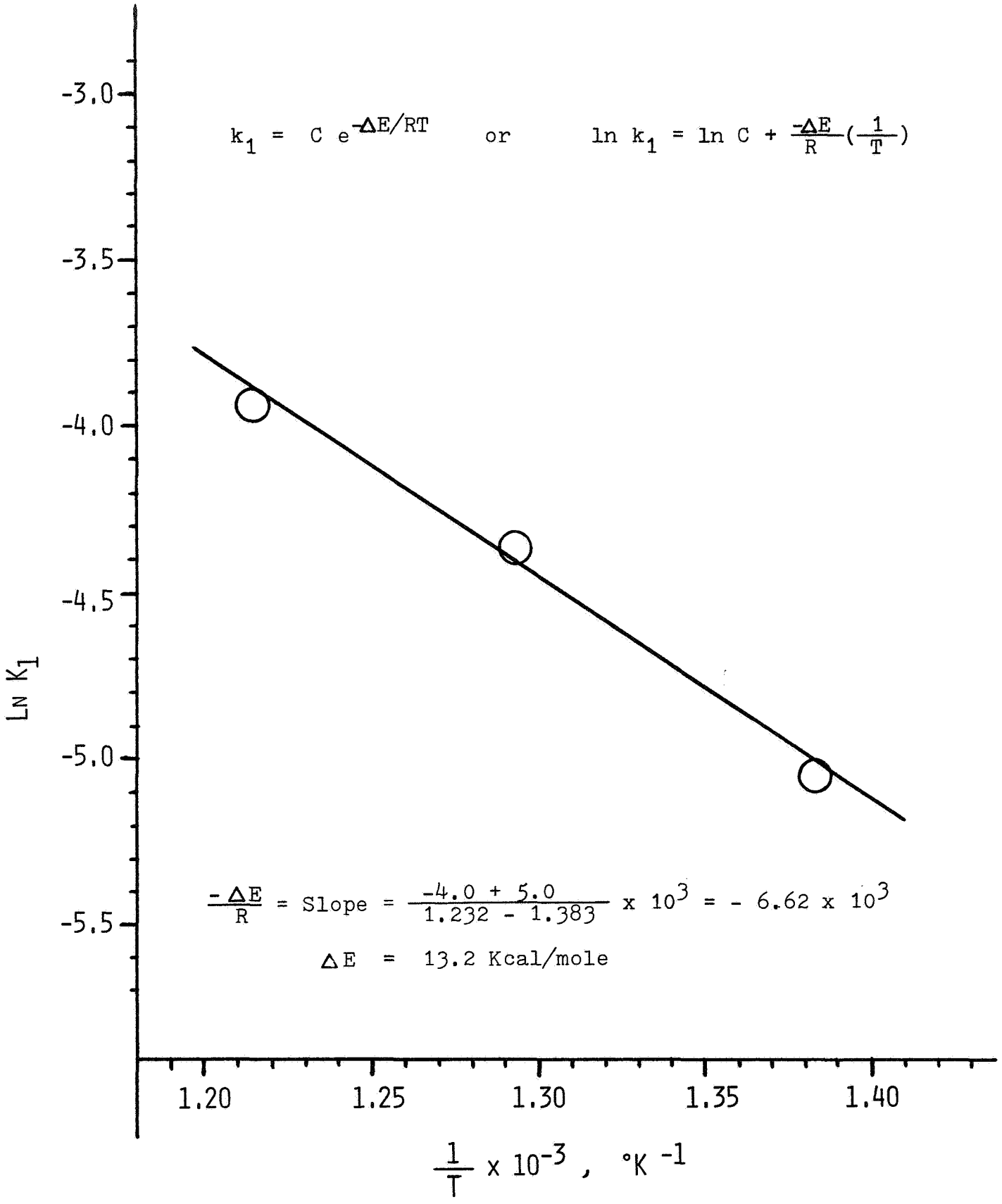

FIGURE XIII HYDROCHLORINATION OF $SiCl_4$ AND M.G. SILICON AT 500°C, $H_2/SiCl_4$ RATIO OF 2.0 AND AT VARIOUS PRESSURES

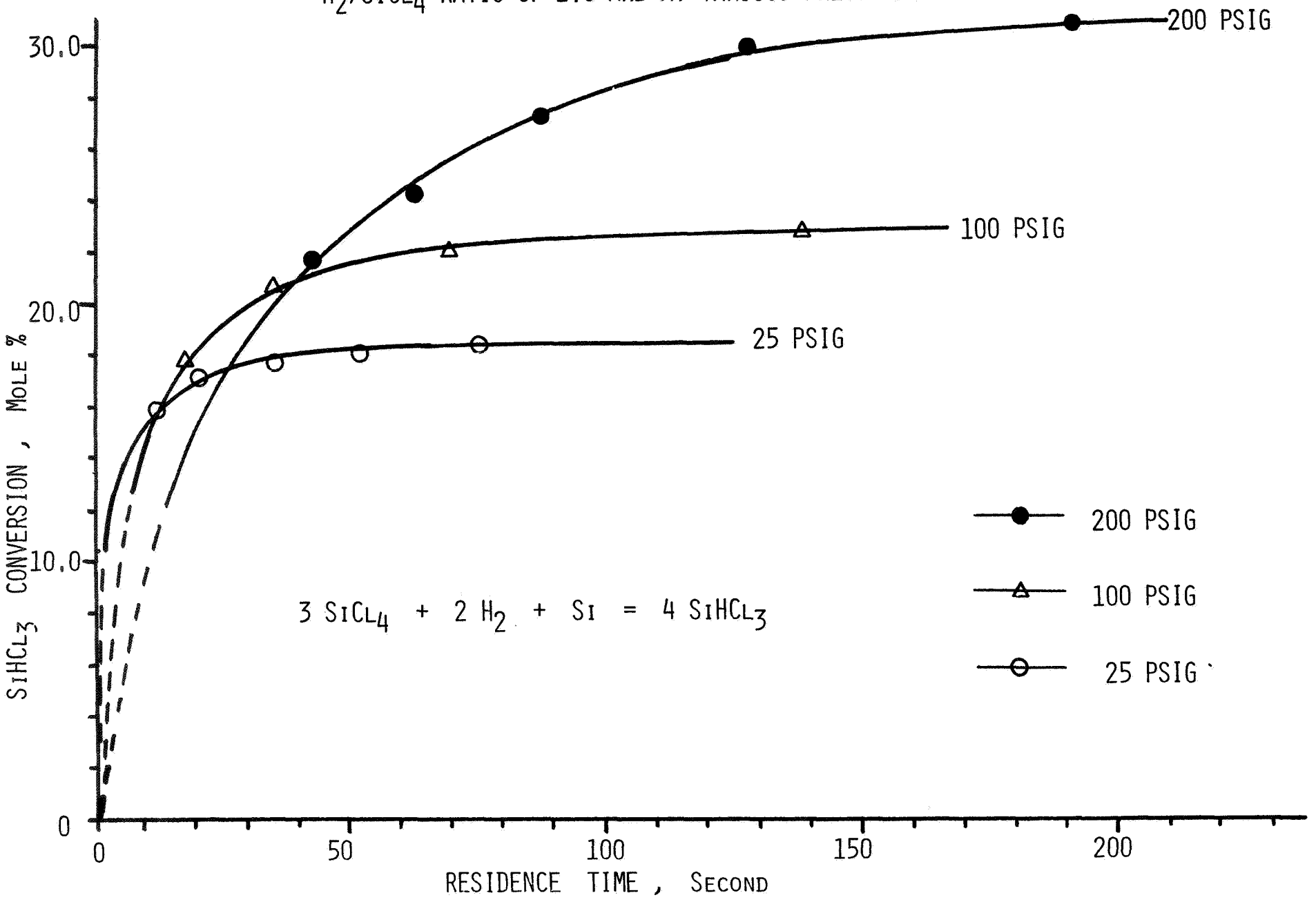

FIGURE XIV SCHEMATIC OF THE QUARTZ HYDROCHLORINATION REACTOR

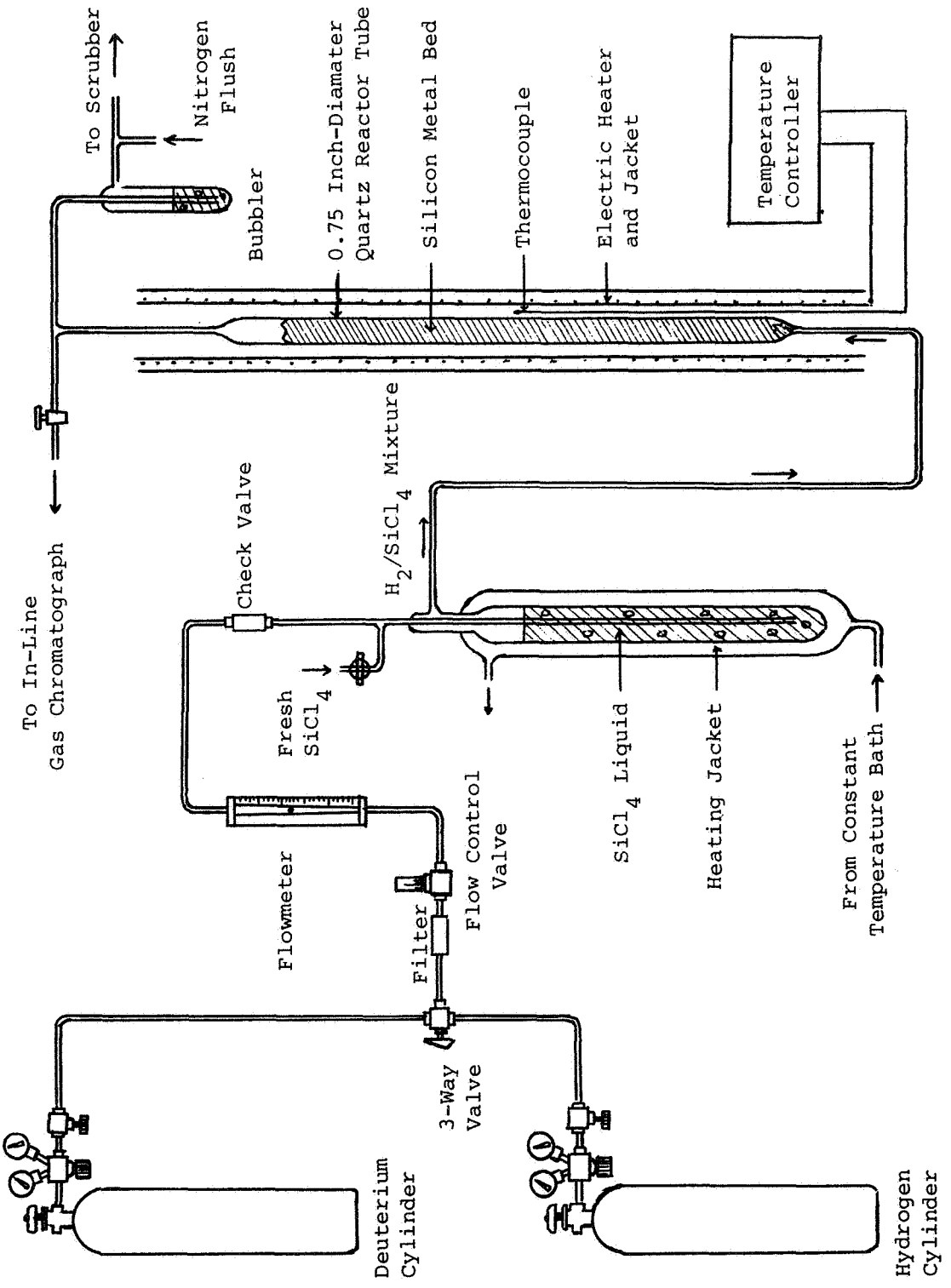

FIGURE XV PLOT OF % $SiHCl_3$ AND % $SiDCl_3$ CONVERSION VERSUS RESIDENCE TIME

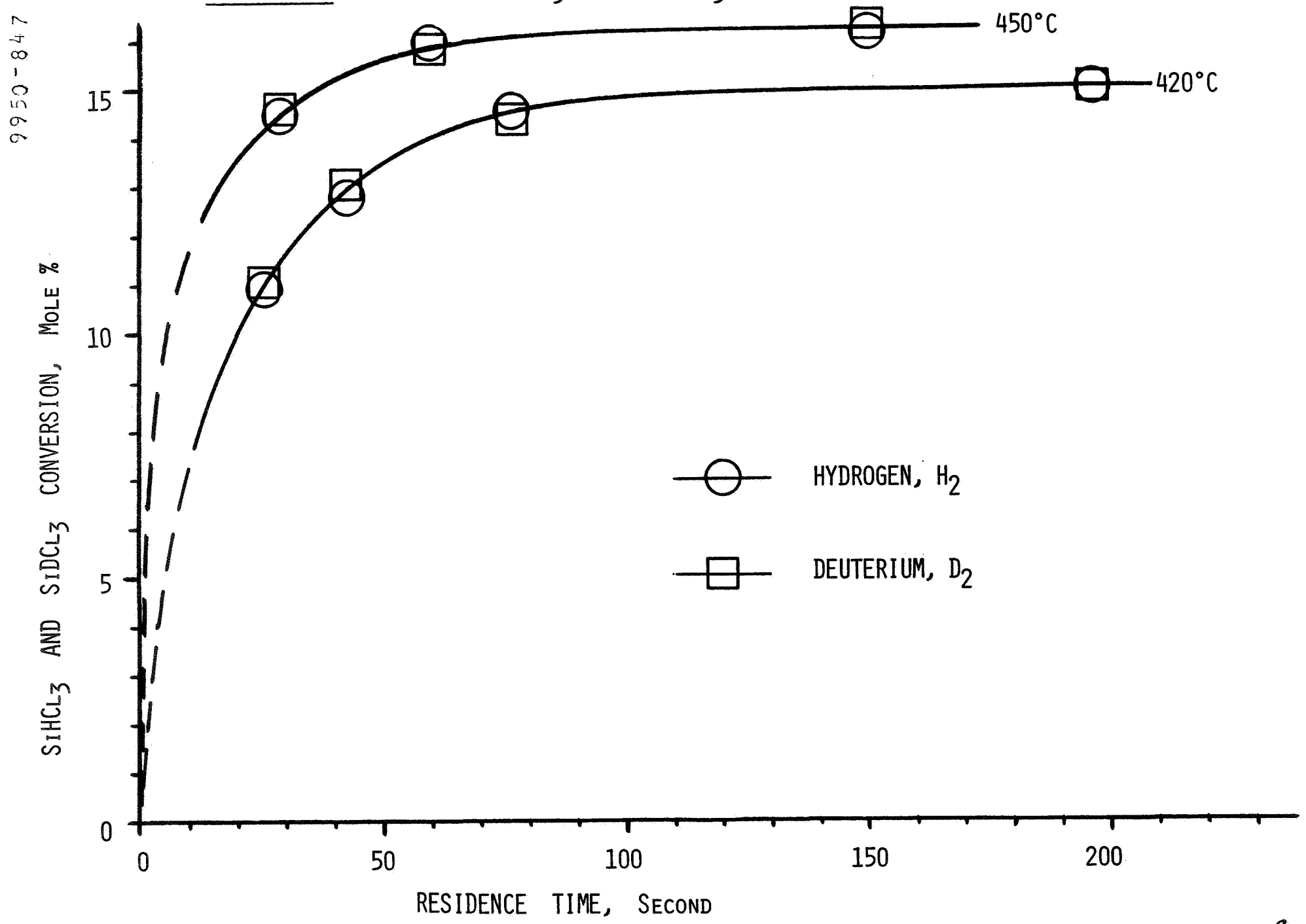

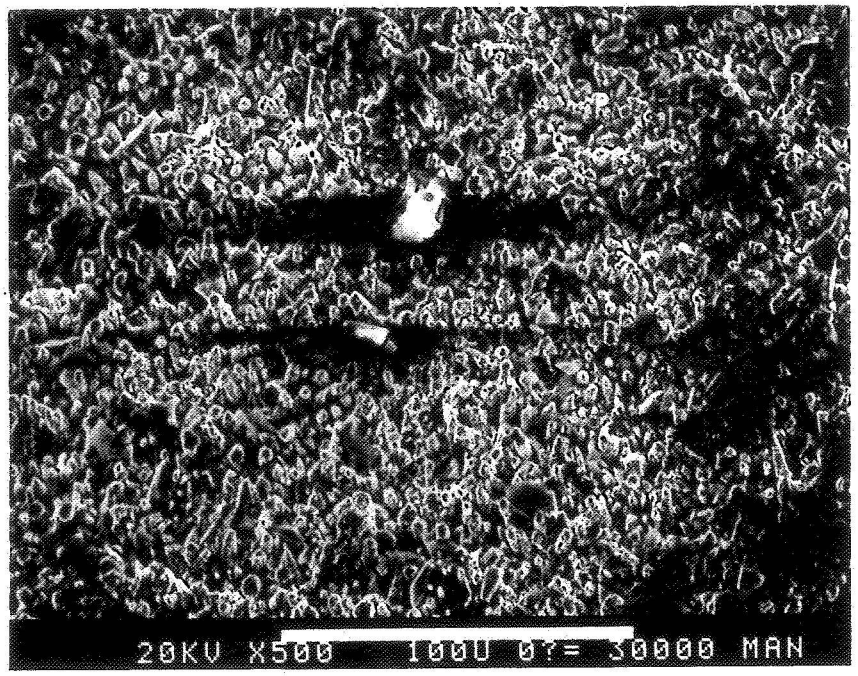

FIGURE XVI

CORROSION TEST ON PURE NICKEL: 87 HOURS AT 500°C, 300 PSIG AND $H_2/SiCl_4$ RATIO OF 2.0

SCANNING ELECTRON MICROGRAPH OF THE SURFACE OF THE TEST SAMPLE TO SHOW THE MORPHOLOGY OF THE SILICIDE FILM AT VARIOUS MAGNIFICATIONS

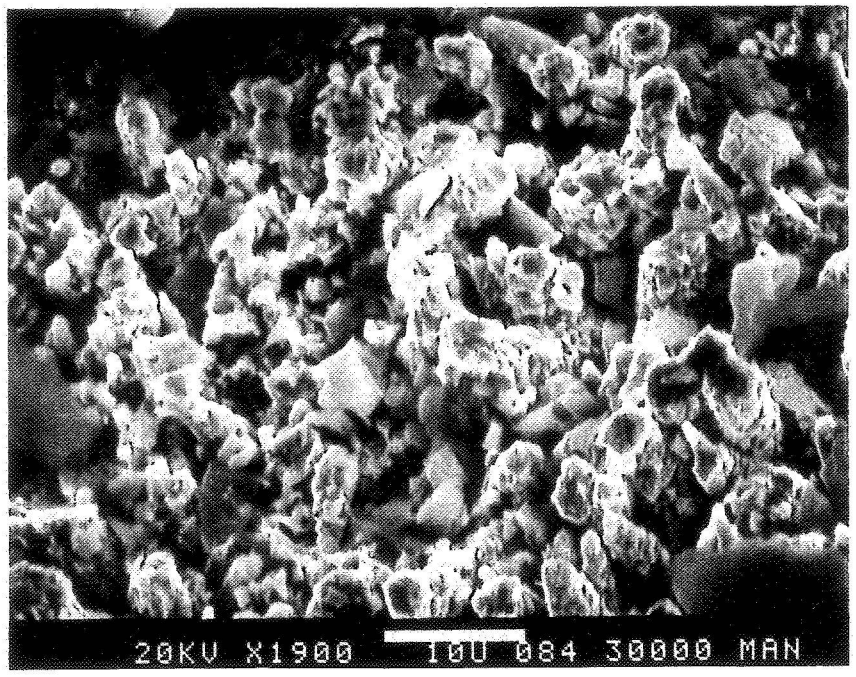

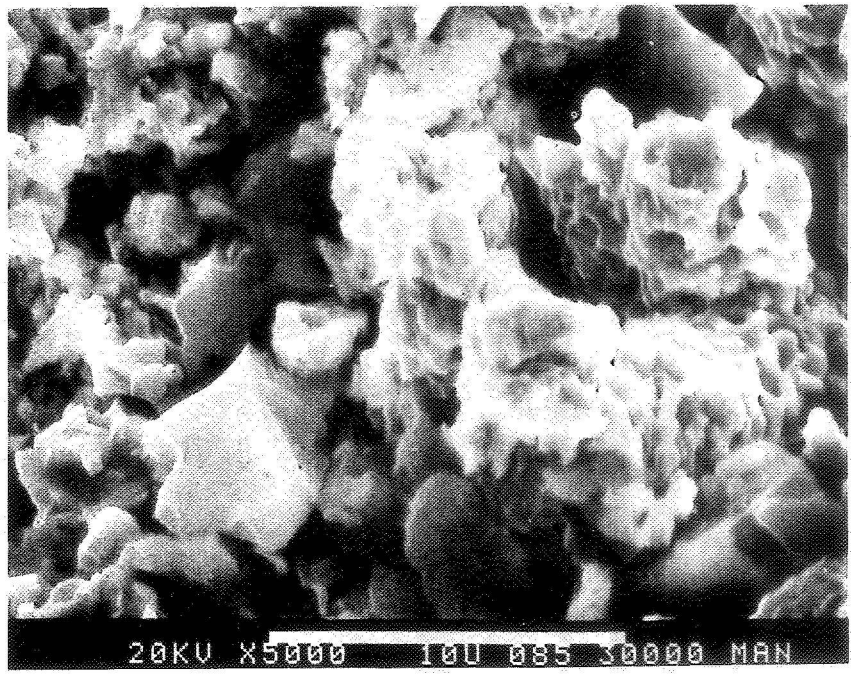

FIGURE XVII SCANNING ELECTRON MICROGRAPH OF A CROSS SECTIONAL AREA OF THE PURE NICKEL TEST SAMPLE: 87 HOURS AT 500°C, 300 PSIG, $H_2/SiCl_4$ RATIO OF 2

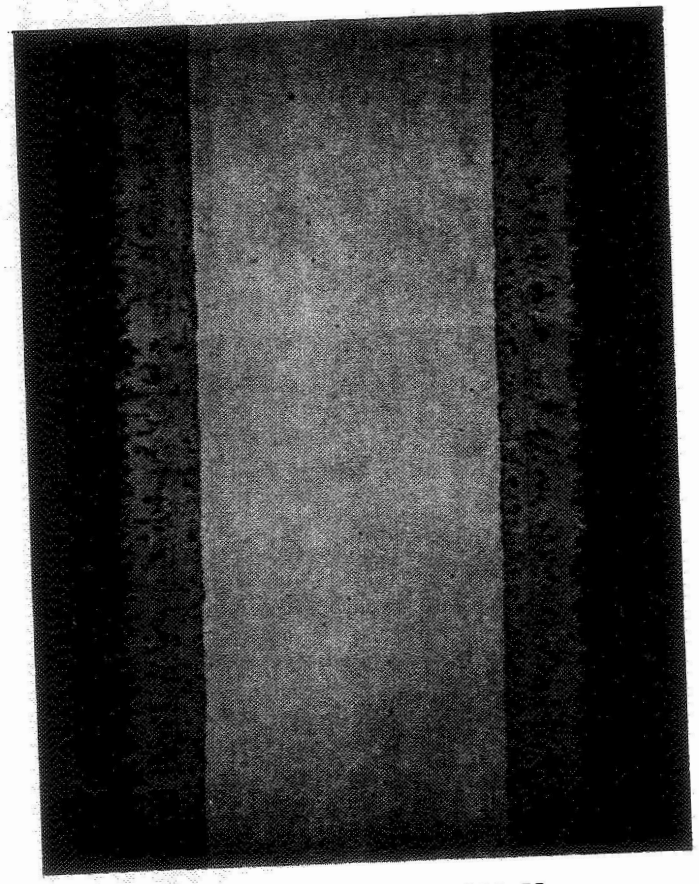

#3 Silicon on Nickel 100 X

#3 Silicon on Nickel 500 X

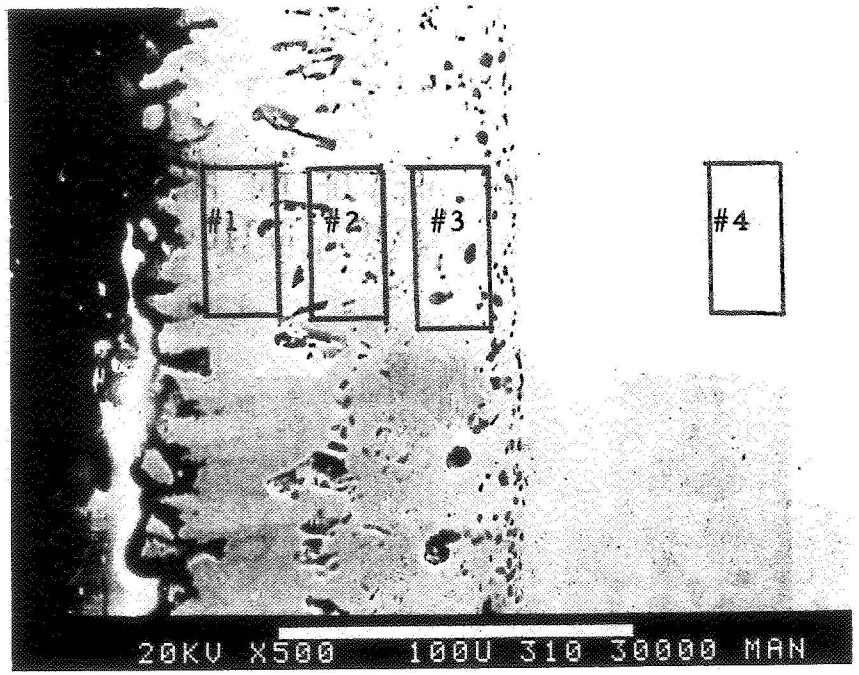

FIGURE XVIII SCANNING ELECTRON MICROGRAPH AND X-RAY DISTRIBUTION MAPS OF THE CORROSION TEST SAMPLE ON NICKEL

AREA #	ATOMIC % Si	Ni
1	46.40	53.60
2	42.88	57.12
3	33.94	66.06
4	0.00	100.00

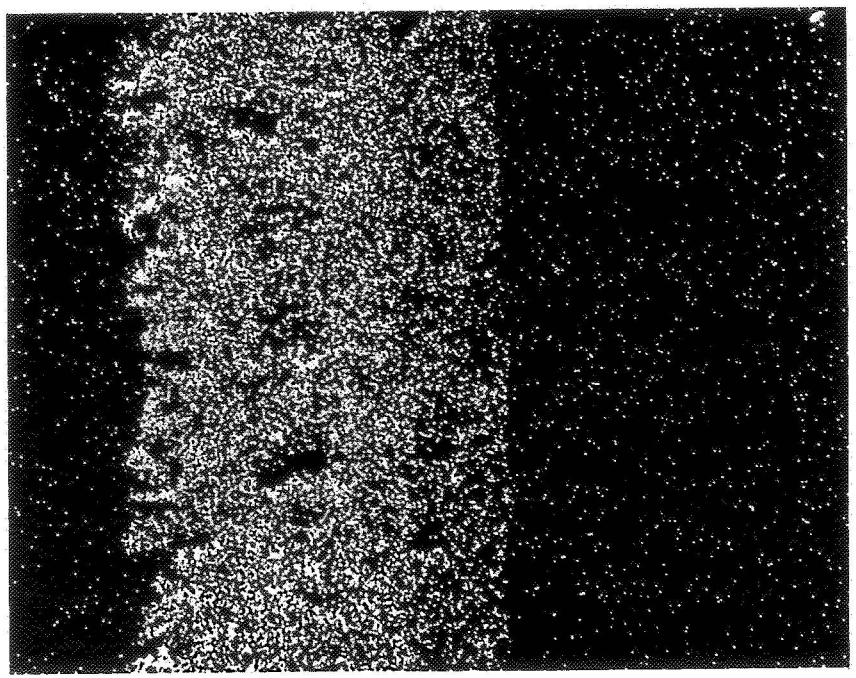

Silicon X-ray Distribution Photo 310 30000

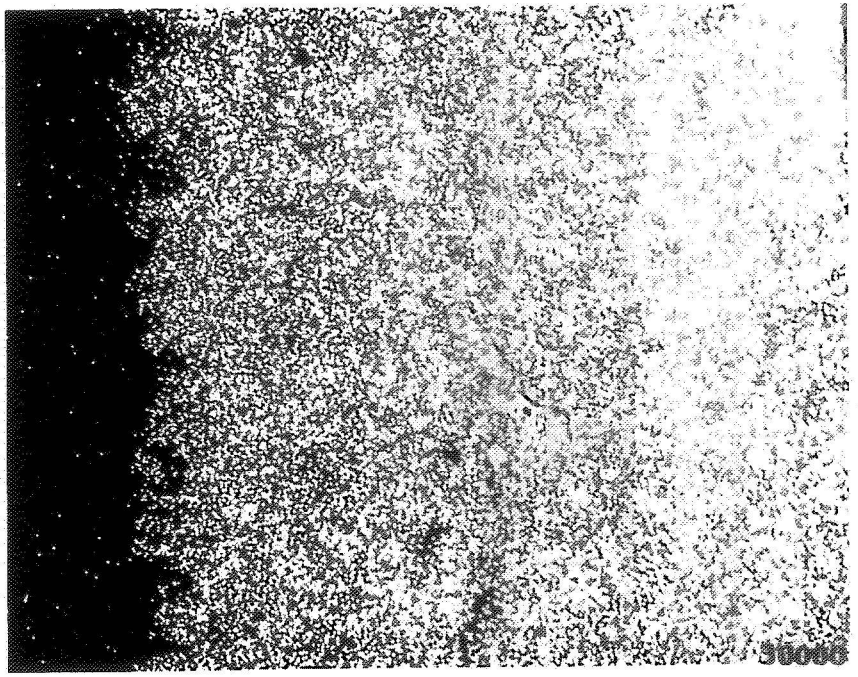

Nickel X-ray Distribution Photo 310

9950-847

FIGURE XIX

CORROSION TEST ON ALLOY 400 (MONEL)
87 HOURS @ 500°C, 300 PSIG, $H_2/SiCl_4$= 2.0

SCANNING ELECTRON MICROGRAPH OF THE SURFACE OF THE TEST SAMPLE TO SHOW THE MORPHOLOGY OF THE SILICIDE FILM AT VARIOUS MAGNIFICATIONS

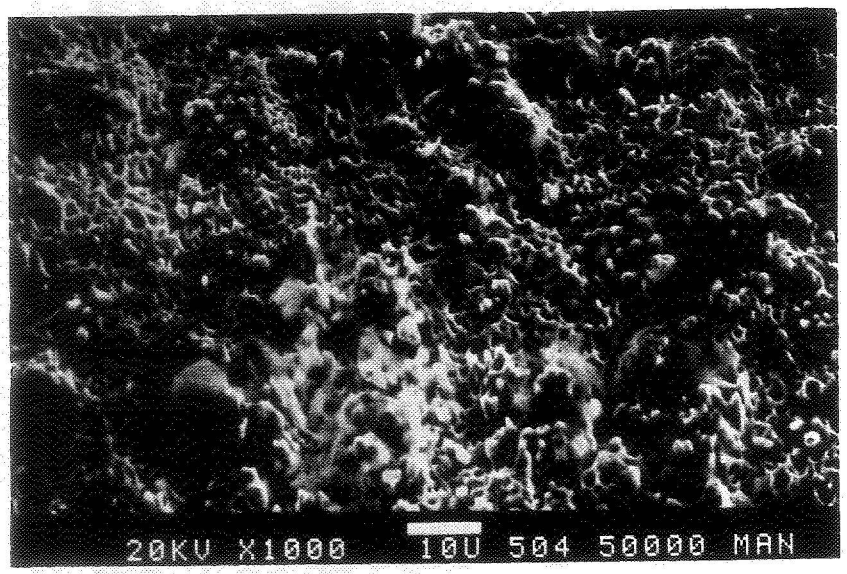

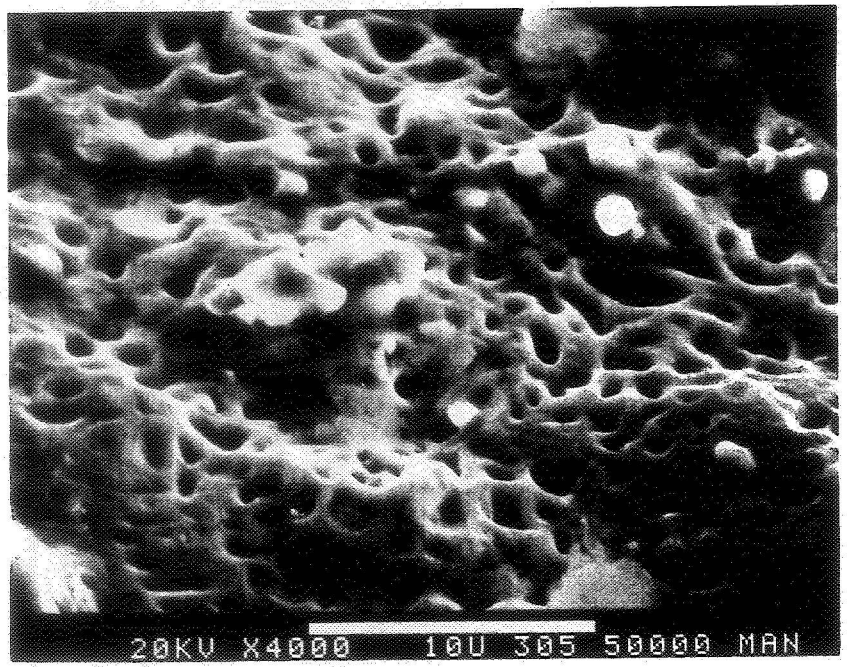

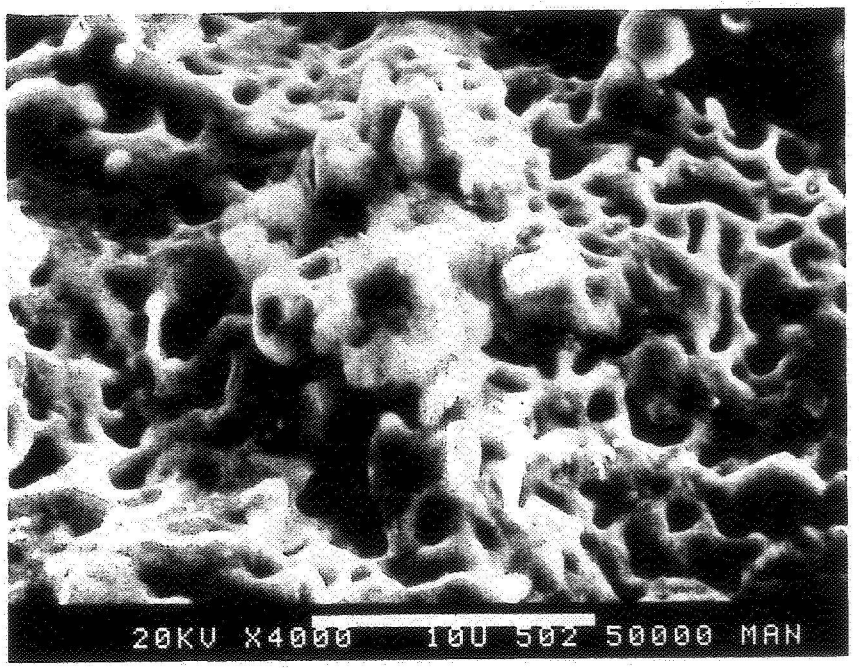

FIGURE XX CORROSION TEST ON ALLOY 400, CROSS SECTIONAL AREA AND X-RAY MAPS

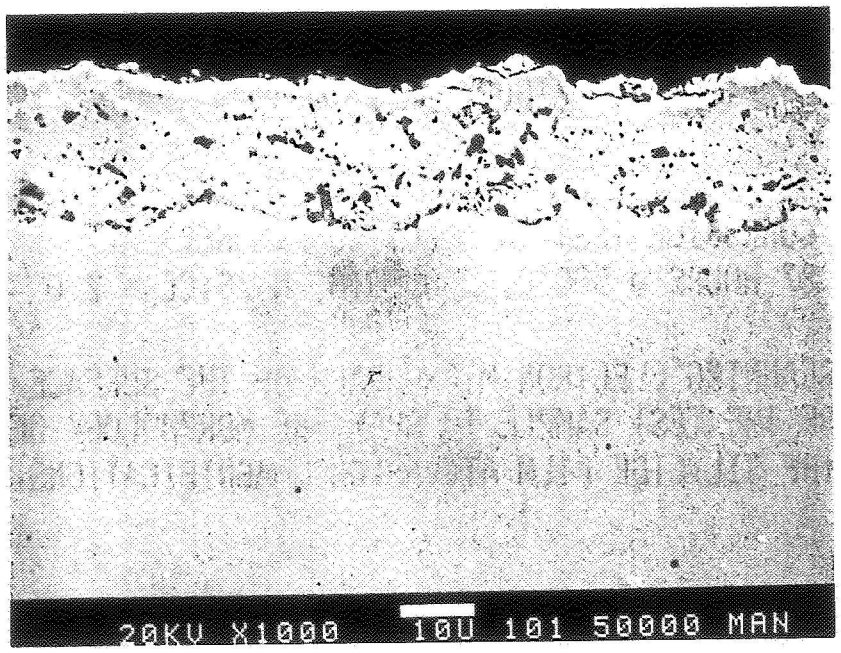

Coating Chemistry Sample # 5 (Silicon over Monel Metal) O.D. Surface

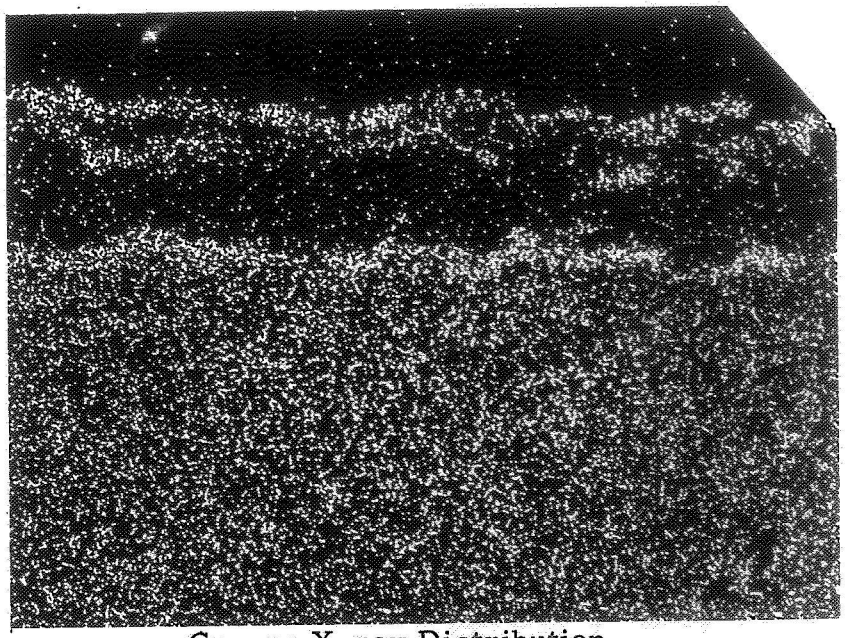

Copper X-ray Distribution

FIGURE 5

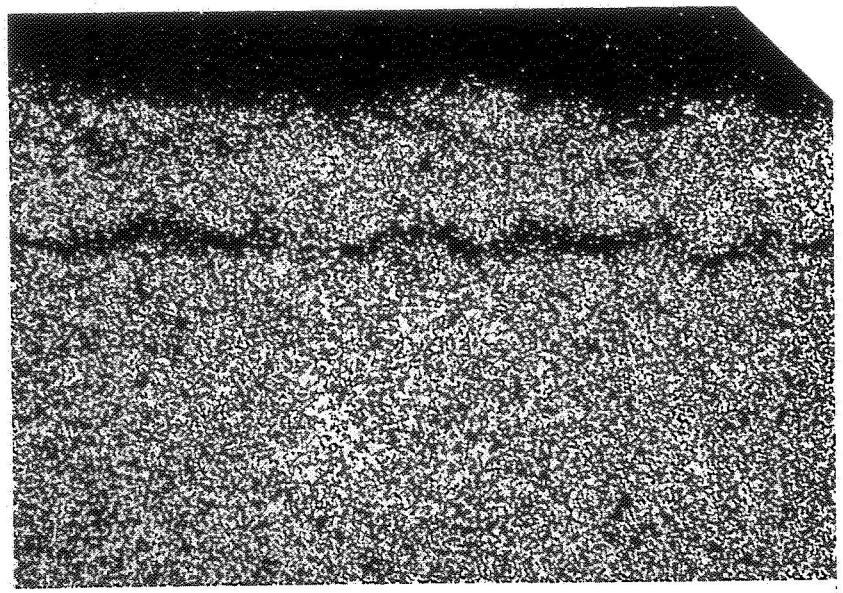

Nickel X-ray Distribution

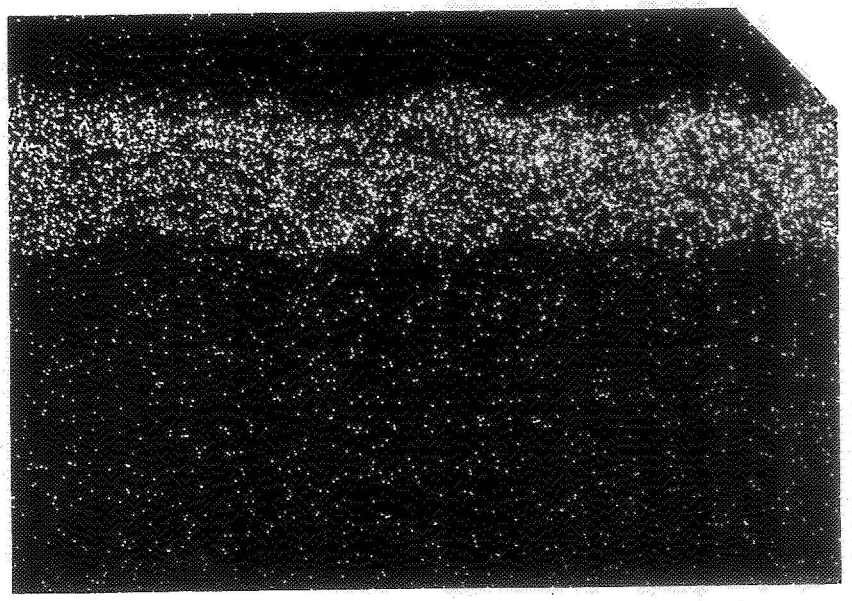

Silicon X-ray Distribution

9950-847

FIGURE XXI CORROSION TEST ON ALLOY 400: X-RAY MICROPROBE ANALYSES ON FOUR DIFFERENT AREAS AT THE CROSS SECTION OF THE SAMPLE

9950-847

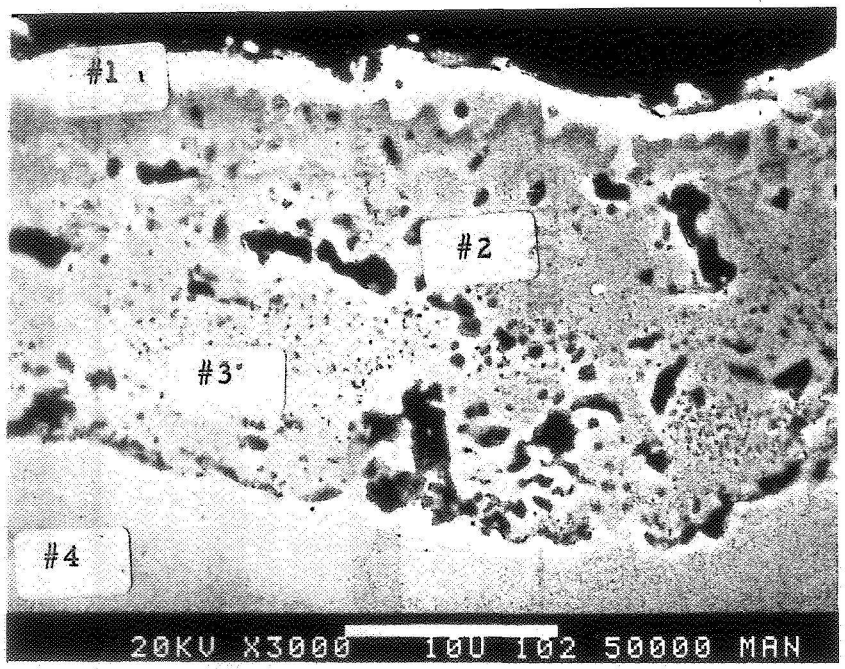

S OD AREA 4
KV=20 TILT=30 TKOFF=29
BKG PT1= 3.0 BKG PT2=14.0
NOST
21-APR-82

CONCENTRATION

	WT.%	AT.%	% S.E.
SIK	1.11	2.36	8.86
MNK	0.77	0.83	9.23
FEK	1.45	1.55	5.74
NIK	59.86	60.74	0.93
CUK	36.81	34.52	1.38
	100.00		

S OD AREA 1
KV=20 TILT=30 TKOFF=29
BKG PT1= 3.0 BKG PT2=14.0
NOST
21-APR-82

CONCENTRATION

	WT.%	AT.%	% S.E.
SIK	20.52	36.55	1.47
NIK	13.17	11.22	2.17
CUK	66.32	52.22	1.07
	100.00		

S OD AREA 2
KV=20 TILT=30 TKOFF=29
BKG PT1= 3.0 BKG PT2=14.0
NOST
21-APR-82

CONCENTRATION

	WT.%	AT.%	% S.E.
SIK	24.64	40.88	1.19
FEK	1.76	1.47	5.09
NIK	61.01	48.42	0.92
CUK	12.59	9.24	2.46
	100.00		

S OD AREA 3
KV=20 TILT=30 TKOFF=29
BKG PT1= 3.0 BKG PT2=14.0
NOST
21-APR-82

CONCENTRATION

	WT.%	AT.%	% S.E.
SIK	23.23	38.77	1.25
CLK	0.35	0.47	15.92
FEK	1.73	1.45	5.15
NIK	69.27	55.31	0.87
CUK	5.41	3.99	4.11
	100.00		

FIGURE XXII

CORROSION TEST ON
INCOLOY 800H

238 HOURS @ 500°C,
300 OSIG, $H_2/SiCl_4$ = 2

SEM ANALYSIS OF
CROSS SECTIONAL AREA

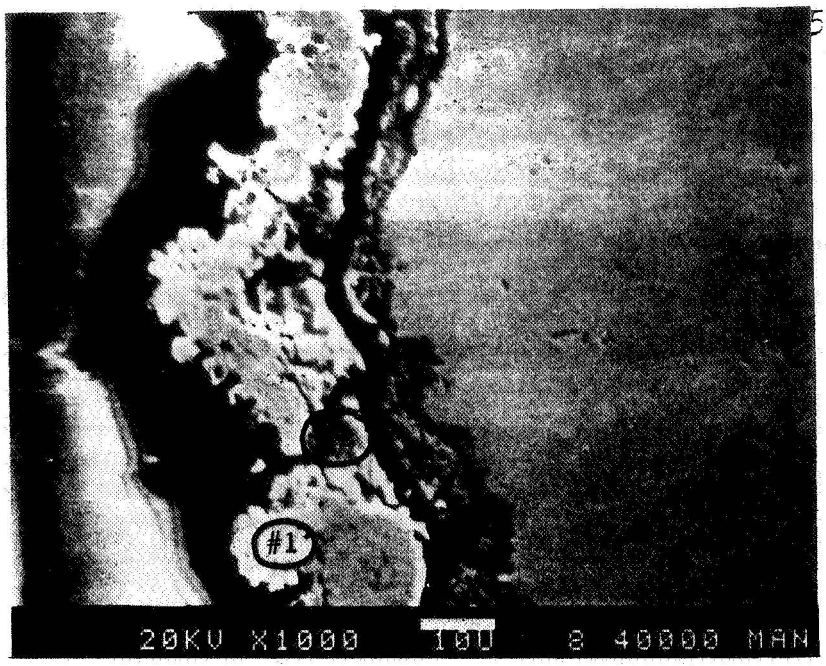

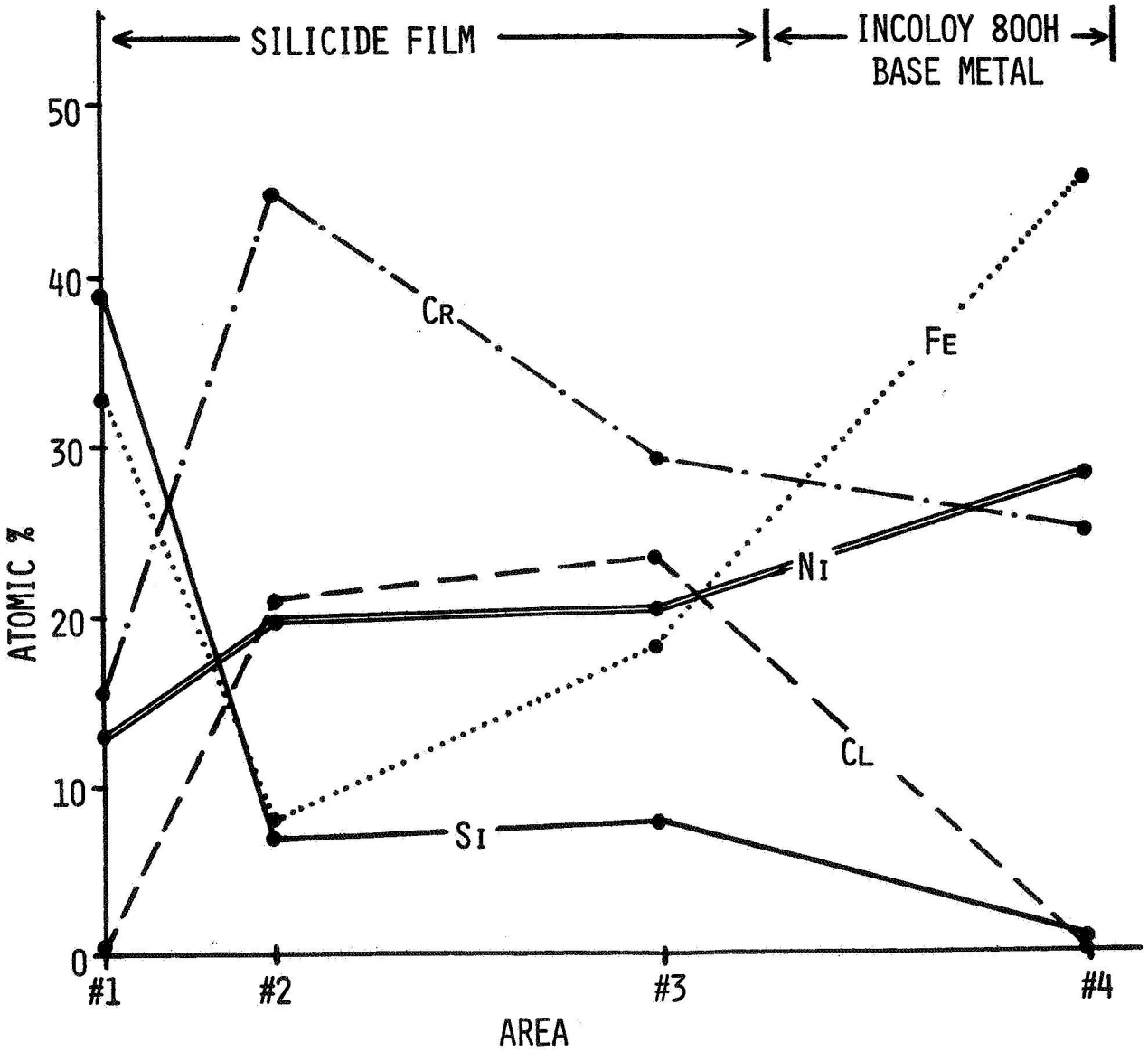

FIGURE XXIII X-RAY DISTRIBUTION MAPS OF A CROSS SECTIONAL AREA OF INCOLOY 800H TEST SAMPLE (SEE FIGURE XXII ALSO)

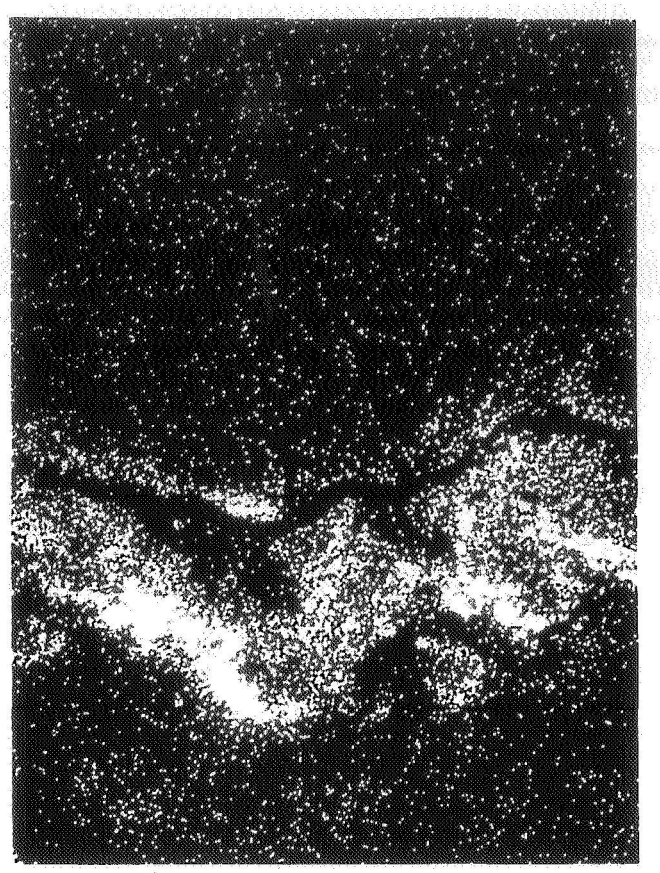

Silicon X-ray Distribution Photo 8 40000

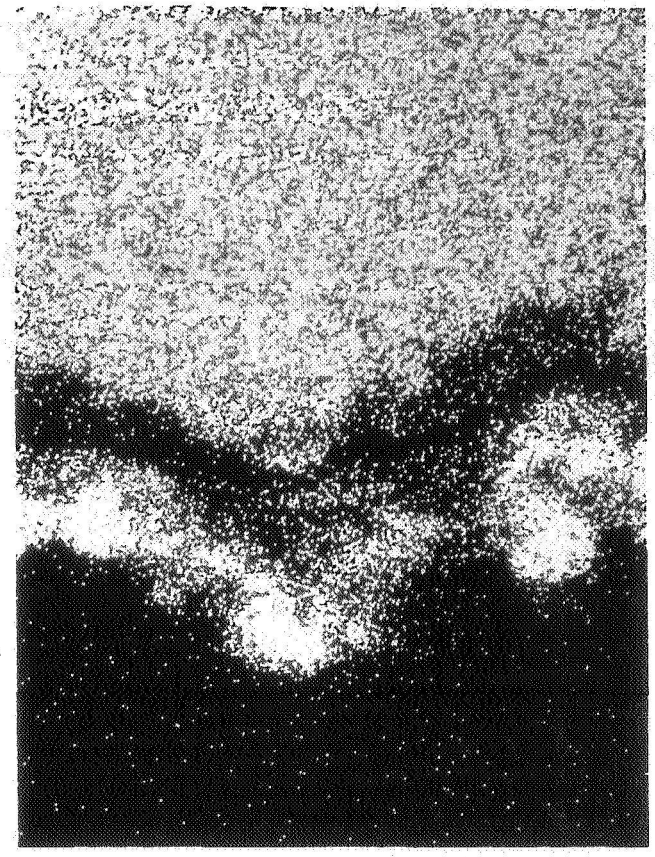

Iron X-ray Distribution Photo 8 40000

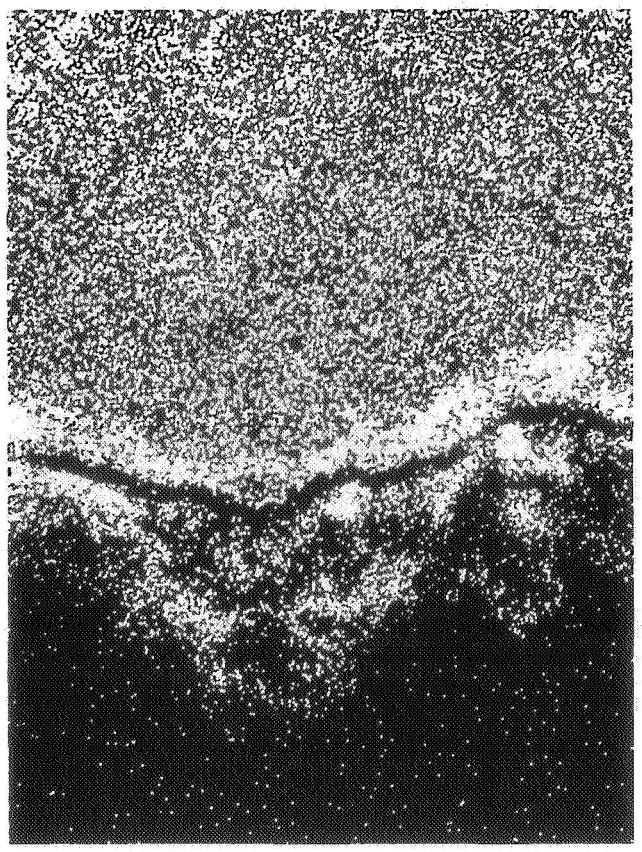

Nickel X-ray Distribution Photo 8 40000

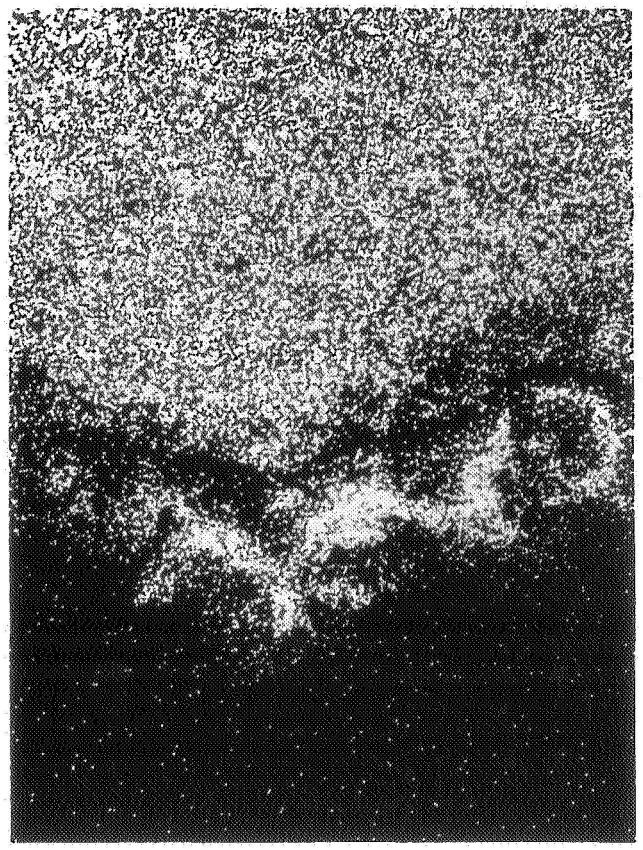

Chromium X-ray Distribution Photo 8 40000